ICT-777137

5G-RANGE

5G-RANGE: Remote Area Access Network for the 5th Generation

Research and Innovation Action
H2020-EUB-2017 – EU-BRAZIL Joint Call

D6.3: Performance Evaluation and Simulation

Due date of deliverable: 30th July 2020
Actual submission date: 25th November 2020

Start date of project: 1 November 2017
Duration: 36 months
Lead contractor for this deliverable: UnB
Version 1 date 20th November 2020
Confidentiality status: Public

Abstract
This deliverable shows the integration of the multiple block in the 5G-RANGE PHY, cognitive MAC and Network layers. A software simulator was used to perform and test this integration. The PHY layer has been simulated using Matlab and C languages, providing link level block error rate for the cognitive MAC and network simulator, which has been implemented in NS3. The integrate software simulator will be used to analyze the system performance and also to show 5G-RANGE features that will not be present in the proof-of-concept testbed. The PoC will be used to demonstrate three use cases defined in D2.1 and the SDR approach employed in its development will lead to an advanced Technology TRL prototype, which will be easily transferable to the market.

Target audience
The primary target audience for this document is the radio access network research and development community, particularly those with an interest in mobile communication physical and MAC layers. This material can be fully understood by readers with a background in mobile wireless cellular systems, especially those familiar with 3GPP standards for 4G and 5G.

Impressum
Full project title: 5G-RANGE: Remote Area Access Network for the 5th Generation

Document title: D6.3 – Performance Evaluation and Simulation

Editor: Priscila Solís, UnB (BR)

Project Co-ordinator: Marcelo Bagnulo, UC3M (EU), Priscila Solís, UnB (BR)

Technical Manager: Luciano Mendes, Inatel (BR), Yaning Zou, TUD (EU)

WP leaders: Ivo Bizon, TUD (EU), Luciano Mendes, Inatel (BR)

This project is co-funded by the European Union through the ICT programme under H2020.

Executive Summary

The 5G-RANGE network has been designed to support a large set of services in remote area, covering four use cases, as described in D2.1. However, the evaluation of all 5G-RANGE features demands the implementation of the entire architecture described in D2.2, D5.1, D5.2 and D5.3. Considering the budget and time restrictions of the project, the project planned that implementation of the main features will be integrated in a real-time PoC (Proof of Concept) that will cover smaller versions of the most important uses cases which are voice and data connectivity, smart farms and wireless backhaul. Therefore, to validate the PoC results and demonstrate all capabilities of the 5G-RANGE Network in more complex scenarios for the four uses cases defined in D2.1, the strategy is to use a software simulator, to be developed during the project, that integrates the PHY and MAC functionalities of the 5G-Range Network with a customized IP layer in terms of end-to-end applications, for each of the four use cases.

The software simulator is composed by a link-level simulator and a system level simulator. The link-level simulator is able to analyze the physical layer performance in terms of bit error rate and block error rate under different channel conditions. All numerologies and features have been implemented in the link-level simulator which provides block error rate curves that feeds the system level simulator, abstracting the physical layer. With these curves, the behavior of the physical layer can be mapped in a set of tables that are accessed to inform the performance of the lower layer. With this approach, the performance of the entire network can be simulated in a feasible amount of time. A similar approach was taken to integrate the spectrum sensing capabilities in the software simulator, however, the features regarding 5G-COSORA and 5G-DARA modules were fully implemented in the software simulator with some extensions for security and collaborative spectrum sensing optimization.

The adopted strategy to develop the real-time PoC and the 5G-Range software simulator allowed to validate the PoC performance results as well as a software tool that can be used in future developments of the 5G-Range network. Also, the software tool, that can be considered as a customized experimental testbed, allows to evaluate the performance and metrics of miscellaneous configurations of the 5G-Range use cases, which may also aid in future developments and research activities for 5G.

List of Authors

Alexandre Carvalho Ferreira (Inatel)
Luciano Leonel Mendes (Inatel)
Roberto Michio Marques Kagami (Inatel)
Wheberth Damascena Dias (Inatel)
Gabriel de Carvalho Ferreira (UnB)
Geraldo Pereira Filho (UnB)
Luis Alberto Belem Pacheco (UnB)
Priscila Solis (UnB)
Marcos Fagundes Caetano (UnB)
Rafael Amaral Soares (UnB)

Table of Contents

List of Figures

Definitions and Abbreviations

ACLR	Adjacent Channel Leakage-Power Radio
ADC	Analog to Digital Converter
AI	Artificial Intelligence
ARMA	Auto Regressive Moving Average
AR	Auto Regressive
AWGN	Additive White Gaussian Noise
BLER	Block Error Rate
BS	Base Station
CB	Code Block
CDL	Cluster-Delay Line
CDL-D	Cluster Delay Line with Rician Distribution
CDN	Content Over the Network
CFD	Cyclostationary Feature Detection
CMAC	Cognitive Medium Access Control
CP	Cyclic Prefix
CQI	Channel Quality Indicator
CSI	Channel State Information
CSS	Common Spectrum Sensing
DAC	Digital to Analog Converter
DCI	Download Control Information
DL	Downlink
DPD	Digital Pre-distortion
EESM	Exponential Effective SINR Mapping
EROS-5	Synthetic Traffic Generator for 5G Networks
IP	Internet Protocol
F-OFDM	Filtered Orthogonal Frequency Division Multiplexing
FPGA	Field Programmable Gate Array
GFDM	Generalized Frequency Division Multiplexing
iSAC	Internet Speech Audio Codec
IR2A	Inner Receiver for Remote Areas
LOS	Line of Sight
LTE	Long Term Evolution
LSM	Link to System Mapping
MA	Moving Average
MCS	Modulation and Coding Scheme
MIMO	Multiple-Input Multiple-Output
MIESM	Mutual Information Effective SINR Mapping
MNOs	Mobile Network Operators
NLOS	Non-Line of Sight
OFDM	Orthogonal Frequency Division Multiplexing
OOBE	Out-of-Band Emissions
PD	Probability of Detection
PFA	Probability of False Alarm
PSD	Power Spectral Density
PHY	Physical Layer
PoC	Proof-of-Concept
QAM	Quadrature Amplitude Modulation
QPSK	Quadrature Phase-Shift Keying
RA	Resource Allocation
RB	Resource Block
RBG	Resource Block Group
ROC	Receiver Operating Characteristic

ROI	Return of Investment
ROM	Read-only Memory
SDU	Service Data Unit
SINR	Signal-to-Interference-plus-Noise Ratio
SISO	Single-Input Sigle-Output
SLS	System-Level Simulator
SNR	Signal-to-Noise Ratio
SS	Spectrum Sensing
TB	Transport Block
TRL	Technology Readiness Level
TVWS	TV White Space
UCI	Unique Client Identifier
UE	User Equipment
UL	Uplink
ULA	Uniform Linear Arrays
USRP	Universal Software Radio Peripheral
VNF	Virtualized Network Function
WIBA	Window Based

1 Introduction

The 5G-RANGE network has been designed to provide reliable broadband access connection, in remote areas. In D2.1 were described the four use cases of application of the 5G-Range Network in remote areas. Then, the specification of the entire architecture of the 5G-Range Network was described in D2.2, D5.1, D5.2 and D5.3. The budget limitations and time restrictions of the project allow the implementation of the main features in a real-time PoC (Proof of Concept) that covers smaller versions of the most important uses cases which are voice and data connectivity, smart farms and wireless backhaul. Then, in D6.1 and in this deliverable, D6.3, the goal is to integrate the developments made in WP3, WP4 and WP5, i.e., the Physical Layer (PHY) blocks designed and specified in WP3 are combined with the Cognitive Medium Access Control (CMAC) developed in WP4, with the network functions to provide a simulation platform that can be used to evaluate the overall system performance and also to demonstrate features that will not be available in the proof-of-concept (PoC) demonstrator.

In D6.1, the main strategy of the system integration was presented. The strategy consists of using an event-based environment, the NS-3 with a specific module for LTE networks called LENA, i.e. NS-3/LENA, to integrate the 5G-COSORA and 5G-DARA functions and the network functions in order to create a system level simulator. Also, the strategy defined that the PHY layer will be abstracted through a set of block error rate (BLER) performance curves, which are provided by a PHY simulator developed using Matlab. The goal is to use the system simulator and its measures as a reference design for the final PoC and its field measures. With this approach, the software simulator is composed by a link-level simulator and a system level simulator and in D6.1 some previous results of the initial phase of development were presented and validated.

In this deliverable, D6.3, the goal is to present the final version of the software simulator, integrating all the proposed features in WP3 and WP4, also with some basic features from WP5 that allow the evaluation of different applications related to different configurations of the four use cases defined in D2.1.

To facilitate the understanding of the software simulation tool and its features, the deliverable is structured in different sections that provide a view of the developments made for the PHY and MAC Layer, as well as the access for the GITHUB repositories, where some simple demonstrations are available. For each of these layers there is verification procedure, which shows that the software implementation satisfies all the expected requirements.

It is clear that any software simulation tool may have its limitations, some of them imposed by the development environment and programming language and others for the theoretical models that are implemented with some restrictions and approximations. Therefore, a common practice is to validate the software simulation tool when comparing its simulation results with real-time measures. This procedure was adopted in this deliverable, making a comparison of the PoC results and the simulation results for similar scenarios. It is important to note that because of the COVID-19 Pandemic, the field measures that were planned to be performed during June 2020 and July 2020 were drastically reduced, and for this reason, the real-time measures were performed in Santa Rita, at Inatel’s laboratory using the last version of the software prototype described in D6.2. The comparison of the real-time measures with the simulation results showed satisfactory results and provided an interesting feedback to improve some features in the software simulation tool.

After the validation, the next step was to develop the performance evaluation of the four use case scenarios using the software simulation tool. The four scenarios, i.e., Voice and Data Connectivity, Smart Farming, Backhaul and e-Health were simulated using different configurations regarding a 50km cell and varying parameters such as mobility, distance from the gNodeB, number of UEs/clients in the cell and customized traffic for each application in the network layer. The results of each simulation were compared with the KPIs defined for each use case, as described in D2.1 and the results show the applicability of the 5G-Range Network for remote areas.

1.1 Deliverable Structure

The remaining of this document is structured as following: Section 2 presents the description of the System Level Simulator, recalls from D6.1 the adopted strategy for the implementation and shows the integration with the developments described in D4.4. For both layers, PHY and MAC, there is a detailed description of the software developments that were made to implement the feature of the 5G-Range Network, considering the NS-3/LENA. In this section, there are also available the references to the repositories with the implemented code.

Section 3 presents the PoC Performance Evaluation and Verification, which is divided in a Phy Performance Evaluation, that presents 5G-Range software prototype performance evaluation in a laboratory environment, performed at Inatel's venues after March 2020. Then, this section also presents the PoC Simulation and Evaluation using the software simulation tool in a similar scenario, that we named as COLAB-5 when integrating the 5G-Range implementations for the PHY and MAC Layers into the NS-3/LENA. The results obtained in this section shows similar results and allowed to perform a preliminary validation of COLAB-5.

Section 4 presents the simulation using COLAB-5 of the four use cases, defined previously in D2.1. For each use case, a number of different scenarios is simulated, and the results are compared with their specific KPIs. Finally, Section 5 presents the conclusion of the tasks and developments made in this deliverable.

2 General Description

Basically, the tool was implemented by following a modular approach that allows the incorporation of physical layer characteristics in the simulator through a set of pre-defined interfaces.
The link-level simulator, mainly implemented in MATLAB, provides as a set of tables that describe and model the behavior of the channel in different scenarios. The link-level simulator enabled simulations relative to the physical layer only, such as channel coding algorithms, channel models, and waveform, as was described in Deliverable 6.1. Results from other channel models can be generated by other tools and loaded in the same format, adapting the simulator to different needs. The values provided are SNR (Signal-to-Noise Ratio), spectral efficiency, the flow achievable using a given modulation and coding scheme (MCS), the error rate per block (BLER) and the size of the block or frame (TBS), the latter describing the resilience of the MCS to interference.
The spectrum sensing (SS) information is also produced in MATLAB, which is represented by curves of probability of detection of primary users, as described in D4.4. These curves are used in the NS-3/LENA to implement the collaborative sensing mechanism.
All the information produced in the MATLAB environment for the physical layer and spectrum sensing is exported in JSON format and loaded by the NS-3/LENA during the system level simulation.
As described in D4.4, the 5G-Range proposes the use of a Cognitive Cycle, that has as main feature the opportunistic use of spectrum. Then, the 5G-RANGE Cognitive MAC layer is integrated in the NS-3 code and the PHY layer is integrated with the L2S (Link-to-System) interface. In this way, the properties of the physical layer are incorporated into the system simulator and integrated with the upper layers, which allows the simulation of more complex scenarios. This approach reduces the computational complexity of the simulation, by separating the process into two stages and allows greater flexibility in the integration of both layers.

2.1.1 PHY Layer Implementation

Figure 1 recalls the 5G-RANGE simulation approach, as was described in D6.1. The link-level simulator provides SINR/BLER mapping tables by using the Exponential Effective SINR (Signal-to-Interference-plus-Noise Ratio) mapping (EESM). In order to simplify the obtaining of the SINR in the 5G-RANGE Module within the NS-3, it was defined to use the EESM technique based on the Chernoff Union bound as L2S Interface. As described in D6.1, such a technique gets good results with low complexity in comparison to MIESM (Mutual Information Effective SINR Mapping). As the EESM does not use the MI values, it is easy to get the look-up tables and the Link-to-System Mapping (LSM) because only the β parameter is necessary. With this, the 5G-RANGE Module can make use of the direct mapping of SINR values to BLER values and embed the link-level performance curves into the SLS (System-Level Simulator).
In the proposed channel error model, the Transport Block (TB) was divided in N_{K-} code blocks of size K- and N^{K+} code blocks of size K+. Therefore, the overall TB BLER can be expressed as described in Eq. (1).

$$TBLER = 1 - \prod_{i=1}^{C}(1 - CBLER_i) \quad \textbf{(1)}$$

where the $CBLER_i$ is the BLER of the CB_i (Code Block) obtained according to the link-level simulations curves within one of 9 CB sizes. For estimating the $CBLER_i$, the look-up tables to each code block are used jointly with the SINR got from the EESM technique. According to the interleaving assumption over CBs belonging to a TB, they might be decoded and successfully received individually or as a whole in the TB.

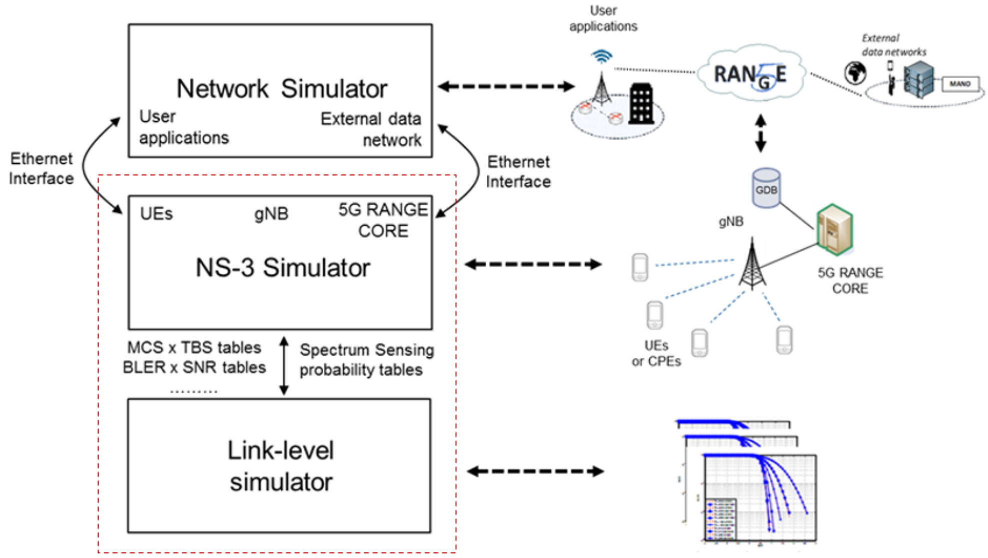

Figure 1. 5G-RANGE simulator overview

The development strategy for the SLS consisted of the modification of the LTE module provided by the NS-3/LENA simulator. LTE module includes the LTE Radio Protocol stack that resides entirely within the UE and the eNodeB nodes.
The development took place in two stages. In the first stage, the features not related to the channel modeling were implemented, as presented in Deliverable 6.1. The main features implemented in this phase are listed below:

- Subframe duration changed from 1 ms to 4.6 ms;
- Spectrum range changed to 170 to 400 MHz and 450 to 700 MHz;
- Frequency range changed to 4 MHz, 6 MHz, and 24 MHz;
- Resource Block bandwidth changed to 180 kHz;
- Usage of CQI (Channel Quality Indicator), MCS, and TBS parameters from 5G-RANGE; and
- Resource Block Group size changed to 1.

The second stage consists of the channel model implementation, in which the EESM tables were imported, the computation of the TBLER (Transport Block Error Ratio) based on the CBLER was implemented, and the CDL A and CDL D propagation loss models were ported into NS-3. Therefore, this stage focused on the implementation of the channel model, MIMO (Multiple-Input Multiple-Output), numerology, and scripts to automate the execution and analysis of simulations. The sections below describe in detail the features implemented.

2.1.2 5G-RANGE channel model

The 5G-RANGE channel model implementation encompasses the propagation loss model, which are the Cluster-Delay Line for Line of Sight (CDL D), No Line of Sight (NLOs), and the mapping and calculations of the SINR to Transport Block Error Rate (TBLER). The two features encompass the entire channel abstraction in NS-3/LENA, where transmitting nodes send a PSD to the channel class, which applies the propagation loss model. Then the receiving node calculates the SINR, acquires the CBLER from the mapping tables, and finally calculates the TBLER and determines the transmission's success.
The propagation loss model was adapted into NS-3/LENA from a repository provided by the UFC partner[1], which had this model implemented in C++. The porting was conducted by adopting the provided code to the NS-3 structure. CDL A and D implementation was performed using the `SpectrumPropagationLossModel`. Such a model receives a Power Spectral Density (PSD)

[1] GitLab Community Edition, https://5grange.gtel.ufc.br

representing the transmitting signal outputs the attenuated PSD. The CDL model implementation required modifying the PHY layer of both eNodeB and UEs. Precisely, the Uniform Linear Arrays (ULA) were modeled for each node antenna (uplink and downlink). ULA represents the node antenna in greater detail, enabling a more accurate model. In the ULA, each antenna has several antenna elements, and the propagation loss is calculated related to each antenna element of the transmitter to each antenna element of the receiver. For this, the `Ula5gRange` class was implemented in each node PHY layer to model the ULA, that allows to use parameters such as the bearing, spacing, number of antenna elements, polarization type, among others.

Figure 2 shows a class diagram related to CDL A and D models implementation in NS-3. The `CdlSpectrumPropagationLossModel` implements both CDL A and D, using the `SpectrumPropagationLossModel` abstract class, which interfaces with the `SpectrumChannel`. The `SpectrumChannel` is a singleton class in which all nodes that want to transmit and receive must register, and every transmission is broadcasted to all nodes registered to this channel. For this, when communication occurs, the `CdlSpectrumPropagationLossModel` is executed, and the loss is calculated. If the node is type `LteSpectrumPhy`, uses the related `Ula5gRange` object to obtain the necessary parameters to execute the loss models.

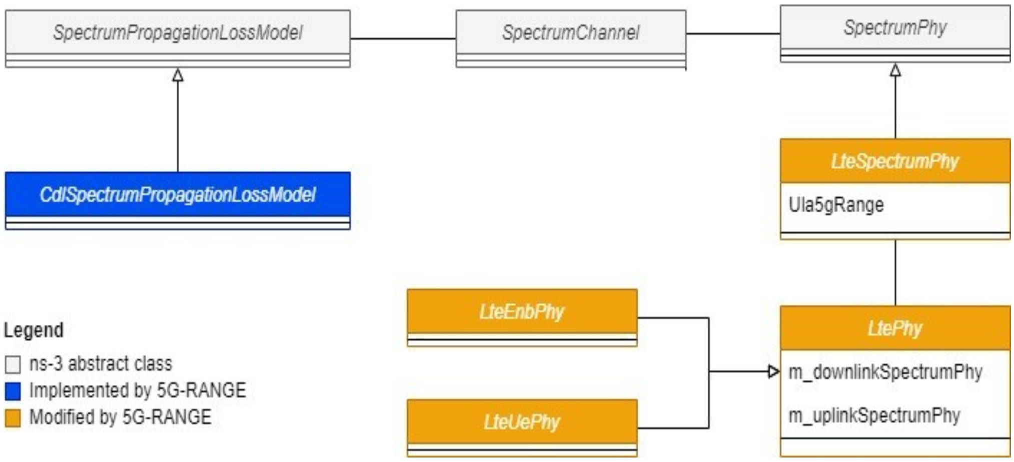

Figure 2. Class diagram of the channel model implementation.

It is worth noting that the channel propagation model implementation takes into account the temporal correlation of the generated values, giving temporal stability. The same model, however, does not implement a spatial correlation between the shadowing values. This implies that the values are not spatially stable and that different users, even co-located, have diverging shadowing values. Such unrealistic representation of space-based shadowing losses is mitigated through shadowing maps. The maps are generated for the 3D Cartesian space occupied by the simulation devices. The shadowing samples with known distribution are drawn for each cell and correlated to each other through a weighted average with the exponential drop. Thus, we obtain the simulated channel's temporal and spatial stability, as presented in Figure 3.

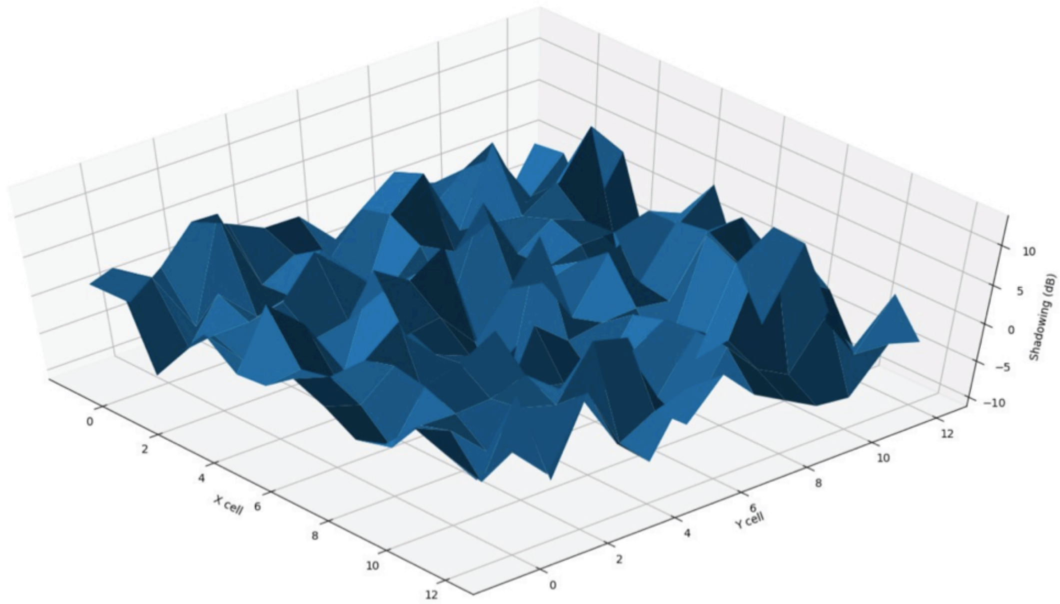

Figure 3. An example of the shadowing map used in the simulation

Therefore, the `SpectrumChannel` class (see again Figure 3) sends the PSD attenuated by the `CdlSpectrumPropagationLossModel` to all nodes attached to this channel. The nodes then calculate the SINR and use the mapping tables to acquire the CBLER and calculate the TBLER to stipulate if the received frame is corrupted.

2.1.3 Performance evaluation of PHY Layer

This section shows the scenario used in NS-3 to generate the experiments to verify the implementations carried out on the PHY Layer. The verification of the 5G-RANGE channel model in the PHY Layer was divided into two stages. In the first stage, we verified the implemented features that are not related to the channel propagation model, such as the usage of spectrum bands and the subframe duration. In the second stage, the channel propagation model and all related features were analyzed.

2.1.3.1 Simulation setup in the PHY Layer

To verify the implemented features, the following configurations were used:

- Usage of spectrum bands 170 to 400 MHz and 450 to 700 MHz;
- The bandwidth of each Resource Block, which is 180 kHz. Therefore, the number of RBs (Resource Block) of a subframe, which changes from 132 RBs in 24 MHz;
- Duration of subframe from 1ms to 4.6 ms;
- Usage CQI, MCS, and Transport Block Size configuration from 5GRANGE.

It is essential to notice that those features were selected considering the parameters defined in the previous deliverables of WP3. The 5G-RANGE allows the use of 3 bands of 8MHz or 4 bands of 6 MHz, for a total of 24 MHz in both cases. Each RB can contain a maximum of 5152 bits of useful data (Numerology 0 at MCS 26). Thus, the maximum throughput achieved in 5G-RANGE in numerology 0 and MCS 26 is 147.84 Mbps. In the simulation environment of the NS-3/LENA, both situations may be implemented using Carrier Aggregation. However, the simulator does not allow the implementation of cross-carrier scheduling, requiring a separate control channel and scheduler per carrier. To override this limitation, we used a single channel of 24 MHz, logically partitioned into either 4x6MHz or 3x8MHz subchannels. That allows the use of a single control channel and a single scheduler that has control over the entire available bandwidth. As the project assumes a separate control channel on a licensed band, the control part of the frames was reduced and assumed ideal (error-free). The simulation scenario was implemented to verify maximum throughput with only one UE and several UEs.

PHY Layer verification

In this scenario, an external agent connected to the eNodeB sends data to all active UEs. The traffic generated by the external agent is equivalent to 5.152 bits every 4.6 ms, that is, the maximum amount of data from a Resource Block in numerology 0 and MCS 26. Thus, when increasing the number of UEs, the traffic increases proportionally until the maximum amount of Resource Blocks reaches the maximum amount. The distance between the UEs and the eNodeB is 1 km; however, this parameter does not affect the results, as the fading algorithms are not being used in this part of the verification. Figure 4 shows the results obtained when we have 8, 16, 33, 66, and 132 UEs active. It can be seen that the UEs receive the traffic generated by the external agent. In addition, the results show that maximum achievable theoretical throughput of 5G-RANGE was reached, which was taken from Table 12 of D3.2. As can be seen, the Expected and Achieved Results are compatible and also limited by the theoretical throughput. This shows that the simulated results reflect the expected throughputs and are a first demonstration that validates the implementation of the 5G-RANGE PHY in the NS-3.

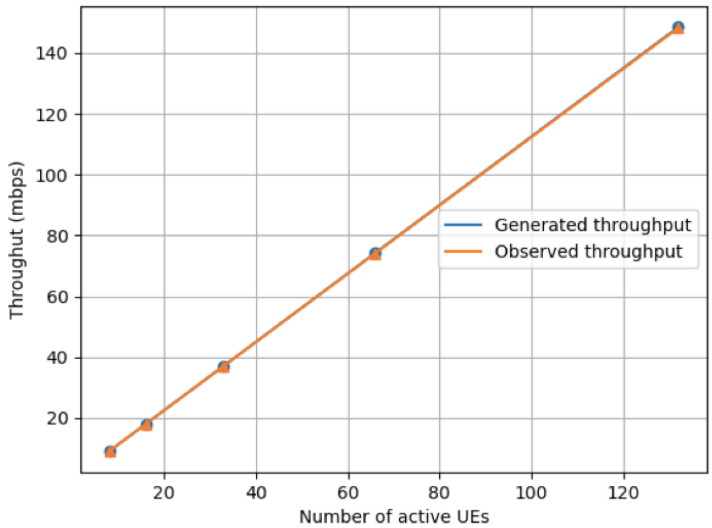

Figure 4 Generated and observed throughput according to the number of UEs.

After checking the achievement of maximum throughput with multiple UEs, it was verified with only one UE. In this case, the single UE receives all traffic generated by the external agent, which increases until reaching the maximum flow supported by 5GRANGE in numerology 0.
Figure 5 shows the results obtained throughput with a single UE. As can be seen, the traffic generated by the external agent is received by the EU in its entirety until it approaches the 5GRANGE limit. When the traffic generated exceeds the limit, the UE receives the maximum, and the rest remains in the buffer. In this case, the buffers have a very big size limit. Therefore, small variations in flow are observed due to the delay in communications and the battery.

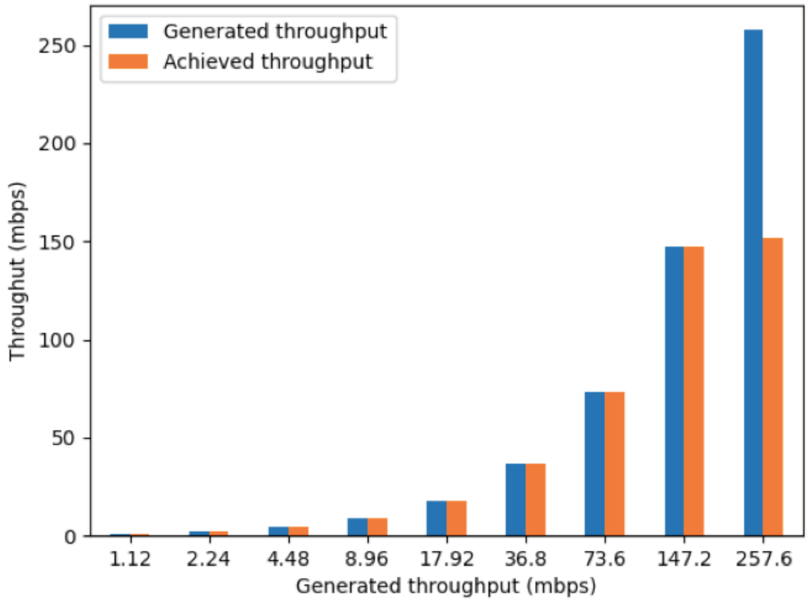

Figure 5 Generated and achieved throughput with a single UE.

It is worth noting that the fixed MCS is not representative of real-world scenarios, where a multitude of factors such as movement, obstacles, temperature, and others can affect the channel conditions. The link adaptation is made by adjusting the used MCS to keep the TBLER lower than a target threshold. That variation of MCS through time results in a Gaussian distribution of MCSs. To show the distributions of the MCS values, simulations were run assuming K = 0 dB, eNodeB TxPower = 40.8 dBm, 40 simulation batches, 95% confidence interval, MIMO 2x2 TxDiversity, UE and eNodeB antenna gains of 9dBi, and the downlink channel centered in 525MHz, using a fixed shadowing value. In Figure 6, we show the distributions of MCSs for the same topology using LOS and NLOS channel models. In the LOS model, the Gaussian is centered in the maximum MCS (27) for all distances. In the NLOS model, the Gaussian center moves away from the maximum MCS as the distance increases.

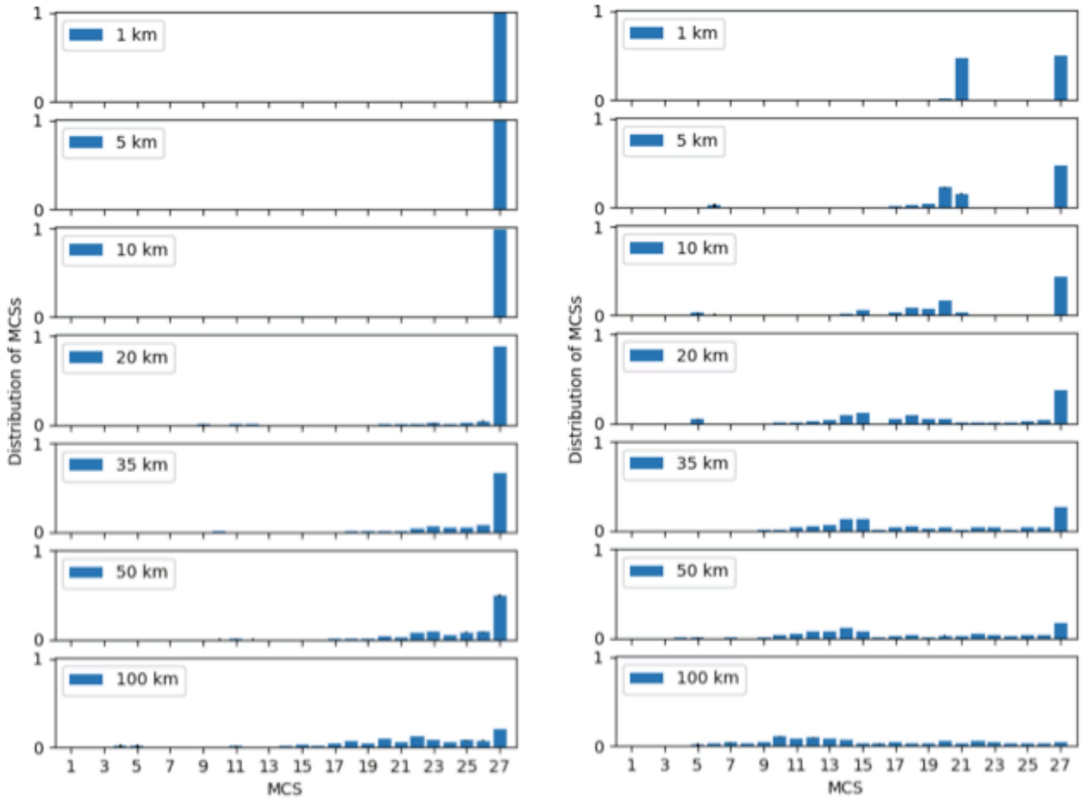

CDL D (LOS) CDL A (NLOS)

Figure 6. Distribution of MCSs for CDL D (LOS) and CDL A (NLOS).

The link adaptation also reflects on the throughput and TBLER of the network. Figure 7 shows the impact of previous MCSs distributions is shown in terms of throughput and TBLER, assuming a TBLER threshold of 10%, same used in 3GPP LTE-A networks. We use the shadowing distribution defined in deliverable D3.1 in this scenario. Throughput for LOS (CDL-D) is very stable within the first 20 km of distance between the UE and eNodeB, well above 100Mbps.

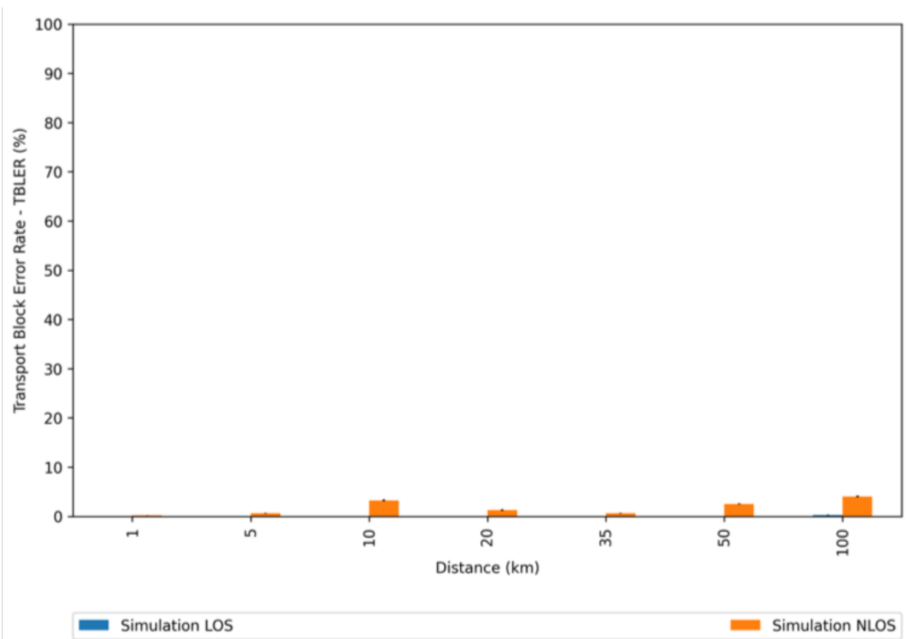

Figure 7. Transport Block Error Rate with a single UE.

2.1.3.2 5G-Range Channel Model Verification

In this section, the channel propagation model is assessed through computational simulation in NS-3/LENA. To that end, the implementation of the fading models CDL A and CDL D, as well as the import of mapping CBLER tables were implemented. Therefore, the validation of the 5G-Range channel model was compared with the models CDL A and D.

The scenario configuration was chosen to make a fair comparison between the models. The sets of parameters established to carry out the performance evaluation are shown in Table 1. In this scenario, the eNodeB transmission power and antenna gain are 53dB and 9dBi, respectively. The UE transmission power and antenna gain are 23dB and 9dBI. The distance has been changed from 1km, 20km, and 50km. The bandwidth used was 24 MHz, and the central frequency was 172 MHz.

Table 1. Simulation parameters for 5G-Range channel model verification.

Parameter	**Value**
eNodeB transmission power	53 dB
eNodeB antenna gain	9 dBi
UE transmission power	23 dB
UE antenna gain	9 dBi
Distances	1 Km, 20 Km and 50 Km
Bandwidth	24 MHz (132 RBs)
Central Frequency	172 MHz
Propagation Loss Model	CDL D and CDL A

Figure 8 and Figure 9 show the results obtained from the attenuated signal when the distance is varied by 1km, 20km, and 50km. It is noted that the 5G-Range channel model has similar results compared with the CDL A and D models. As can be seen, the results show that 5G-Range channel model was reached and is compatible with CDL A and D models, as confirmed in Deliverable 3.1. Therefore, it is possible to verify that the 5G-Range channel model was implemented correctly in the NS-3/LENA.

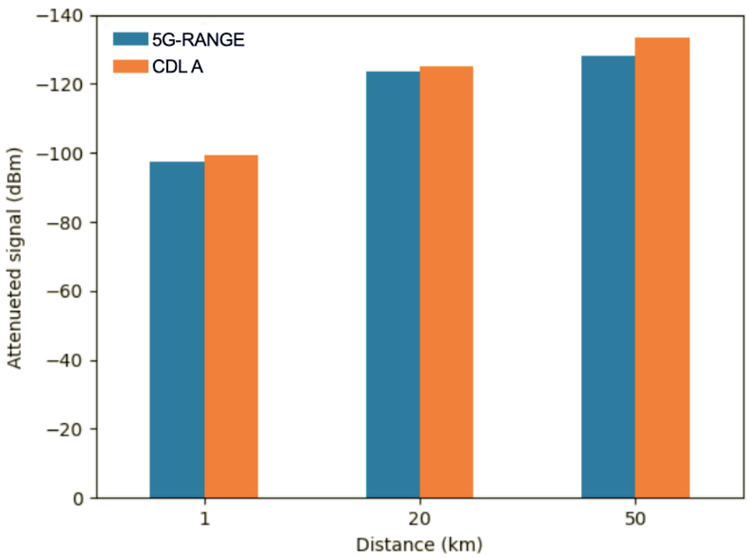

Figure 8. CDL A NS-3/LENA port validation

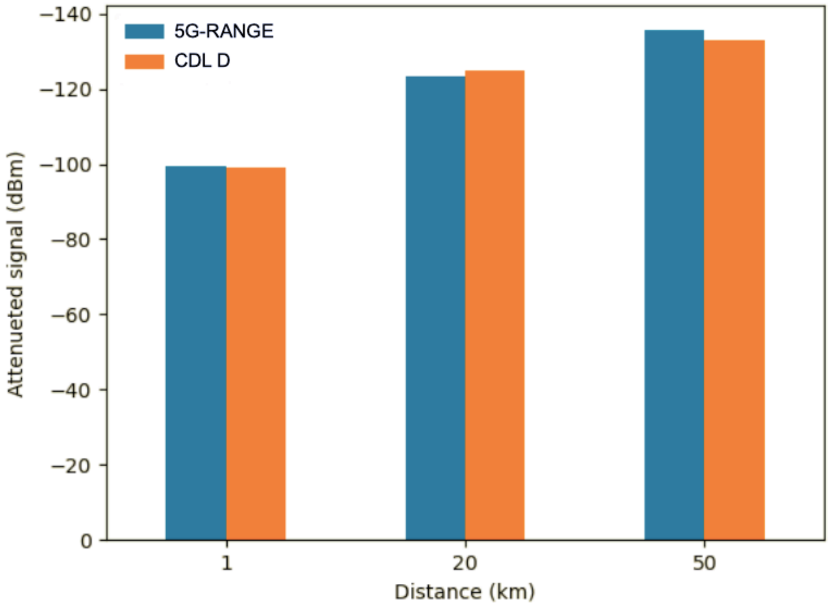

Figure 9. CDL D NS-3/LENA port validation

2.1.4 MAC Layer Implementation

The first part of the implementation of the 5G-RANGE Cognitive Cycle into the NS-3/LENA required the adaptation and inclusion of specific functionalities into the multiple classes available of the NS-3/LTE implementation, as was described in D4.4. The 5G-RANGE project proposes a licensed control channel and a TVWS 24 MHz bandwidth divided into 3 x 8 MHz (Europe) or 4 x 6 MHz (Brazil) data channels. To follow the specification of the 5G-Range system, it was necessary to implement a separated control channel in the NS-3/LENA as was described in the preliminary results in D4.4. D4.3 also described the Cognitive Cycle specification for the 5G-RANGE system, with the 5G-RANGE MAC and PHY layers integrated with the 3GPP standard procedures.

After the developments presented in D4.3 and D4.4, some changes were required to include the Fusion Algorithm with the 5G-COSORA module, and the Spectrum Allocation function with the 5G-DARA module. Considering the use of standard Channel State Information (CSI) procedure for Spectrum Sensing (SS) report management, the change in NS-3/LENA is the use of the DCI (Download Control Information) for SS report request and unique client identifier (UCI) for SS report transmission, with addition of a new format for both control channels. Figure 10 shows a conceptual view of the functionalities implemented in the MAC Layer of the NS-3 simulator. The PU broadcast is sensed by the UEs, which report the PU presence on the channel, using the control channel, and with this information, after the fusion procedure, the gNodeB prevent the scheduling of transmission on the channels identified as occupied.

To better understand the internal procedures on the UE and the gNodeB, Figure 11 and Figure 12 illustrate the logic flow implemented in the LENA/NS-3 modules to include the functionalities for spectrum sensing and opportunistic access. It is important to highlight that an important improvement was introduced on both flows, to optimize the control channel and include functionalities to lead with attackers in the cell, that may send malicious information about spectrum usage. The details of those improvement are presented in detail in Section 2.1.4.1.24

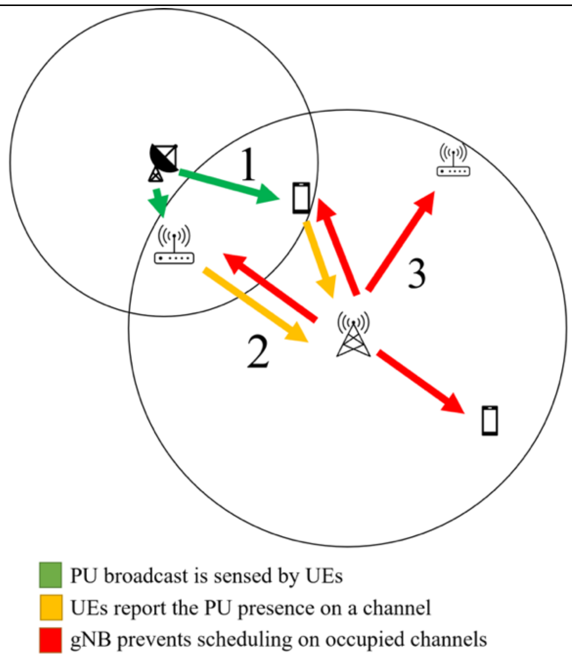

Figure 10. Implemented Functionalities for Spectrum Sensing in NS-3/LENA

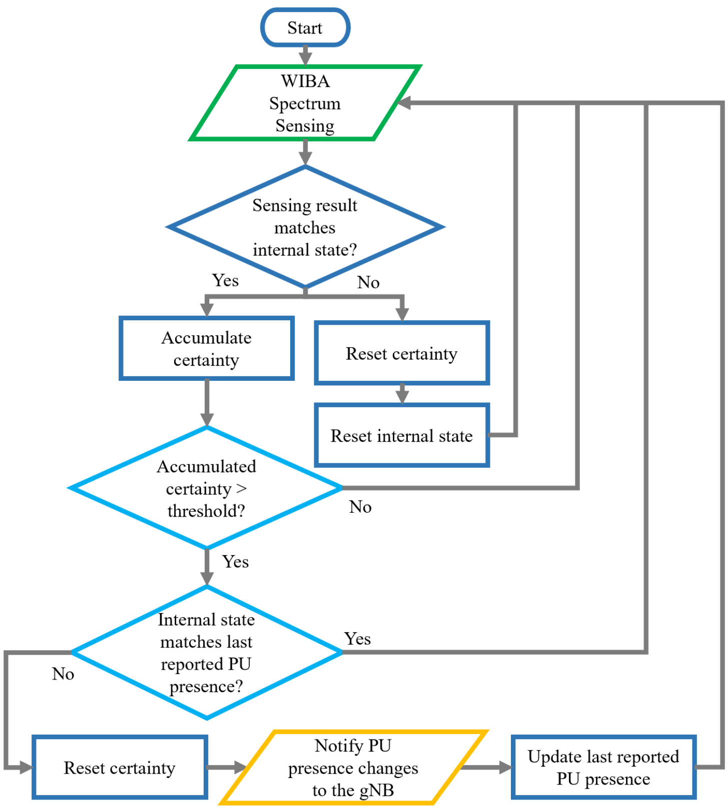

Figure 11. Logic Flow of the internal UE procedure implemented in NS-3/LENA

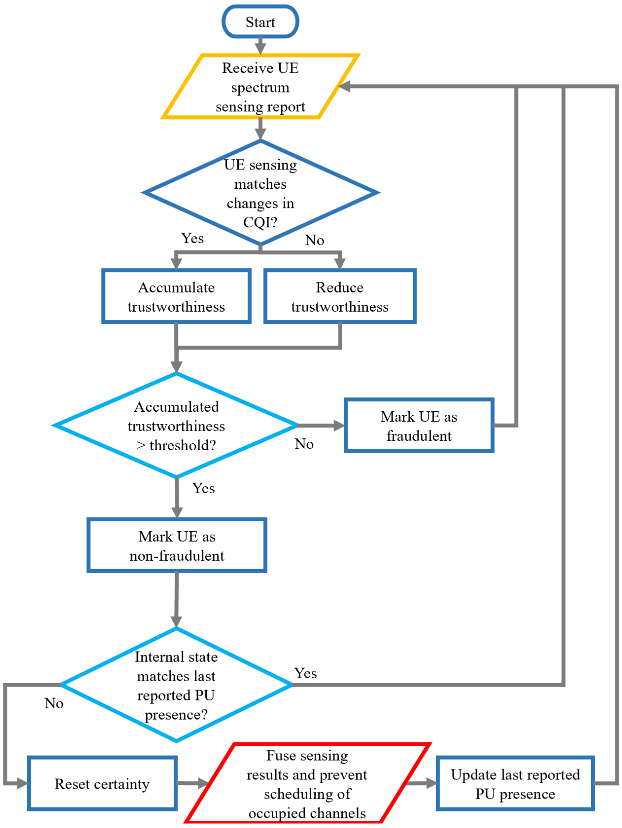

Figure 12. Logic Flow of the internal gNodeB procedure implemented in NS-3/LENA

NS-3/LENA includes the MAC scheduler that works with MCS module to determine the TB bit capacity for user data transmission and provides the TB to the PHY, to the Channel Model for TB transmission and reception simulation. It implements the RA (Resource Allocation) Type 0 grouping the use data bits in Resource Block Groups (RBG) of different sizes determining frequency domain resource allocation. The MAC TB implementation provided by the simulator is simplified with respect to the 3GPP specification, with the class `PacketBurst` used to aggregate MAC Service Data Unit (SDU).

The 5G-SCHED includes the MAC scheduler adapted for Cognitive Cycle Spectrum Allocation function and Resource Allocation (RA). Considering the use of aggregated TVWS (TV White Space) channels of maximum bandwidth size of 24 MHz, with 6 MHz for each TV channel, this implementation was also implemented and changes included the `LteSpectrumPhy` class to check the DCI for unused RBs, `LteSpectrumPhy::StartRX` to allow the forwarding to a sensing function `Sense`, the `LteSpectrumPhy::StartRxDlCtrl` function was also modified to allow the reception of control messages with sensing results. With this arrangement, the LteSpectrumPhy implements the channel sensing function `Sense`, which performs the individual sensing of the station. For this, the channel sensing algorithm uses the SINR parameters and a primary user detection probability curve, generated externally in MATLAB.

The implemented sensing algorithm `sensingProcedure`, checks the SINR ratio of each of the RBGs, or the relationship between the average SINR of the RBGs, and estimates the chances of a PU being transmitted based on the probability curve. The class `LteEnbPhy` was modified to forward sensing messages to the MAC layer of the associated gNodeB. Also, a function was added to the MAC layer of the UE module to assemble the control message with sensing results `SendCognitiveMessage`. Several functions were added to the MAC layer of the gNodeB to process sensing messages from different stations: `ReceiveCognitiveMessage` and to merge the results `mergeSensingReports`. Likewise, the LTE `DoSubframeIndication` function has been modified to implement the merging of results before executing resource scheduling. Still in the MAC layer of gNodeB, the schedulers `DoSchedDlTriggerReq` function now receives an additional parameter, containing a bitmap informing busy RBGs, preventing their use by the scheduler.

2.1.4.1 Other Improvements in the Collaborative Sensing Model: Performance and Security

Based on the results presented in D4.4 regarding sensing procedure in the MAC Layer, we developed two techniques to increase CSS performance and resilience to attackers. Considering CSS, a challenging issue is security, since CSS relies on information provided by third parties (UEs) and normally, there is not a precise procedure verify this information, which may lead to what is known as the Byzantine general problem. Malicious nodes may send false sensing data to the FC, increasing the probability of wrong results that lead to poor network performance or even unavailability.

A novel approach developed for the MAC layer in COLAB-5 [22] aims to improve performance and reduce the reporting overhead along with Byzantine attack mitigation. This approach is based in Markov-chains to improve the collaborative sensing fusion accuracy, while optimizing reporting overhead and increasing resilience against attackers, using a hard-combining fusion technique.

The Markov chain model is used in both techniques to aggregate the UEs individual sensing results, assuming that multiple individual sensing procedures are executed for each PU transmission. The Markov chain transition states with probability *P* for each consecutive value, while different values lead to state transitions with probability *1-P*. After at least *N* consecutive results, the Markov chain reaches a final state *S*. The first technique filters noise of the hard-combining individual SS using the Markov-chain, reducing unnecessary reporting and saving CCC bandwidth. The second technique filters less relevant reports from the CSS fusion, using a Markov-chain and the harmonic mean, to improve the resilience against attacks.

Figure 13 shows the flowchart of the first technique. For each execution cycle, if the result of the current sensing *R_sense* is equivalent to that of the past *R_prev*, the uncertainty of identical events accumulates consecutively *P_accum*. The results of the sensing are binary and the accumulation of probability is done in jumps of 1-*P_acum*/2. When this uncertainty *P_accum* reaches a certain threshold, for example 90 %, it is assumed that the sensing result *R_ sense* is correct and thus, the value to be reported is stored in *R_markov* . If the threshold P*_accum* has not been exceeded, the UE does not report the result of the current sensing, and the gNodeB assumes that the result reported in the past remains valid.

The second technique uses Markov chain-based mechanism like in the first technique, which is used to discard reports from UEs that are less relevant to fusion. The filtering policy is based on the Harmonic mean of the CQI reported by the UE, as illustrated in Figure 14. The first check in Figure 14 halves the relevance *relev* of UEs that are either far from the PU or approximating to the eNodeB, since they are considered to be potential attackers. The second check increases the relevance *relev* of UE that reported no PU presence and have a stable CQI.

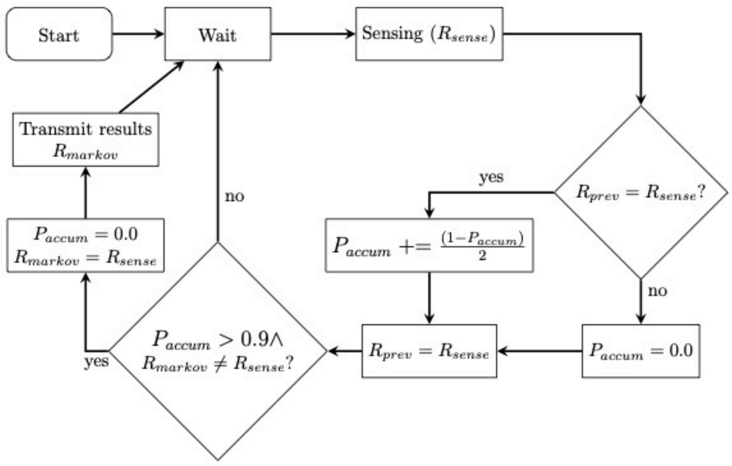

Figure 13. Individual Sensing using Markov Chains.

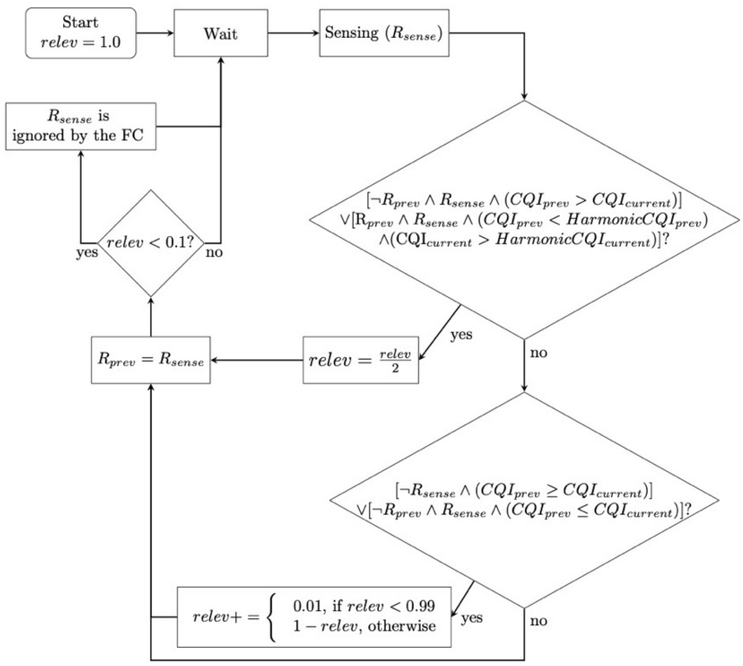

Figure 14. Individual Sensing using Markov Chains and Harmonic Mean

2.1.4.2 MAC Layer Verification

This section provides the results to demonstrate that the implementation of the MAC Layer described in the previous sections works properly and show accurate results. To evaluate the MAC Layer implementation, we performed a simulation in a remote area using a 50km radius cell. The simulation parameters are listed in the Table 2. The SS probability of detection probability used is based on the link-layer results of the WIBA [21], also from the 5G-RANGE scenarios, shown in Figure 15.
The PUs are distributed randomly throughout the cell and different numbers of UEs are distributed either the same or into randomly placed clusters of 5 km radius. The randomly distributed scenario may be unrealistic for such a large cell, but provides the best-case scenario for most fusion techniques, as it provides more diverse data. The clustered scenario is more realistic and represents micro-regions, such as small villages. Examples of both simulated scenarios are shown in Figure 16 and Figure 17, respectively.

Considering *SF* as the number of simulated subframes *SF_active* and *SF_inactive* as the number of subframes the PU transmitted or not, *FP* and *FN* as the number of fusions indicating the PU presence when it was not transmitting, or the inverse. In the simulation, three performance metrics are used to evaluate the techniques:

a) false positive ratio *P_fp=FP/SF_inactive*
b) false negative ratio P*_fn=FN/SF_active*
c) fusion accuracy *Acc=SF-FN-FP/SF*.

Table 2. Simulation parameters for 5G-Range MAC Layer verification.

	Scenario / Simulation parameters	Markov and Harmonic technique evaluation
General	Simulation time	10 s (10^4 subframes)
	Propagation model	5G-RANGE
	Band	5 ($\sim$ 850 MHz)
	Number of channels	4
	Channel bandwidth	3x5.2 MHz + 1x4.4MHz
	PUs per channel	1
	Noise floor	-174dBm/Hz
PU	Tx power	40 dBm
	Tx period	[1-5] s
	Tx duty cycle	[0.1-0.4]
eNB	Tx power	53 dBm
	Antenna gain	9 dBi
	Fusion techniques	[OR, AND, [2,3]-out-of-n UEs]
UE	Number of UEs	[10, 20, 50, 100]
	Number of attackers	[0, 1, 2, 5, 10]
	Tx power	23 dBm
	Antenna gain	9 dBi

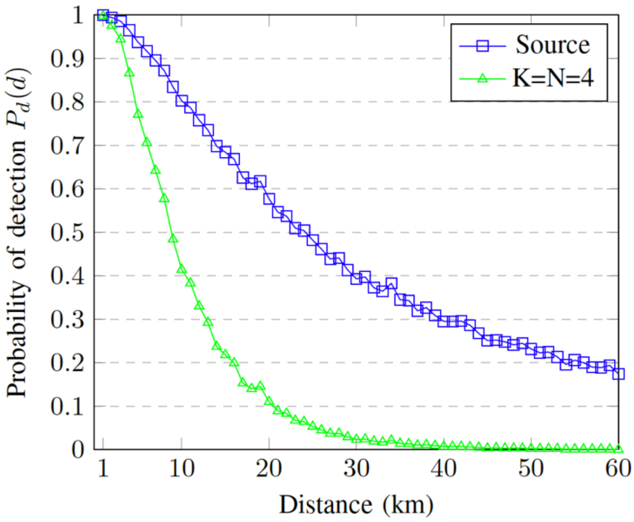

Figure 15. Probability of detection curve based on distance (blue squares)

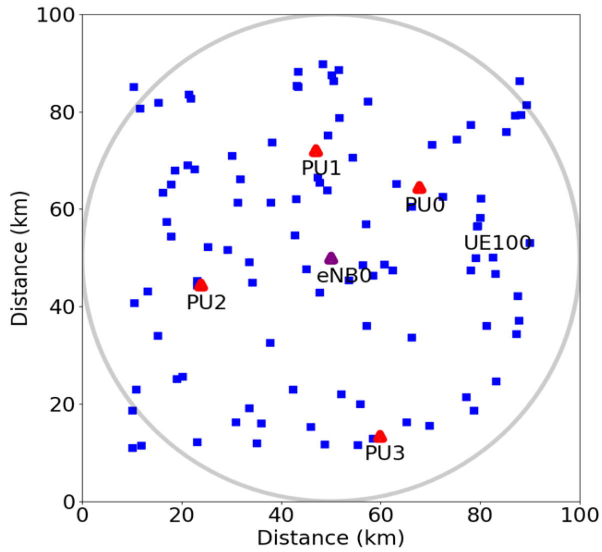

Figure 16. Randomly distributed scenario, 50km cell

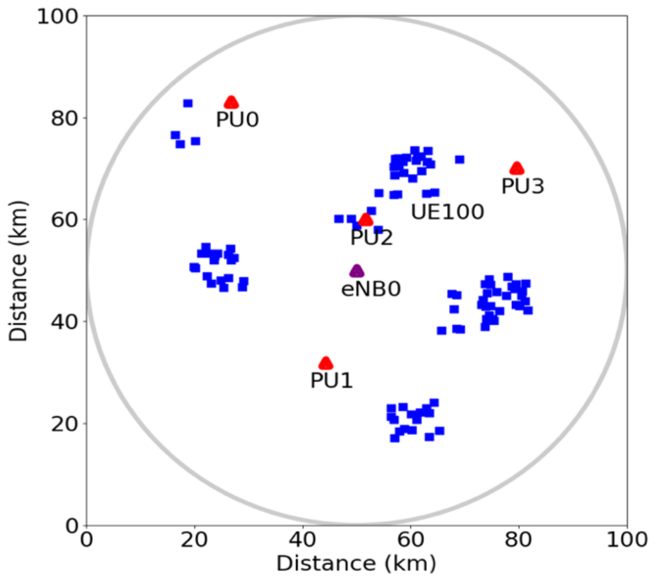

Figure 17. Clustered scenario, 50km cell

Figure 18 shows the compiled results for the same scenarios, where (a) and (b) represent simulations with 0 and 5 attackers, varying UEs within 10, 20, 50 and 100. The results include the standalone fusion, along with its combinations with the Markov-chain techniques. The figures illustrate how the Markov-chain technique reduces false positives while keeping false negatives low (if there is no attacker) and how the harmonic-mean based technique mitigates attacks (behaving as the standard fusion in the scenario without attackers).

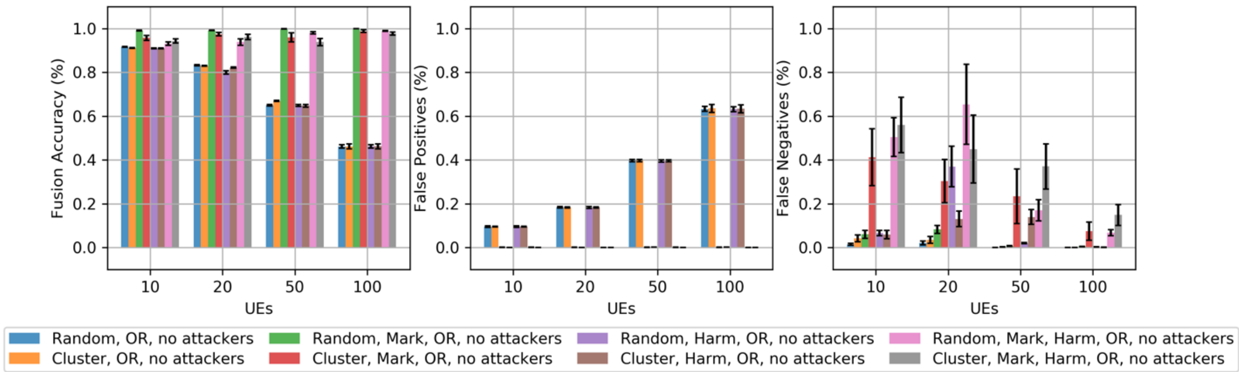

(a)

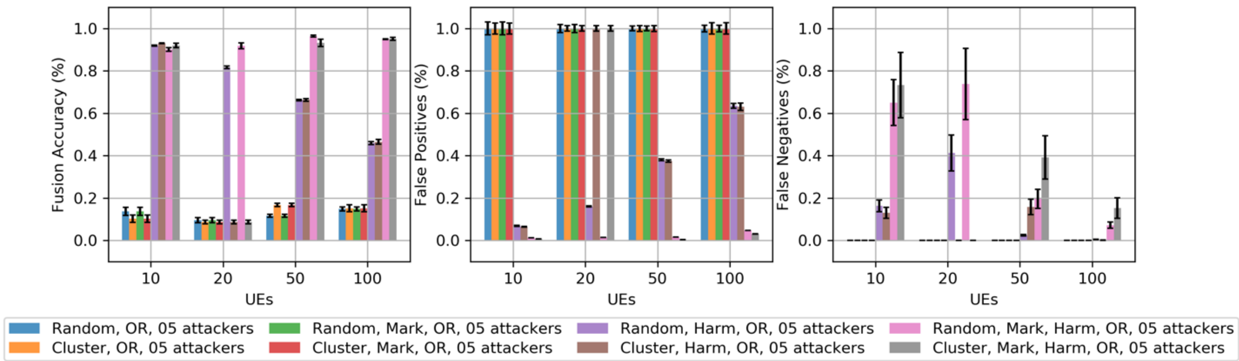

(b)

Figure 18. OR fusion results with different numbers of attackers, on clustered and randomized UEs distributions throughout the cell (Cluster and Random), with and without the Markov technique (Mark), with and without the Harmonic technique (Harm)

The performance for the OR fusion is shown in Figure 19. For the case with 100 UEs, the implementation is able to reduce the false positives to a minimum (from 0.6323 +/- 0.0110 to 0.0008 +/- 0.0002 in the random scenario, 790 times reduction), at the cost of increasing false negatives (from 0.0000+/-0.0000 to 0.0047+/-0.0005, in the random scenario, and to 0.0744+/-0.0419, in the clustered scenario). The large difference in the false negative values of the random and clustered scenarios shows how the number of UEs and their distribution within the cell may influence the results when using the Markov-chain based technique.

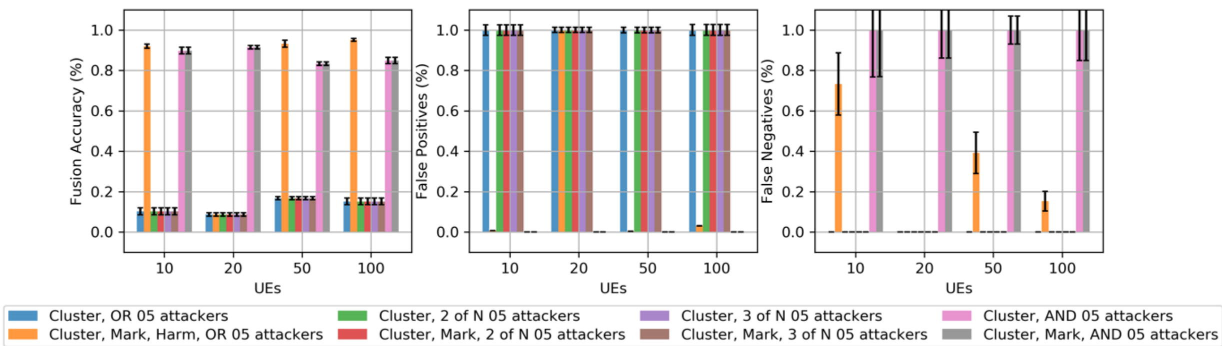

Figure 19. Performance of different fusion techniques, including the combination of the Markov-chain technique in orange.

Another important result is that for all the scenarios, the Markov-based technique effectively reduced the number of reports by 2 orders of magnitude, as shown in Figure 20 which presents the mean percentage of reported frames per UE for all the simulations.

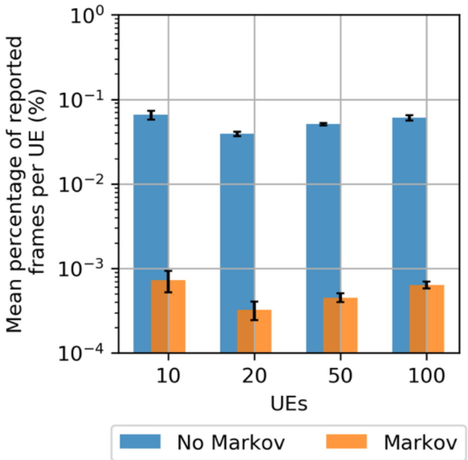

Figure 20. Sensing report overhead with and without the proposed Markov-chain based mechanism

The results show that the MAC Layer implementation behaves as expected in different scenarios and that the results are coherent with the expected theoretical results, therefore it is possible to verify that the 5G-Range MAC Layer implementation was implemented correctly in the NS-3/LENA.

2.1.5 Network Layer

As described in the D4.4 and in the previous sections, the LENA LTE Module in NS-3 modifications implemented all the features regarding the PHY and the MAC Layer for 5G-Range. The aspects regarding SDN/NFV provide mainly the description of 5G network slicing and most of the ongoing work and research regarding testbeds and simulation tools in this area are still limited to standardization activities related to 5G network slicing and open challenges on how SDN, NFV and Cloud computing will integrate 5G and network slicing [16]. In this project, the Network Architecture described in D5.1, D5.2 and D5.3 which includes the VNF (Virtualized Network Function) Environment with the Control and Data Plane specified in the latest 3GPP specification [28], are still not feasible of being implemented in simulation tools in a short to medium period of time. Some ongoing works and projects are approaching this problem with testbeds that are still in testing and developing stage [15][16]. Then, the focus of the simulation tool is to validate the 5G-Range PoC and evaluate the potential performance in the different core scenarios described in D2.1. The impact of NFVs and network slicing cannot be taking in account in this phase of the 5G-Range Project. With this in mind, our approach is to integrate the different applications from the four use-cases in the simulation tool considering an end-to-end IP connection between UEs and the remote host, as shown in Figure 21. Then, the performance evaluation is carried between the UE and the remote host and the different KPIs will be evaluated for each simulation scenario.

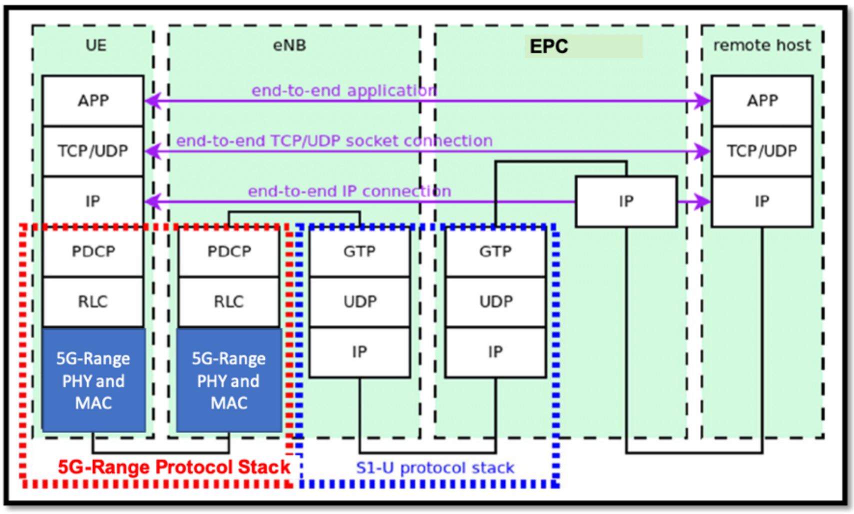

Figure 21. Network Layer for NS-3 Simulation in 5G-Range

2.1.5.1 Traffic Generation for the use-case scenarios

Considering that in an end-to-end application the type of traffic has a relevant impact in QoS metrics, we developed a specific traffic generator tool called EROS-5 (Synthetic Traffic Generator for 5G Networks) [17][18] which allows simulating a variety of applications such as video streaming, VoIP Web and IoT, in 5G network scenarios. EROS-5 is an open source and configurable tool that allows the easy coupling of new mathematical models to generate new types of traffic. The traffic generated is in the form of time series in JSON format, which presents the necessary flexibility to be used by several simulators such as LENA/NS-3. EROS-5 is implemented using Python language and, in this tool, the application traffic as implemented as a temporal time series using statistical modeling as described in Figure 22, where θ is the size of the message, δ is the time between two messages, ϵ is the variation in time between two messages and T is the duration of the load. The first three variables characterize the loads individually while the last two model the behavior between loads. In this sense, the tool does the modeling of θ, δ and ϵ making possible the parametrization of the load duration (T) and leaving the start time open. Normally, in real applications, this last variable is highly dependent on human behavior and the devices.

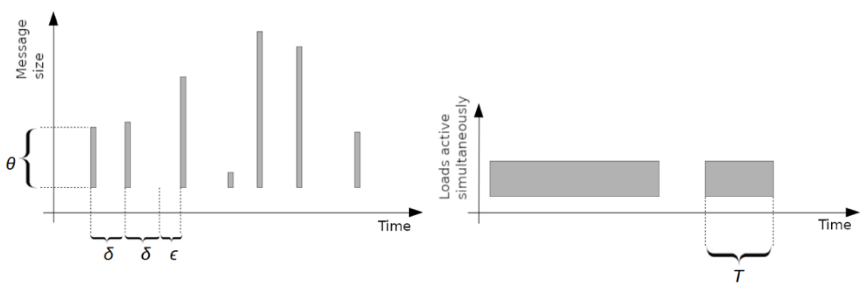

Figure 22. Statistical modelling of traffic for 5G-Range Use Cases

Figure 2 shows the architecture of EROS-5. The class `Ui_Gerador` implements the static graphical interface of the tool that is used by the classes of layout for visualization, generation, and analyses of the loads generated. The output of the load generator is introduced on the analyzer for the extraction of statistical information such as mean, standard deviation, and series parameters. For aggregated traffic, for example, the traffic that is generated from different applications, we use fractal traffic characterized mainly by the Hurst exponent. Some properties can be extracted from this exponent: H ∈ [0.5, 1] means that the series has a long-term dependence and values persist over time, which is mainly used to characterize aggregated traffic and multimedia traffic. The architecture facilitates the integration of other models on EROS-5, which can help in its future evolution. The next sections describe the statistical models used for the generation of VoIP, Video Streaming, Web, and IoT loads, which describe the main applications in the 5G-Range scenarios described previously in D2.1.

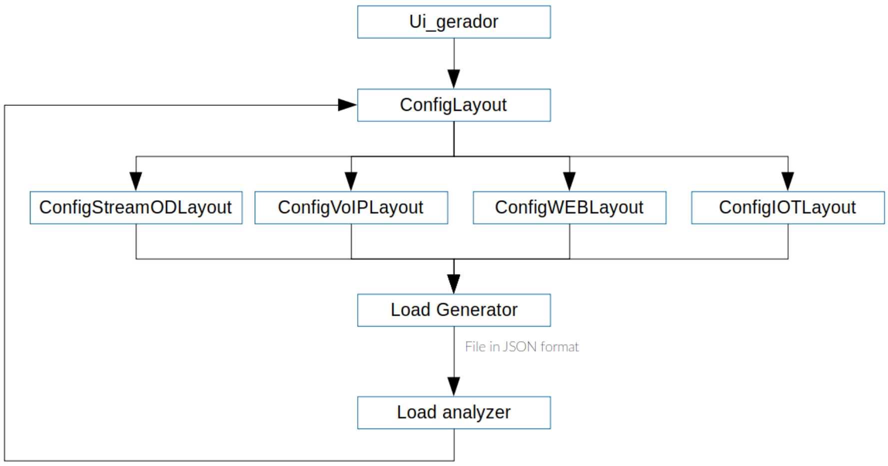

Figure 23. EROS-5 Operating Architecture

VoIP Traffic Generation

VoIP applications are characterized by requiring a small delay and jitter. Voice transmission is done through a sampling process and transmission of an encoded bitstream. On the receiving side, the sequence is decoded, and the voice is reproduced, using different codecs such as ITU G.711, ITU G.729, iSAC (internet Speech Audio Codec), SILK, etc. Each encoder has a message generation rate that can be modeled according to a Gaussian distribution and the size of the messages changes according to the codec used. For example, ITU G.711 and ITU G.729 have fixed sizes while iSAC and SILK have variable sizes. The iSAC and SILK encoders use the ARMA (Auto Regressive Moving Average) function, in which the value of the X_t term of a series is influenced by X_{t-k} previous terms, where t refers to the current term. The combination of the AR (Auto Regressive) and MA (Moving Average) models results in Eq. (2, where X represents the terms of the series, c is a constant, ψ represents white noise, φ_i are parameters of the AR model, β_i are parameters of the MA model. The value of ψ is the result of a Gaussian distribution with a mean of 0 and a known standard deviation. The parameters taken from [29]79 for modeling the variable message size of iSAC and SILK and ARMA are shown in Table 1.

$$X_t = c + \psi_t + \sum_{i=1}^{p} \varphi_i X_{t-i} + \sum_{i=1}^{q} \beta_i \psi_{t-i} \qquad \textbf{(2)}$$

Table 3. ARMA function parameters

	φ1	φ2	β1	ψσ	c
iSAC	1,117	-0,190	-0,631	22	159
SILK	1,281	-0,332	-0,600	22	159

Video Streaming over-demand

In this type of applications, normally are used techniques of adaptation to the available band during the transmission of segments. The principle behind band adaptation methods is based on dividing long videos into smaller segments and the prior storage of these on the client side. Several versions with different encoding rates are generated, making it possible to choose the correct version according to the network conditions. In addition, the distribution of content over the network (CDN) is a factor strongly present in video provider systems. The model used for generating video streaming on demand is very similar to the ON-OFF model in which during the ON state the segment is transmitted while in the OFF state nothing is transmitted. The sum of the times in which the transmitter performs a complete cycle represents the time between two requests, that is, $T_{IR}=T_{ON}+T_{OFF}$. The idea presented is based on the fact that, given a segment of τ seconds in duration, the time for transmission of this must be less than or equal to the time of the segment, that is, $T_{ON} < \tau$, otherwise the reproduction will find pauses. Having the distribution that models the time between two requests (TIR), it is possible to build a series with characteristics similar to the application. The message size can be obtained by multiplying $T_{ON} * c$ where c is the average encoding rate of the video. Using tools such as dash.js and TAPAS [19], is possible that the Burr12 and t-*Student* distributions correctly model T_{ON} and T_{IR}, using the parameters in Table 4, but to ensure the correct autocorrelation it is necessary to use a Z transform.

Table 4. Parameters for TON and TIR

	$T_{ON}(Burr12)$	$T_{IR}(t - Student)$
Dash.js	α = 1,469; k = 1,915; c = 3,014	μ = 1, 938; σ = 0, 245; ν = 2,086
TAPAS	α = 1,033; k = 1,451; c = 2,671	μ = 1,953; σ = 0,001; ν = 0,402

Web traffic generation

A WEB page is made up of one or more main and secondary objects. The HTTP protocol is predominant and when obtaining a page, a user usually takes time to interpret its content. The ON-OFF model can be used to describe the behavior of users on the Web. In the ON state the user is receiving files from the server, while in the OFF state the user is passive, and no files are received T_{OFF}. In this way, the model that takes into account the size and number of primary and secondary objects in addition to the time between objects and T_{OFF}. Recent studies show that the size and number of objects has changed considerably due to the insertion of dynamic content and the addition in the number of images, much due to the incremental access to social networks like Facebook and Instagram. Table 5 list some of the distributions that best fit to model a series that represents a user's behavior.

IoT traffic generation

The operation of IoT devices differs from the traditional communication standard in that they are designed to operate in low power mode, extending the operating time to months or even years. The flow of information occurs mainly in the direction of the uplink and the sinks aggregate messages, which produces an information generation pattern that can be divided into two categories: synchronous and asynchronous. The asynchronous category can be divided into periodic and non-periodic and it is observed that these applications have a characteristic periodicity and average message size. Using this approach, the model used is focused on generating asynchronous and periodic messages, according to the initial transmission time t_i of the *i-th* device that can be modeled according to a uniform distribution$T_i \sim U(0, T)$, where T represents the period. With the number of devices, the size of the messages and the transmission frequency, traffic with characteristics of IoT applications can be obtained.

Table 5. Distributions to model Web user behavior

	Distribution
Size of main objects	Weibull $\lambda = 28242{,}8$; $k = 0{,}814944$
Number of main objects	Lognormal $\mu = 0{,}473844$; $\sigma = 0{,}688471$
Time between two secondary objects	Gama $k = 0{,}16$; $\theta = 5{,}375$
Size of secondary objects	Lognormal $\mu = 9{,}17979$; $\sigma = 1{,}24646$
Number of secondary objects	Exponential $\mu = 31{,}9291$
T_{OFF}	Lognormal $\mu = -0{,}495204$; $\sigma = 2{,}7731$

3 PoC Performance Evaluation and Verification

This section is divided in two parts. The first part shows the Phy Performance evaluation that was performed in laboratory environment. The second part shows the comparison of results of the PHY performance evaluation with the results produced by the COLAB-5 when simulation the PoC scenario.

3.1 Phy Performance Evaluation

This section presents 5G-RANGE's prototype performance evaluation in laboratory environment, considering different technical aspects related to the PHY layer. The parameters analyzed in this section are:

- BER and BLER for different channel conditions;
- OOBE (Out-of-Band Emissions) before and after the power amplifier and with the Digital Pre-distortion (DPD);
- maximum throughput;
- communication reliability;
- Probability of detection and false alarm for the spectrum sensing;
- Spectrum sensing sensibility and;
- Time to clear the channel after incumbent detection.

3.1.1 BER and BLER performance

This subsection presents the BER and BLER performance for the implemented 5G-RANGE's prototype in laboratory environment. A real-time channel emulator that mimics the effects introduced in the communication chain has been developed and implemented in the PoC. With this methodology, it was possible to submit the transceiver to specific and known channel conditions. The main challenge here was the high demand for processing power, since the channel emulator must operate at the same sampling frequency of the transceiver's output.
The channels selected for this analysis are: AWGN (Additive White Gaussian Noise) and selective fading channel based on CDL-D (Clustered Delay Line with Rician distribution) profile.
Figure 1 shows the setup considered for the transceiver performance evaluation. The transmission data pattern is a PRBS (pseudo-random bit sequence), which is known on the receive side. The benchmarks for this performance evaluation are the results obtained from a PHY simulator implemented in Matlab, which can be seen as the result assuming perfect implementation and no effects from the RF front end.

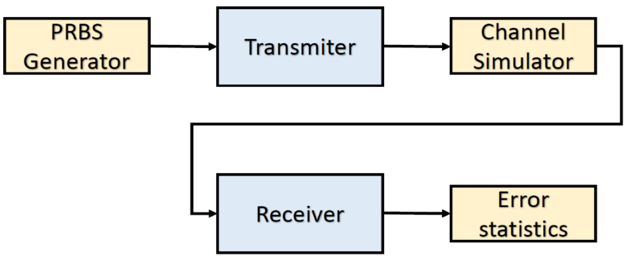

Figure 24. Block diagram for BER and BER performance evaluation.

Numerologies 1 and 3 [1] are have been chosen for the performance evaluation, since these configurations are likely to be employed in the demonstrations. Numerology 1 is interesting for Voice and Data Connectivity and Wireless Backhauling use cases, while numerology 3 is suitable for the Smart Farm use case.
The performance evaluation also considers different MCS (Modulation Coding Scheme), which allows the analysis of several modulation orders, coding rates, and, consequently, distinguished spectral efficiency. The selected MCS values and their respective modulations are MCS 04 (QPSK), MCS 12 (16-QAM), MCS 20 (64-QAM) and MCS 25 (256-QAM).

Figure 25 and Figure 26 show the 5G-RANGE's prototype BER performance evaluation over AWGN channel for SISO (single-input single-output) and MIMO (multiple-input multiple-output) schemes. For each case, both numerologies have been considered with several MCSs.

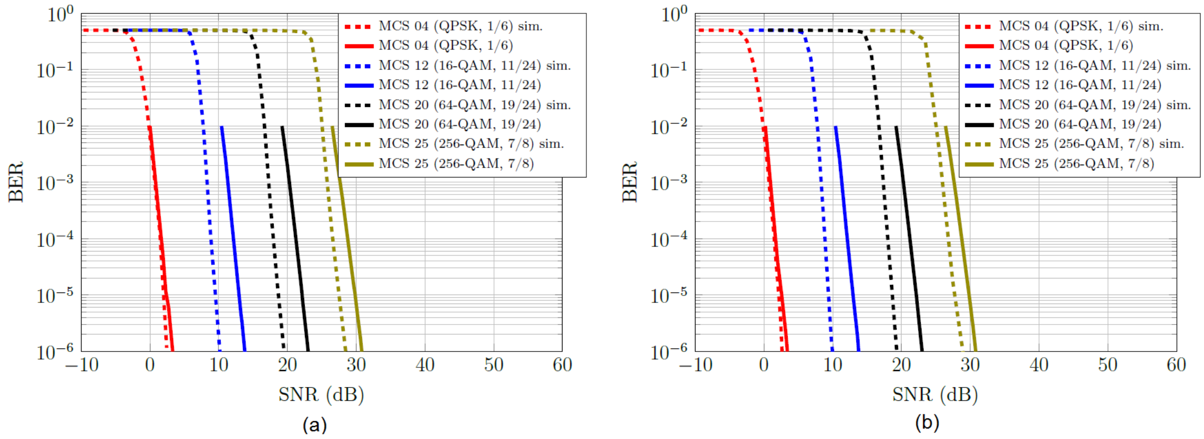

Figure 25. BER - SISO over AWGN channel for numerologies 1 (a) and 3 (b).

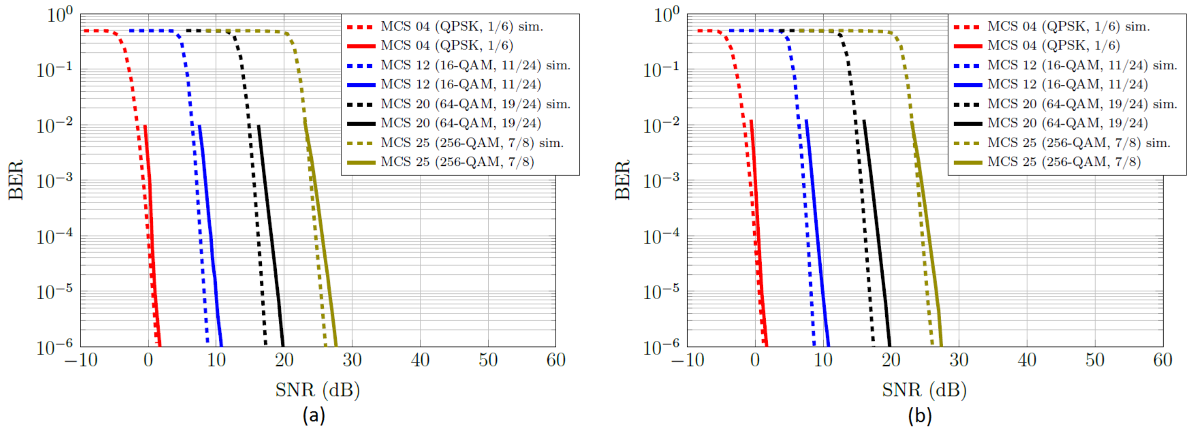

Figure 26. BER - MIMO over AWGN channel for numerologies 1 (a) and 3 (b).

Figure 27 and Figure 28 shows the BER performance over CDL-D channel defined in ETSI TR 138 900 Release 14 [24], assuming SISO and MIMO schemes, respectively. Once again, several MCS were considered for numerologies 1 and 3. The behavior of the curves in this condition are similar to the ones observed in the AWGN channel.

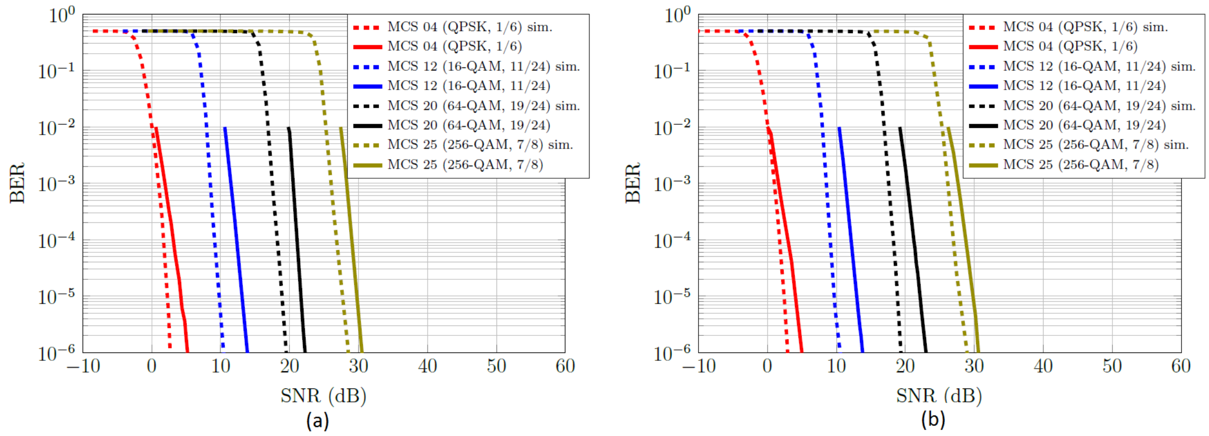

Figure 27. BER - SISO mode and CDL-D based channel for numerologies 1 (a) and 3 (b).

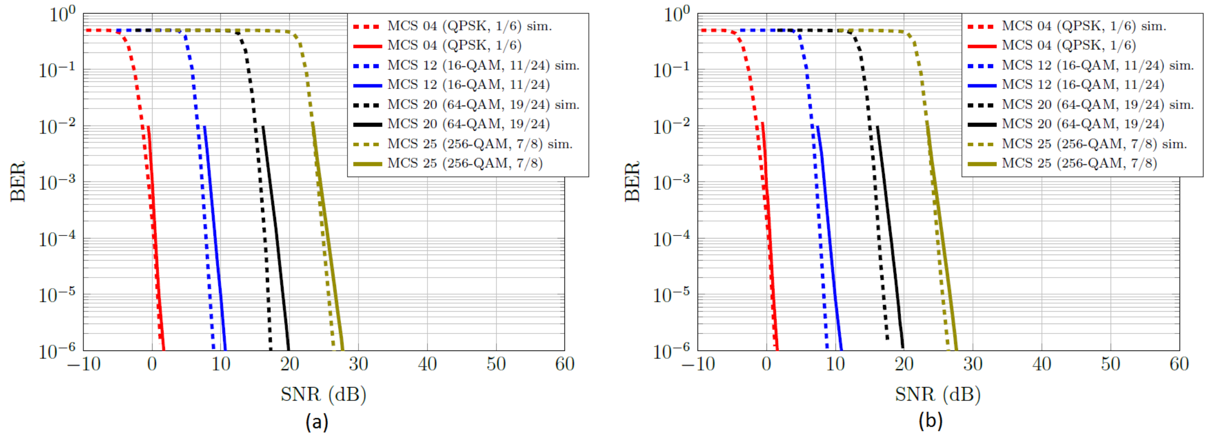

Figure 28. BER - MIMO mode and CDL-D based channel for numerologies 1 (a) and 3 (b).

Figure 29 and Figure 30 shows the BLER performance over AWGN channel, also for SISO and MIMO schemes, respectively, with several MCSs and for numerologies 1 and 3. Figure 31 and Figure 32 presents the same analysis for the CDL-D channel.

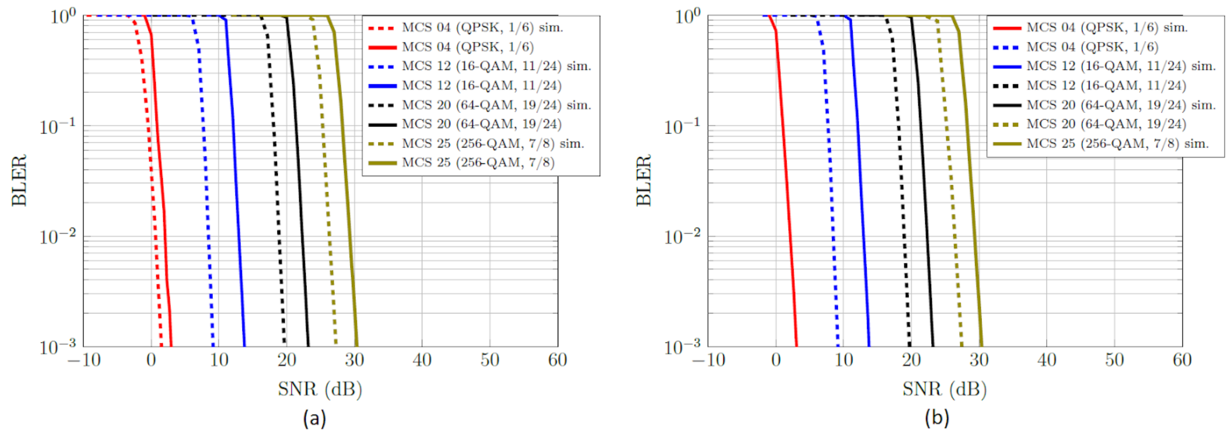

Figure 29. BLER - SISO mode and AWGN channel for numerologies 1 (a) and 3 (b).

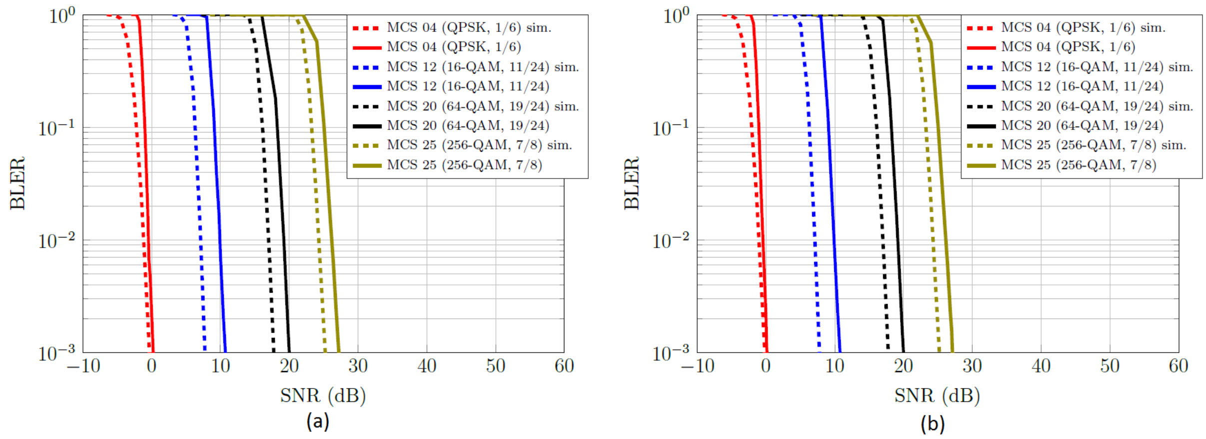

Figure 30. BLER - MIMO mode and AWGN channel for numerologies 1 (a) and 3 (b).

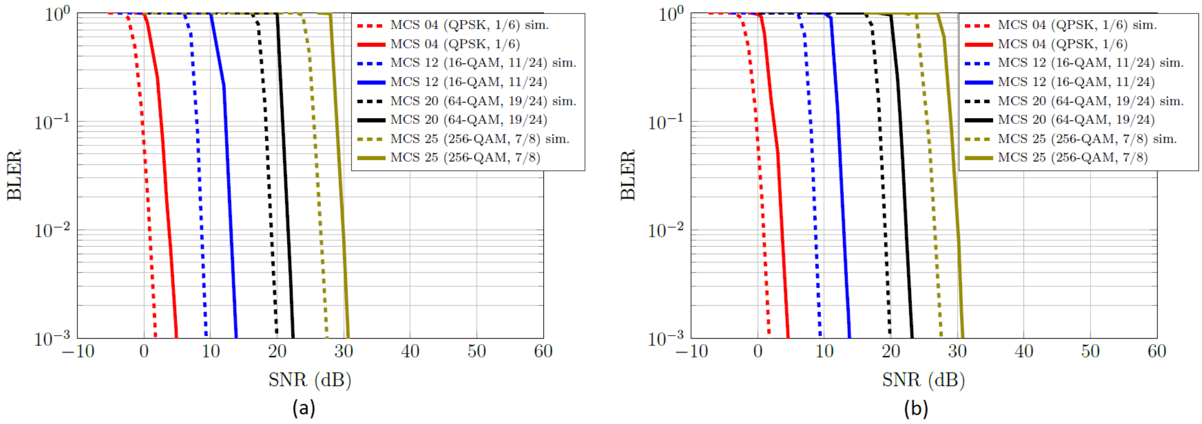

Figure 31. BLER - SISO mode and CDL-D based channel for numerologies 1 (a) and 3 (b).

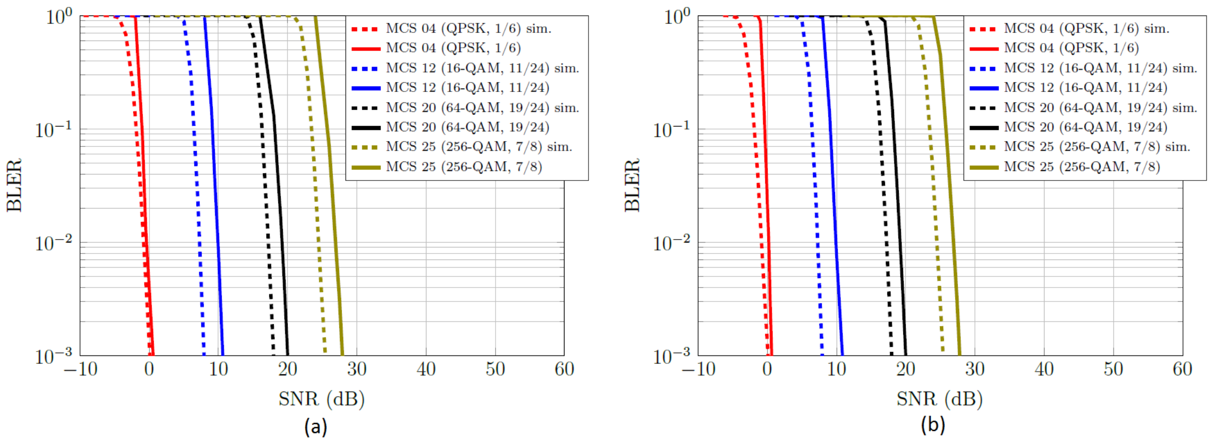

Figure 32. BLER - MIMO mode and CDL-D based channel for numerologies 1(a) and 3 (b).

The results presented in this section show that the loss due to implementation is manageable. The worst SNR (signal to noise ratio) gap is below 3 dB for a BER = 10^{-6} or BLER= 10^{-3} for SISO. It is also interesting to observe that MIMO performs better than SISO, i.e., the gap is smaller for the MIMO case. This can be explained by the diversity introduced by the multiple antennas. Since there are up to four versions of the transmitted signal at the receive side, it is unlikely that impairments introduced by the RF front end will simultaneously impact all signals. Hence, the signal with better overall conditions will bring the BER performance closer to the one observed in the simulations. One can conclude that the impairments introduced by the RF front end do not severely affect the overall system performance, meaning that the frequency and time synchronization, non-linearities of the up and down converters, ADC (Analog to Digital Converter), DAC (Digital to Analog Converter), and channel estimation are working properly. These results corroborate that the design of the IR2A (Inner Receiver for Remote Areas) algorithms can overcome the challenges imposed by the real-world operation.

Another interesting conclusion can be obtained by comparing the results obtained for the AWGN and CDL-D channels. Although the CDL-D channel is a frequency-selective time-varying channel, the BER and BLER performance is similar to the one observed for the AWGN channel. These results show that the 5G-RANGE PHY layer can mitigate the effects of the multipath channel due to the long CP (cyclic prefix) employed by the waveform and high error correction capability of the Pola Code. For the MIMO case, the performance is improved because of the diversity obtained from the two transmit and two receive antennas, which increases the robustness of the system against the doubly dispersive channel and impairments of the RF front end.

3.1.2 Digital Pre-Distortion and Out-of-Band Emissions

The power amplifier is an important element of an RF communication system. The power gain provided by this device is essential to achieve long-range coverage in remote areas. There are different classes of power amplifiers and the most energy efficient architectures introduces high level of non-linearities. This non-linear behavior, without mitigation, causes unwanted interference outside and inside of the occupied band. Interference outside the occupied band, or OOBE, degenerates the good spectrum localization of modern waveforms, such as GFDM (Generalized Frequency Division Multiplexing) and F-OFDM (Filtered Orthogonal Frequency Division Multiplexing). Besides the OOBE, nonlinearities also affect the transmitted signal, reducing the BER and BLER performance. Consequently, it reduces the system throughput and efficiency. The DPD (Digital Pre-Distortion) algorithm is used to compensate the influence of the nonlinear behavior of the power amplifier by pre-distorting the signal before the amplification. Basically, the DPD applies the reciprocal response of the amplifier to the signal's amplitude samples, hence, when the signal is amplified, the combined response of the DPD and the amplifier is linearized within a given dynamic range. In [25], the authors propose a technique where a RF sample of the amplified signal is used to obtain a lookup table that performs the DPD function in the baseband signal. The DPD coefficients can be constantly updated or they can be stored in a ROM (read-only memory) after the system calibration. The former is a more complex and dynamic solution that does not require maintenance for adjusting the coefficients over time. The second approach, which has been implemented in the 5G-RANGE PoC, is simpler but it requires manual updates of the DPD coefficient when the nonlinearities of the amplifier change over time. The DPD must cover an overall bandwidth at least three times higher than the signal's bandwidth to assure that the main intermodulation components will be covered. This means that this algorithm cannot be executed in the GPP and must run in the FPGA (Field Programmable Gate Array) of the RF SDR (Software Defined Radio) board. In the 5G-RANGE PoC, the National Instruments USRP-2954R model is employed for both BS (base station) and UE (user equipment). The power amplifier used in the 5G-RANGE transceiver circuit is the EMPOWER model 1211-002, which technical characteristics are shown in Table 6.

Table 6. Power amplifier characteristics.

Parameter	Value
Operation minimum frequency	500 MHz
Operating maximum frequency	2500 MHz
Peak output power	100 W
Gain	60 dB
Noise Figure	15 dB

The performance parameter used to evaluate the DPD technique is the ACLR (Adjacent Channel Leakage-Power Ratio), which is defined as the ratio between the transmitted power and the power measured in an adjacent channel. Hence, the ACLR indicates how much power is transmitted outside the bandwidth of the signal with respect with the power transmitted within the desired bandwidth. A baseline analysis considered the system without the power amplifier. This procedure ensures that the power amplifier input signal is not limiting the DPD performance. All measurements utilized a probe signal with the properties shown in Table 7. The equipment used to perform the measurements is a Keysight MXA N9020A signal analyzer.

Table 7. Transmitted signal properties.

Parameter	Value
Central frequency	545 MHz
Bandwidth	24 MHz
Power	38 dBm
Adjacent channels bandwidth	5.5 MHz
Channel spacing	15 MHz

Figure 33 shows the ACLR measurement for the power amplifier input signal. As observed, ACLR values are -59.5 dBc and -59.7 dBc in the left and right portions of the spectrum, respectively. This result indicates the maximum possible performance in terms of ACLR that the power amplifier can achieve.

The second measurement has been taken at the output of the power amplifier and without DPD and the result is presented in Figure 34. When the transmission power is approximately +38 dBm, the ACLR measurements achieved -38.2 dBc and -40.9 dBc in the left and right portions of the spectrum. These values do not satisfy the requirement presented in D2.1 (-55 dBc for unlicensed operation and -45 dBc for licensed operation). This means that the DPD is necessary to reduce the OOBE.

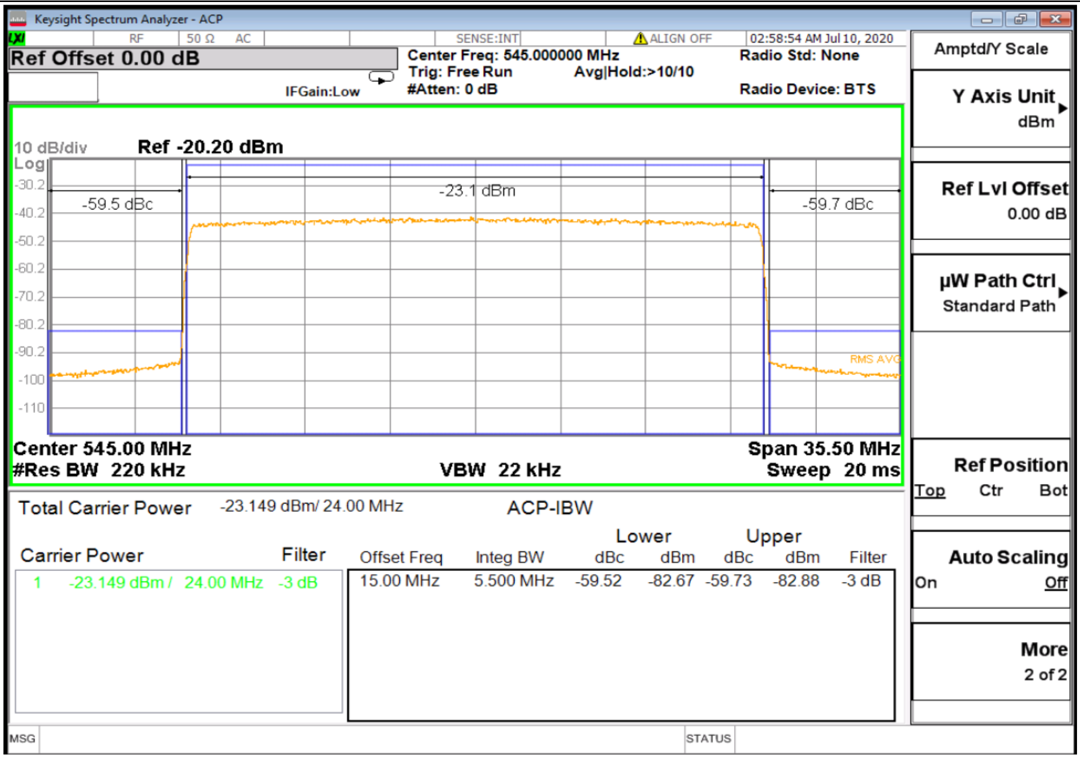

Figure 33. ACLR measurement at the SDR board RF output.

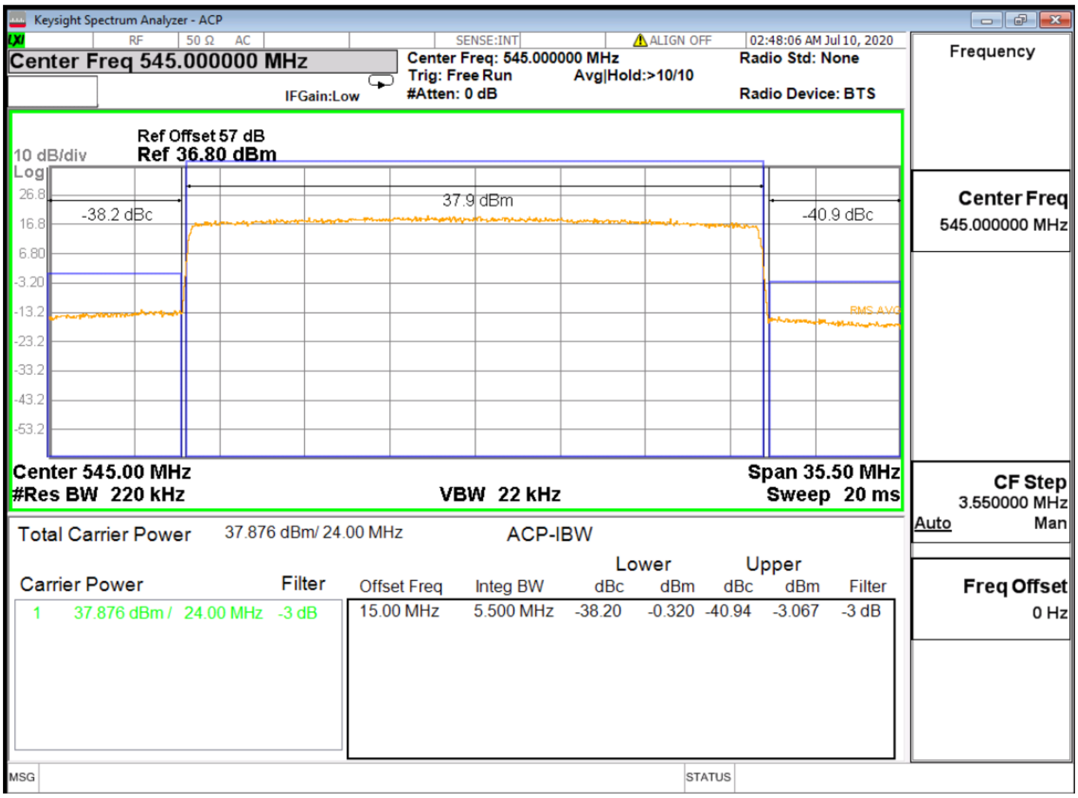

Figure 34. ACLR measurement at the power amplifier's output without DPD.

Figure 35 shows the ACLR measured after the power amplifier with the DPD. The DPD reduced the ACLR from -38.2 dBc to -52.2 dBc on the left side, and from -40.9 dBc to -52.8 dBc on the right side of the spectrum, providing 12 dB of gain for the worst case and 14 dB of gain for the best case. Figure 36 better illustrates the improvement given by the DPD.

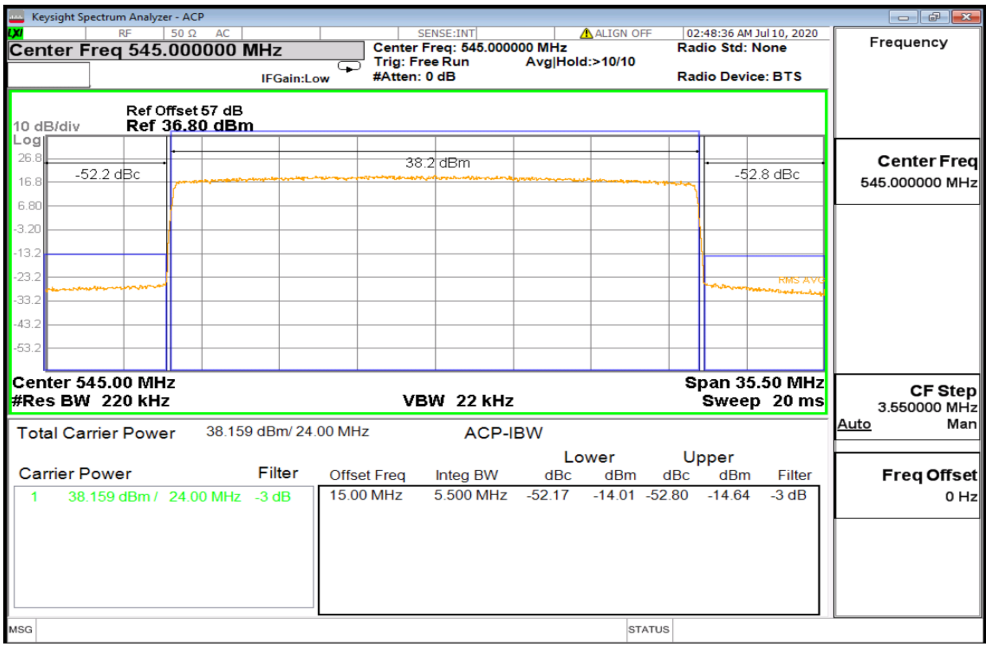

Figure 35. ACLR measurement at the power amplifier's output with DPD.

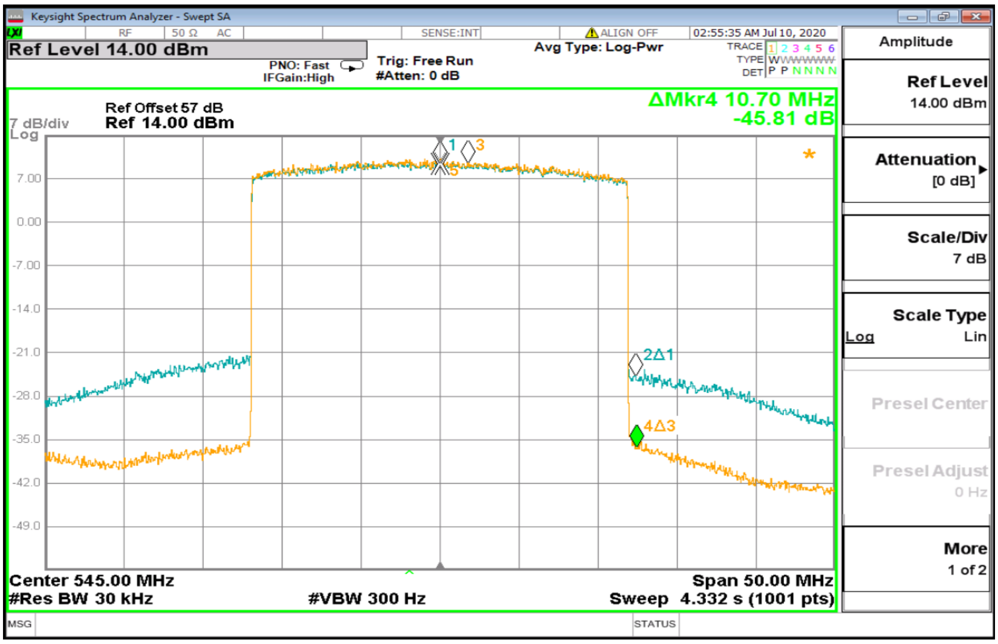

Figure 36. Comparison of the signal's spectrum at the power amplifier's output without (cyan) and with (orange) DPD.

The results presented in this section show that the implemented DPD algorithm is able to reduce the OOBE emissions to levels below the requirement defined for licensed operation. However, refinements are necessary to attend the requirement for TVWS operation. One possible procedure is to implement the self-updating algorithm, allowing the DPD coefficients to be automatically updated. Another interesting approach consists of using AI (artificial intelligence) algorithms [23] that can optimize several parameters simultaneously, i.e., the look-up table, the transmission power and the transistor bias current. Alternatively, a more linear power amplifier with higher back off can be designed to meet the 5G-RANGE requirement for unlicensed channel operation.

3.1.3 System Throughput

The requirement for the 5G-RANGE throughput defined in D2.1 establishes 100 Mbps data rate for a single user at 50 km of from the BS. Initially, the PoC was used to verify this requirement in laboratorial conditions. A channel emulator was used to connect the BS and UE units and the channel model presented in D3.1 was used to evaluate the system performance. The tool iPerf was used to evaluate the overall data rate. This application can measure the maximum achievable throughput using the Internet Protocol (IP) network. Hence, it measures the useful data rate delivered to the final user. Figure 37 shows that the PoC can reach129 Mbps peak throughput. The 5G-RANGE network used 24 MHz for this test. This setup was also used to evaluate the MCS selection and the numerology changes, showing that the system self-configuration is working properly.

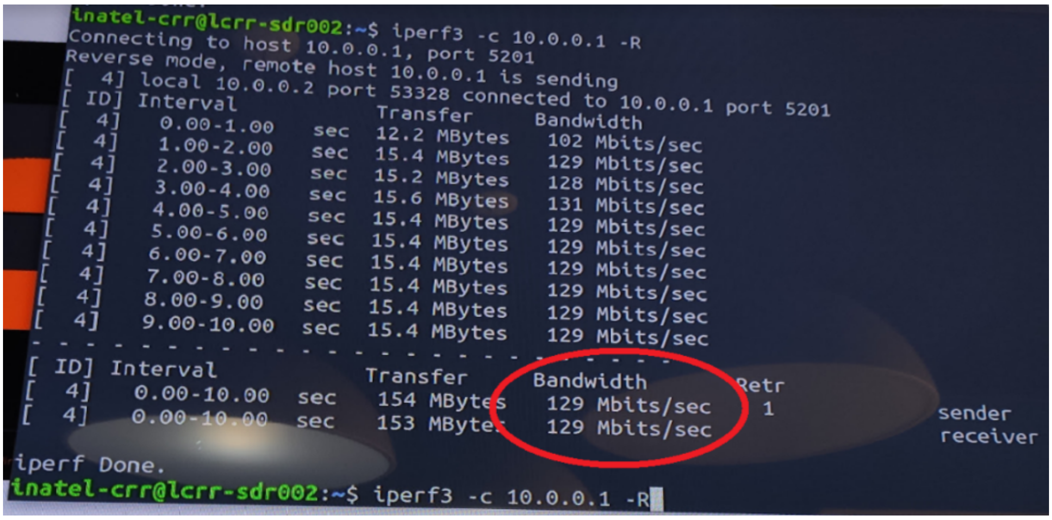

Figure 37. Maximum average throughput achieved by the 5G-RANGE network in laboratorial test.

3.1.4 Access Reliability

The network quality provided by the 5G-RANGE prototype must support, at least, the same level of reliability and latency of other existing communication standards, such as LTE (long Term Evolution). The ping command was used measure the system latency. This application sends packets to the destination equipment and provides statistics accordingly to the packet information responses. This command was used to send packages over the 5G-RANGE network over 24 hours. Figure 38 (top) indicates an estimated number of 86400 packets sent in 24 hours. Figure 38 (bottom) indicates that no packet loss occurred during the test execution ("0% packet loss"). The calculated latency statistics in the network shows an average value of 14.483 ms and a standard deviation of 1.290 ms. These latency scores are acceptable and indicate a good network performance, addressing the requirement of achieving latency compared to the one observed in LTE networks.

```
inatel-crr@lcrr-sdr002: ~
File  Edit  View  Search  Terminal  Help
inatel-crr@lcrr-sdr002:~$ ping 10.0.0.1 -c 86400 -i 1
```

```
64 bytes from 10.0.0.1: icmp_seq=20860 ttl=64 time=15.1 ms
64 bytes from 10.0.0.1: icmp_seq=20861 ttl=64 time=14.9 ms
64 bytes from 10.0.0.1: icmp_seq=20862 ttl=64 time=14.9 ms
64 bytes from 10.0.0.1: icmp_seq=20863 ttl=64 time=14.3 ms
64 bytes from 10.0.0.1: icmp_seq=20864 ttl=64 time=15.1 ms

--- 10.0.0.1 ping statistics ---
86400 packets transmitted, 86400 received, 0% packet loss, time 86491908ms
rtt min/avg/max/mdev = 9.706/14.483/20.459/1.290 ms
inatel-crr@lcrr-sdr002:~$
```

Figure 38. Ping command (top) and the reliability test result (bottom).

3.1.5 Spectrum Sensing

The frequency spectrum is a scarce resource. Therefore, it is essential to optimize its use. The current rules used for spectrum allocation is not flexible and mobile communication services require licenses obtained by auction to operate in a given location. This model is adequate for areas with high population concentration, but it is not adequate for rural areas, where the cost of the spectrum license is prohibitive for local operators and the ROI (return of investment) is not attractive for major MNOs (Mobile Network Operators).

Besides the restriction regarding accessibility of the spectrum, this resource is underused in several remote regions. For instance, most of the frequencies allocated to broadcast TV are idle in the countryside of Brazil. The use of TVWS (TV White Space) through cognitive radio technology has attracted interest in recent years as an alternative to better exploit the vacant spectrum. 5G-RANGE network has been designed to exploit the TVWS as a solution to cover remote and rural areas.

The opportunistic usage of the spectrum demands a strong protection of incumbents. Several mechanisms are used by the cognitive cycle to protect the primary users. 5G-RANGE network employs two complementary approaches to assure that the channels occupied by primary users are not used by the secondary network. The first approach consists of the geolocation data base, where the information about spectrum allocation for a region is provided by the regulatory agency. The second approach consists of the spectrum sensing performed by the 5G-RANGE UEs and reported to the 5G-RANGE BS for fusion and final decision about the availability of the VHF or UHF bands. Since this geolocation data base is not available nowadays, only the spectrum sensing was implemented in the PoC. This section shows the results of a spectral sensing system implemented in the 5G-RANGE transceiver to allow its operation in TVWS.

Figure 39 shows the performance of the spectral sensing technique through the ROC (Receiver Operating Characteristic) curves, that shows the PD (probability of detection) versus the PFA (probability of false alarm) for a specific SNR. The measurements are compared with simulation results for different SNR values. For the calculation of the ROC curve, the used parameter for noise variance is 0.001. This value corresponds to the average variance of a signal at the receiver connected to a 50 ohms impedance load.

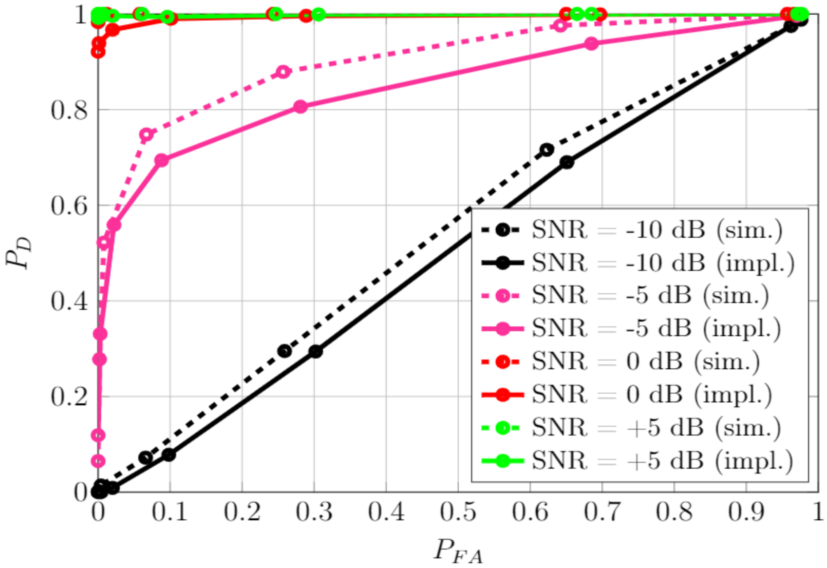

Figure 39. Receiver operating characteristic considering the selected spectral sensing algorithm.

Figure 40 (left) shows the power measurement of an ISDB-Tb Digital TV signal used for spectral sensing tests in the laboratory. Figure 40 (right) shows the signal power measurement at the detection threshold (-88 dBm) for a 5G-RANGE UE. The algorithm used for sensing is the CFD (Cyclostationary Feature Detection), which exploits the OFDM cyclic prefix present in the ISDB-Tb signal.

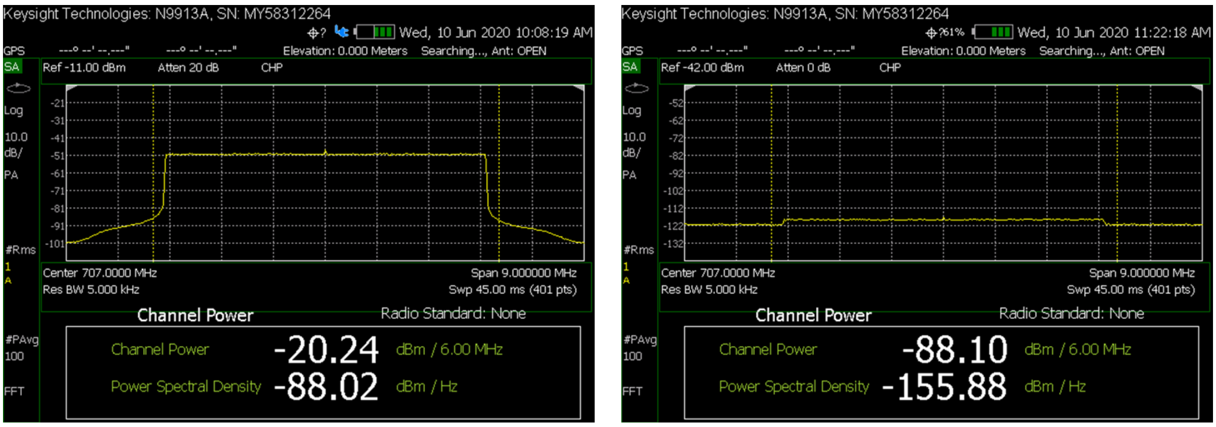

Figure 40. Power level of ISDB-Tb signal (left) and the detection threshold of the implemented spectral sensing algorithm (right).

Figure 41 shows the measurement of the sensing cycle implemented in Python. This test considers the sensing of four consecutive 6 MHz channels, totaling a 24 MHz bandwidth. That is the same band used by 5G-RANGE network to achieve 100 Mbps at 50 km from the BS. The requirement for the sensing cycle is 2 s [27] Hence, the spectrum sensing performed by the 5G-RANGE respects the maximum time limit for the spectrum sensing cycle.

```
------------------------------------------------------------------------------
Sensing cycle measurement (look for DTV signal in four consecutive channels of 6 MHz)
------------------------------------------------------------------------------
Averaged sensing cycle time: 0.7492318892478943 seconds
```

Figure 41. The average cycle time (100 cycles) of spectral sensing in 24 MHz of bandwidth.

The regulatory agencies establish that the spectrum sensing must have PD ≥ 0.9 and PFA ≤ 0.1. Figure 42 shows the performance of a cooperative sensing system implemented in 5G-RANGE where the BS combines the outcome of the spectral sensing performed by the UEs. As can be seen in Figure 42, each user terminal can detect primary signals with a power of up to -88 dBm. Considering the cooperative scheme with n = 5 terminals, signals up to -98 dBm can be detected with the OR fusion algorithm. The spectrum sensing sensibility defined in D2.1 requires the detection of signals with very low power (-114 dBm). From Figure 42, one can conclude that at this power level, the spectrum sensing cannot meet the PD ≥ 0.9 and PFA ≤ 0.1 requirement. One solution for this problem is to increase the measurement time window to collect samples of the signals, improving the correlation properties at the cost of the spectrum sensing cycle time. This is a feasible approach, since the sensing cycle of the current implementation is very short. Another approach consists of implement more advanced spectrum sensing algorithms, such as the WIBA (window based) energy detection. Higher number of UEs making measurements of the channel also improves the spectrum sensing performance.

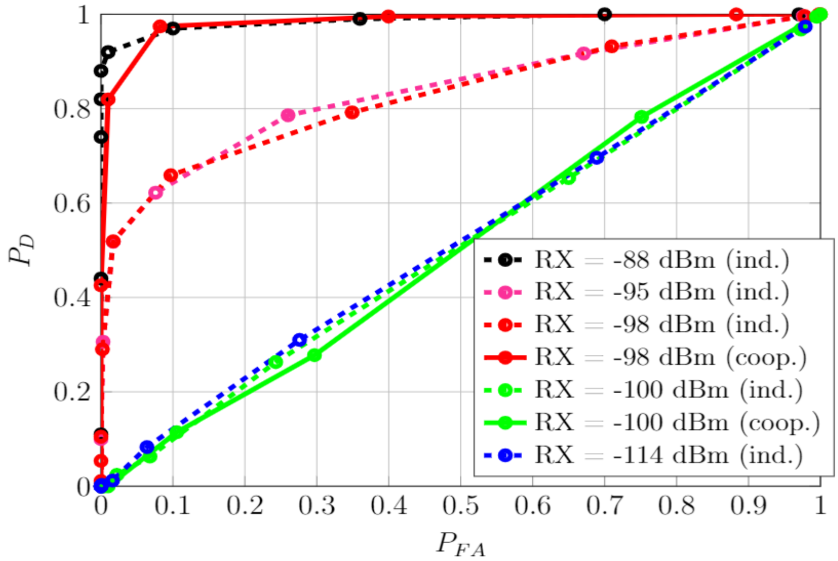

Figure 42. Performance comparison between the spectral sensing for a single UE and cooperative sensing (OR algorithm with n = 5 UEs) for different levels of primary user (PU) signal.

Figure 43 shows the frequency spectrum measurement of 5G-RANGE's downlink. In this scenario, the system detected a TV signal in the third 6 MHz quarter of the 24 MHz bandwidth occupied by the 5G-RANGE network. The 5G-RANGE disabled the subcarriers on the bandwidth occupied by the TV signal and the very low OOBE from the 5G-RANGE waveform does not interfere with the incumbents. These results confirm that the spectral sensing implementation is functional and that the 5G-RANGE network can harmoniously coexist with primary users, although improvements in the spectrum sensing algorithm must be performed to fulfil the requirement defined in D2.1.

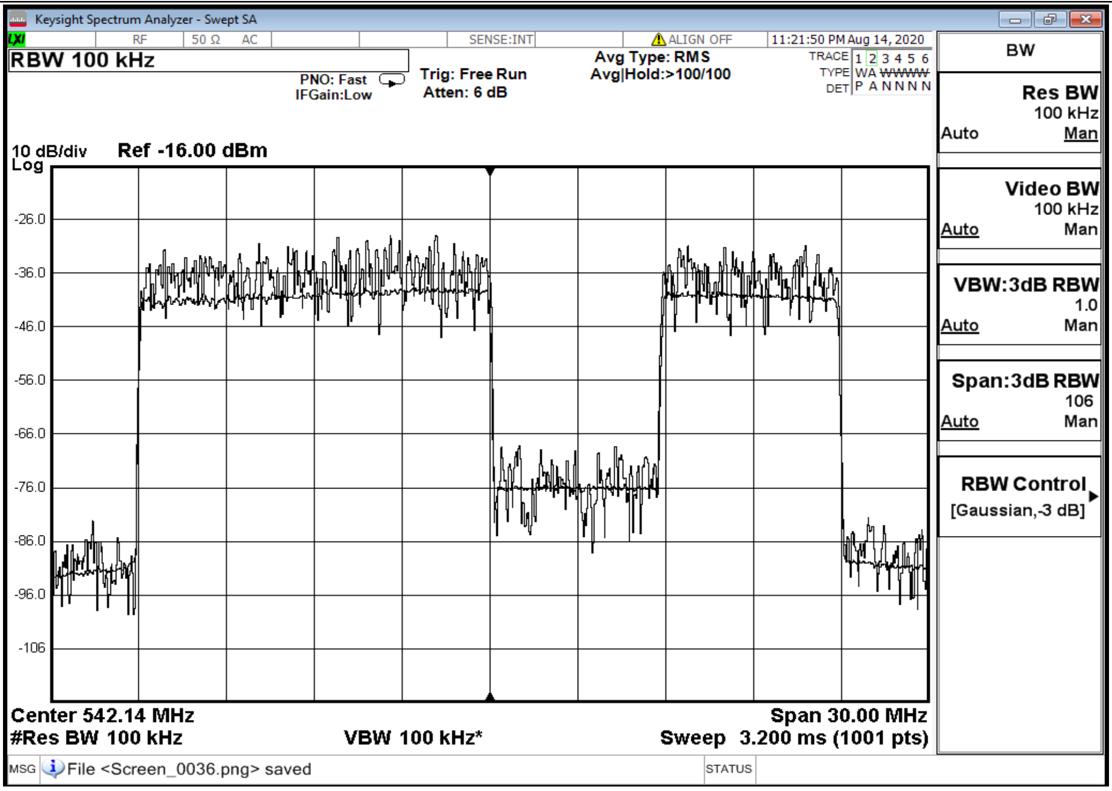

Figure 43. Spectrum of 5G-RANGE's downlink with a Digital TV interference.

3.2 PoC Simulation and Evaluation

In this section is presented the simulation of the basic PoC scenario. The simulation was performed in the COLAB-5 tool, which is the result of the integration of all the 5G-Range developments described in Section 2. So, for that, the simulated scenario for the POC consists of cell of 50km with a single user. Considering the KPIs defined in D2.1, the goal is to achieve 100 Mbps data rate for a single user at 50 km from the BS. For this basic scenario, a CBR traffic was generated at the expected rate from the UE to the remote host, considering the application layer implementation in COLAB-5 as described in Figure 21.
Section 3.1 showed the results of the POC in laboratory conditions. Another set of measures were made in a few field trials that are consistent with the measures in the laboratory trials. For these measures, the details and values are shown in Table 8 and correspond to field measures described in [19]. In these field measurements, the evaluated MCS was chosen by manually adjusting the MCS until the BER was equal or very close to 0%.

Table 8. First field trial measures for 6MHz wide channel

	Line-of-sight (LOS)			Non-Line-of-sight (NLOS)		
Distance to base station (km)	Throughput (Mbps)	MCS	BER	Throughput (Mbps)	MCS	BER
10	22	QAM64 3/4	0	-	-	-
20	22	QAM64 3/4	0	22	QAM16 2/3	0
30	13	QAM16 2/3	0	13	QAM16 2/3	0
40	-	-	-	13	QAM16 2/3	0.5
50	22	QAM64 3/4	0	-	-	-

Table 9. Second field trial measures for a 24 MHz wide channel

	Line-of-sight (LOS)		
Distance to base station (km)	Throughput (Mbps)	MCS	BER
50	102	QAM256 2/3	0

Using COLAB-5, simulations were executed 40 times for each scenario (LOS and NLOS for each of the sampled distances) to achieve a 95% confidence interval of a t-Student distribution. The simulation parameters used were the same defined in the field trials, as follows: eNodeB power transmission 38 dBm, UE power transmission 23 dBm, antenna gain 9 dBi MIMO 2x2.

Figure 44 show the comparative results for measures shown in Table 8 (in red and orange) and simulation (in blue and green) for 24MHz of bandwidth (4x6 MHz or 3x8 MHz). The results show that for all the cases, the simulation and field trial regarding LOS are close, achieving the expected values for each distance. on each 6 MHz channel. Considering the four 4 channels, the received throughputs is around 88 Mbps, using QAM 64. For the NLOS case, the results for 30 and 40 km are in line with the expected results, while there are no points of reference for 10 and 50 km.

Figure 45 shows the results for the TBLER, measured by the trials of Table 8 and simulations. Results for LOS scenarios are in line with the expected TBLER equals to 0%. The TBLER results for 40 km NLOS show some divergence, with simulated TBLER 5 times lower than its trial counterpart, which may result of conditions in the field trial that were not possible to be included in the simulation, for example, shadowing or interference.

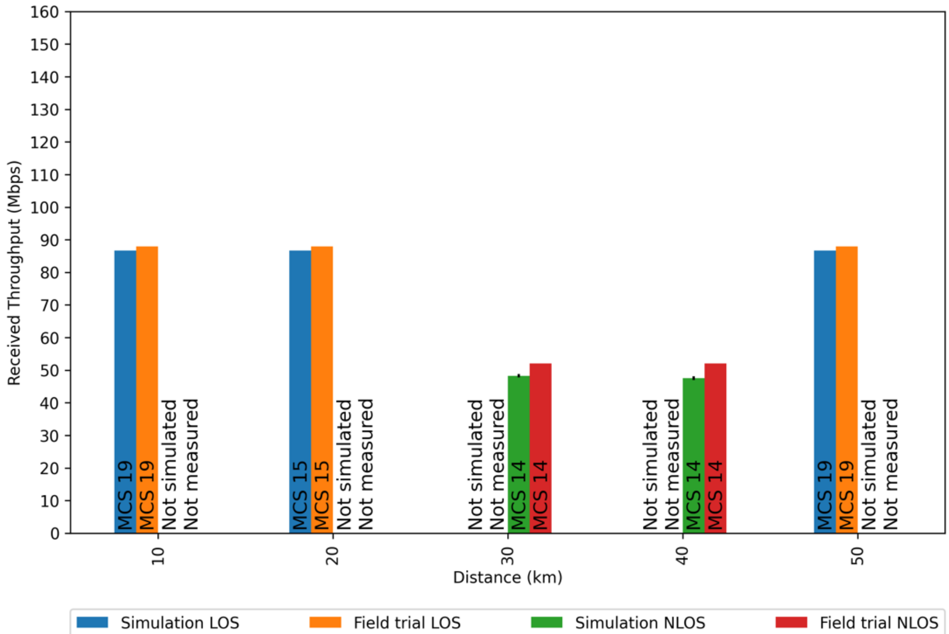

Figure 44. Received Throughput for COLAB-5 simulations and field trials

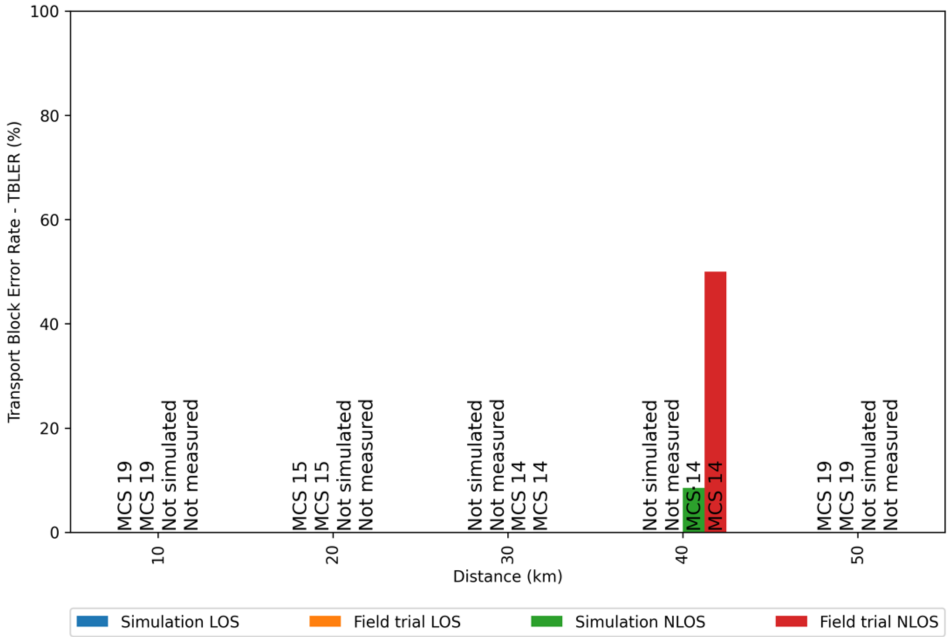

Figure 45. Transport Block Error Rate (TBLER) for COLAB-5 simulations and field trials

Another batch of simulations were executed to compare with the latest field measurements, as detailed in D6.3. Figure 46 shows the area in which these measurements were taken and Table 9 shows the details and the mean throughput value and BER of these trials. For this second trial, the gNodeB transmission power was increased from 38 to 40.8dBm and a 24MHz wide channel in the 500MHz band was used. The MCS 24 used was equivalent to QAM 256 2/3. Field trial measurement (orange) and simulation results (blue) are shown in Figure 45, for throughput, and Figure 47, for TBLER. The simulated results match the field trial measurements.

Figure 46. Field measures, 24MHZ wide channel

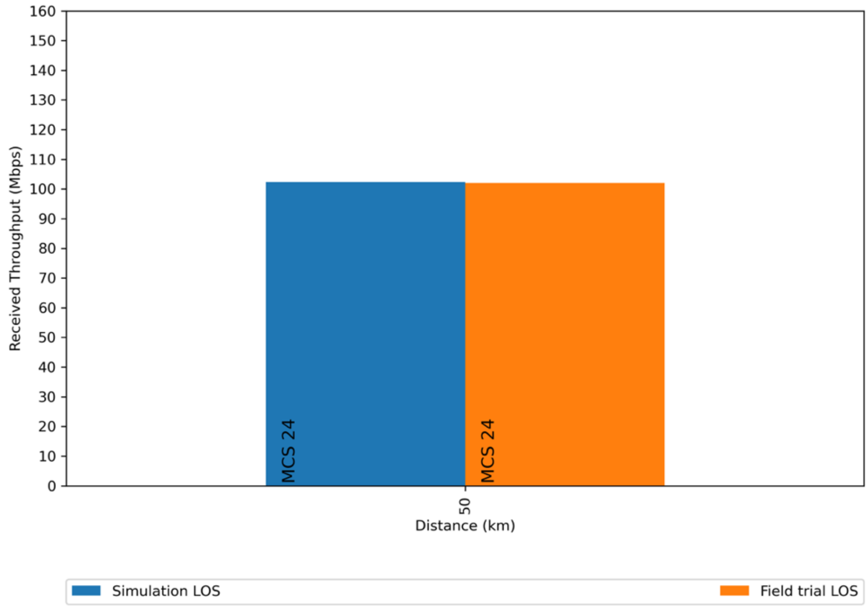

Figure 47. Received Throughput for PoC field trial

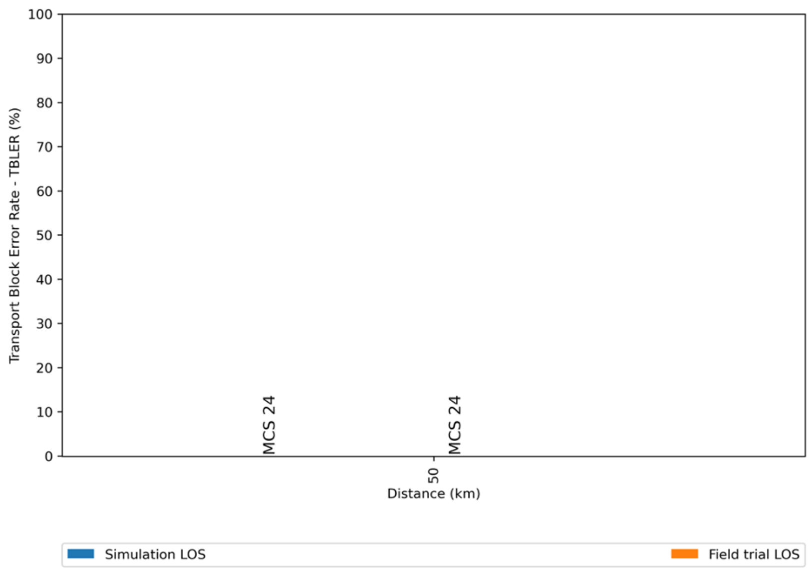

Figure 48. Transport Block Error Rate (TBLER) for PoC Field Trial

The results of this section show that the COLAB-5 is achieving the expected results and can be considered as a validated platform to perform the simulation use case scenarios, to be presented in the next section.

4 Core Use Case Simulations and Evaluation

In this section, it will be presented the scenarios, requirements, simulation parameters, and the results for the four defined core use cases. Using the 5G-RANGE system-level simulator, we were able to evaluate the properties for the voice and data connectivity, backhaul, smart farm, and e-Health scenarios. Table 10 presents the general simulation parameters used to simulate the four scenarios. It gathers all common basic parameters for the ns3 simulator. The Primary User communication impact is also evaluated in all scenarios. We proceed with simulations with and without PU presence and both OR and MHM fusion algorithm are evaluated as well. Table 11 presents the traffic model parameters used to generate the synthetic traffic injected during the simulations. In the next subsections, it will be presented the specifics traffic proportion used in each simulated core use case scenarios.
For all the simulation scenarios, using the EROS-5, a traffic injection was made following the main application which reads an input Json file containing packet sizes and time between packets. The application can be configured to spread the traffic to more than a single port and to use either UDP or TCP sockets, depending on the type of traffic the simulator user wants to inject. A sample of such inputs is shown in the Figure 49, corresponding to VoIP traffic, with uniform packet sizes of 20 bytes and interval between packets around 20ms. Another example of the file format is shown in Figure 50 packet sizes of a few megabytes each and time between packets of a few seconds, corresponding to a 480p YouTube video stream (~2Mbps) using MPEG-DASH.

Table 10. General simulation parameters used in four core use cases.

	Description	**Values**
General	Simulation time	10 seconds
	Propagation model	CDL-A (NLOS)
	Band	713 MHz
	Channels number	4x6 MHz
	MCS configuration	Dynamic choose
	Noise floor	-174 dBm/Hz
	MIMO	2x2 TxDiversity
eNodeB	Tx power	40.8 dBm
	Antenna gain	9 dBi
UE	Tx power	23 dBm
	Antenna gain	9 dBi
	Numerology	0, 2 and 3
	Tx power	40 dBm
	Number of PUs	0 per channel, 1 per channel
PU	Distance from eNodeB	Random placed
	Fusion Algorithm	MHM and OR

Table 11. Traffic model parameters used in four core use cases.

Applications	Description	Values
VoIP	Codec	G.729, G.711
	Packet size	20 bytes, 214 bytes
	Time between packets	Normal distribution with parameters: $\mu = 0.02$; $\sigma = 0.0038$
Web Browsing	Protocol	HTTP
	Main object size	Weibull l = 28242.8, k = 0.814944
	Number of main objects	Lognormal with parameters: $\mu = 0{,}473844$; $\sigma = 0{,}688471$
	Secondary object size	Lognormal m = 0.473844, s = 0.688471
	Time between two secondary objects	Gama k = 0,16; $\theta = 5{,}375$
	Secondary object size	Lognormal with parameters: $\mu = 9{,}17979$; $\sigma = 1{,}24646$
	Secondary object number	Exponential $\mu = 31{,}9291$
	T_{OFF}	Lognormal m = 9.17979, s = 1.24646
Video Streaming	T_{ON}	Burr XII with parameters: $\alpha = 1{,}469$; $k = 1{,}915$; $c = 3{,}014$
	T_{IR}	T-Student with parameters: $\mu = 1, 938$; $\sigma = 0, 245$; $\nu = 2{,}086$
	c	Codification rate (kbps): [91, 180, 469, 978, 2058, 3953, 9581, 21373]
IoT	Period	T
	Time between packets	Uniform distribution ~ U (0, T)


```
{
    "init_time": 0.0,
    "server_port": 5060,
    "packet_size": 20,
    "time_between_packets": [
        0.018284707544248543,
        0.017123366667584194,
        0.023738888862305654,
        0.017783141252863875,
        0.02254070541567553,
        0.020411459104100464,
        0.029559318530178694,
        0.01460540729375764,
```


Figure 49. Example of EROS-5 file format of VoIP traffic

```
{
    "init_time": 0.0,
    "server_port": 81,
    "packet_size": [
        6868617,
        3243554,
        7405134,
        3670405,
        5052687,
        2379423,
        6716185,
        1721599,
```

```
        3989908,
        4656715
    ],
    "time_between_packets": [
        0.0,
        1.8674431822499349,
        2.023905425285999,
        1.5750005872600419,
        2.618789134560008,
        1.4884551185434087,
        2.2625561283393294,
        2.0391791817637994,
        2.1147151740766676,
        5.90663585954772,
        1.8839285114338826,
```


Figure 50. Example of EROS-5 file format for streaming video traffic

4.1 Core Use Case 1: Voice and Data Connectivity

This is one of the fundamental uses case scenarios to evaluate the basics services and infrastructure provided by the 5G-RANGE project. Data and voice connectivity aim to guarantee minimum voice and broadband services at far distances from the base station. Indeed, this is an enabling service that can leverage other potential applications. It focused to provide access to typical Internet applications in very large areas with extreme coverage requirements and low density of users.

There are many Internet applications and services that could be benefited from this use case scenario evaluation. Applications like web browsing, e-mail, VoIP, multimedia on the web, audio-graphic conference, file sharing and interactive video on demand. The QoS requirements will change for different kinds of applications. In this use case, one Internet application from each Voice and Data categories will be chosen to be evaluated. The following applications were chosen for evaluation for this user case.

- **Voice over IP (VoIP)** – This service is characterized by the set of rules that allow voice transmission though IP protocol. This service is especially sensitive to measurements metrics like latency and jitter. Beyond voice traffic over IP, which is a real time user voice data, a VoIP application generates control traffic as well. The control traffic is control data used by the VoIP infrastructure to manage all online users VoIP connections. The 5G-RANGE infrastructure will have to deal with these different kinds of data traffic. QoS requirements for the VoIP connections will need to be achieved.
- **Web Browsing** – This is a very popular and traditional web service, it works using HTTP protocol. The asymmetric characteristics of HTTP data traffic will have a different impact among DL and UL traffic, on 5G-RANGE infrastructure. This directly impact will especially increase when the number of users get bigger in the simulation scenario.

4.1.1 General Description of the Simulation Scenario

Figure 51 presents the topology implemented to simulate the voice and data connectivity use case. In this scenario, the UEs will use 5G-RANGE infrastructure to have Internet access. Using the HTTP protocol, they will be able to access a remote server, localized outside of the local communication infrastructure. They will be able to make VoIP calls with each other, using the 5G-RANGE infra. For this use case simulation, the number of UEs was varied following the values of 2, 3, 20, 50 and 100 nodes. For the traffic model, 30% of the UEs will make VoIP calls and 70% will use HTTP for browsing on the Internet. These parameters are defined in Table 11.

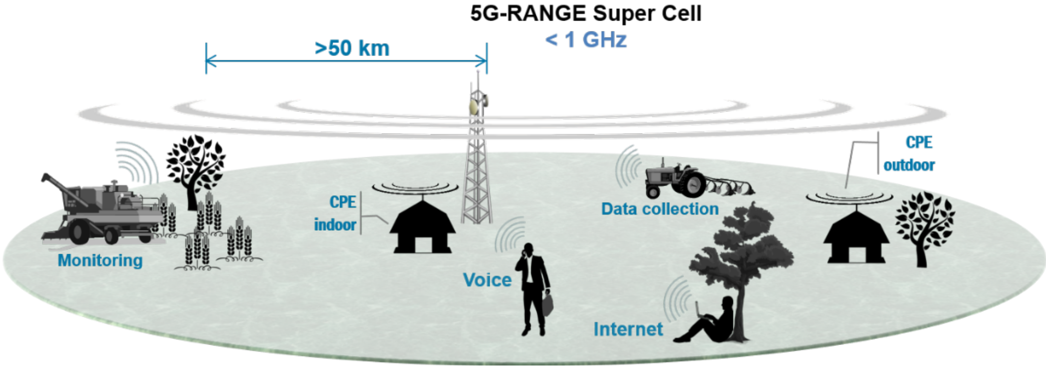

Figure 51. Illustration of the voice and data connectivity scenario.

Table 12 presents the quantitative specific requirements for Voice and Data connectivity use case, originally presented and explained in the deliverable D2.1 [6]. According to D2.1, it is important to highlight the traffic model defined for the user experience data throughput is 100 Mbps. This capacity will be achieved during the peak DL data rate at the cell edge (50 km) with one stationery UE.

Table 12. Specific requirements (Voice and Data Connectivity) [6].

Attribute	Description	KPI	
		VoIP	Web
Spectrum	Carrier Frequency	< 3.5 GHz Priority on 700 MHz band	
Traffic model	Low-density areas	≤ 2 users/km^2	
	User Experience data throughput	500 kbps	100 Mbps
	Uplink/Downlink capacity ratio	50% / 50%	25% / 75%
UE	Medium mobility	Speed up to 60 km/h	
System	Reliability	>90%	
	End-to-end latency	100 ms	
	Jitter	400 ms	100 ms
	Cell range	Up to 100 km	

Figure 52 shows the VoIP traffic series used to simulate the user traffic at the application level in the COLAB-5 tool in different scenarios. The traffic series achieves 8 kbps using codec G.729 and it generates the payload that the application will use at the application layer. Figure 53 shows the web traffic series used in the simulations.

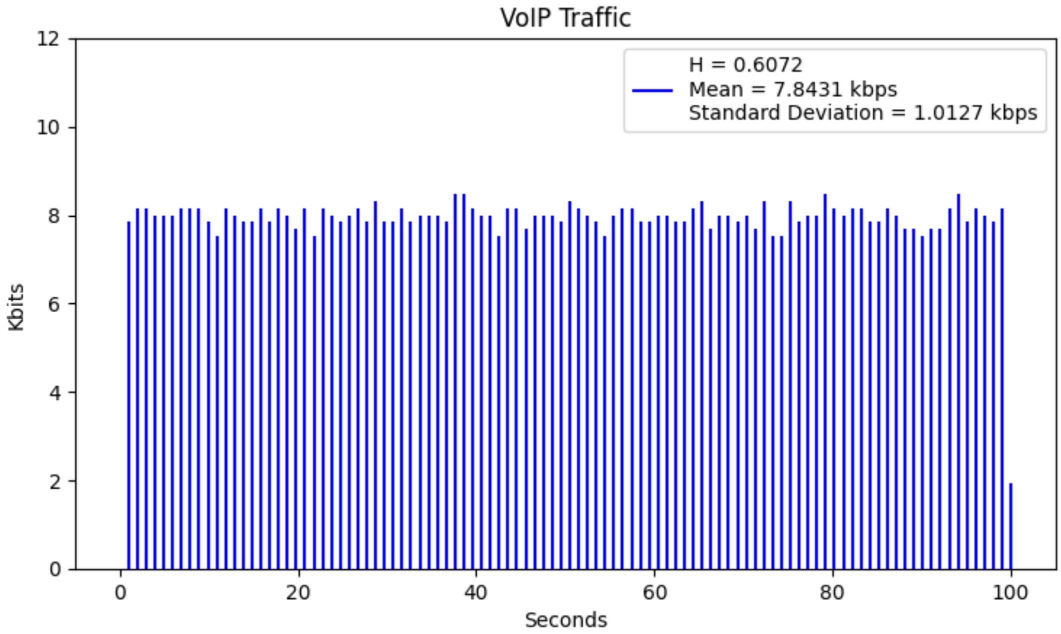

Figure 52. VoIP Traffic Series (per UE).

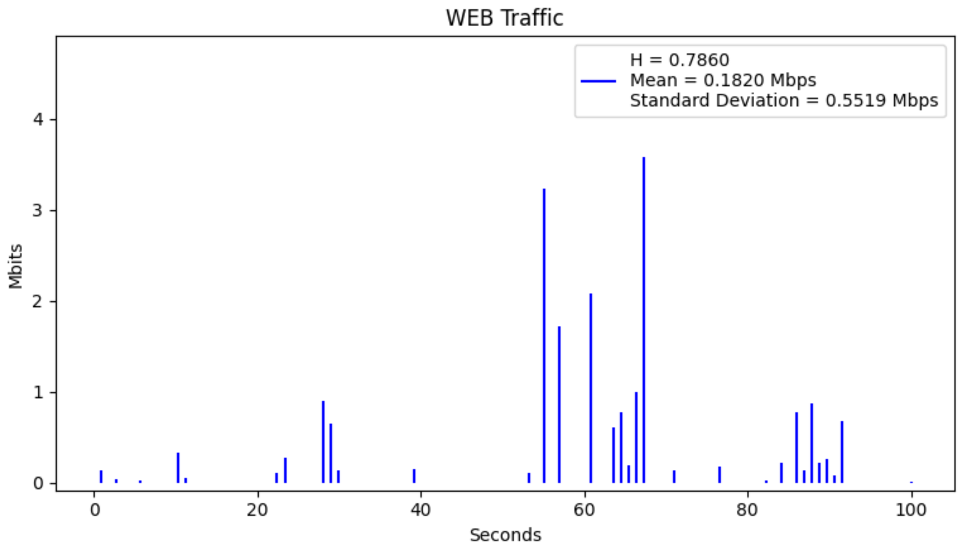

Figure 53. Web Application Traffic Series (per UE).

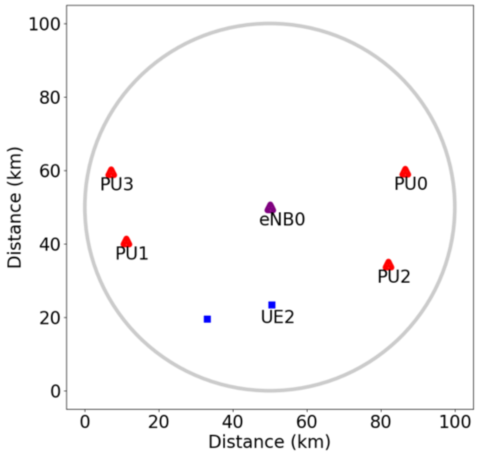

Figure 54. Example of simulation topology with 2 UEs and 4 PUs within the 50km radius

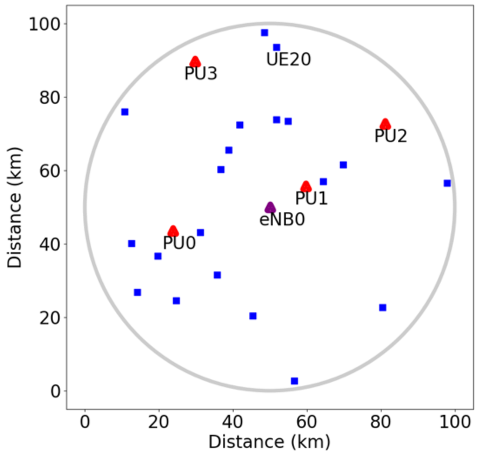

Figure 55. Example of simulation topology with 20 UEs and 4 PUs within the 50km radius

4.1.2 Simulation Results

This section presents the evaluation results for the VoIP and data connectivity scenario. For each scenario were executed 20 simulations with UEs in random positions and the results show the mean values of each simulation.

The first scenario is very simple with a 50km cell with two UEs near the cell border, as illustrated in Figure 54. Both UEs establish a VoIP call between them. The simulation results are presented for 03 cases: (1) without PU interference, i.e, when all the UEs have the 24MHz available for transmission, (2) with PU interference using a simple CSS procedure, already presented in D4.4, and (3) with MHM CSS control, which includes control for potential attackers and improves the control channel efficiency.

Figure 56 shows the aggregate throughput for the downlink (DL) and uplink (UL) channels for the three cases. The first two columns show the results of throughput for transmission without PUs interference. Third and fourth columns show the results for simulations with PU presence and the fifth and sixth columns show the results for the MHM fusion algorithms. As defined in Table 11, the G.729 is one of the used codecs in VoIP calls simulation, with a packet size of 20 bytes. Considering the control overhead of the IP transport and network layer, 8 and 20 bytes for UDP and IP headers are added respectively, and the achieved rate is 384 bits every 0.02 seconds, which follows the parameters described in Table 11. That is, a VoIP call using G.729 codec generates 19.2 kbps, for each UE communication direction. As we expected, in Figure 56, the aggregate throughput for VoIP application is near 40 kbps. With PU interference, the throughput drops to near 30 kbps. This degradation is generated by the interference with the PU, which may not be correctly detected due to the low number of UEs performing CSS. This may result also in higher transport block error rates due to lower SINR. At the same time, the link adaptation scheme selects lower performing MCSs in order to keep error rates under control. The results show that, as expected, the MHM mechanisms do not show an effective result for a small number of sensing nodes.

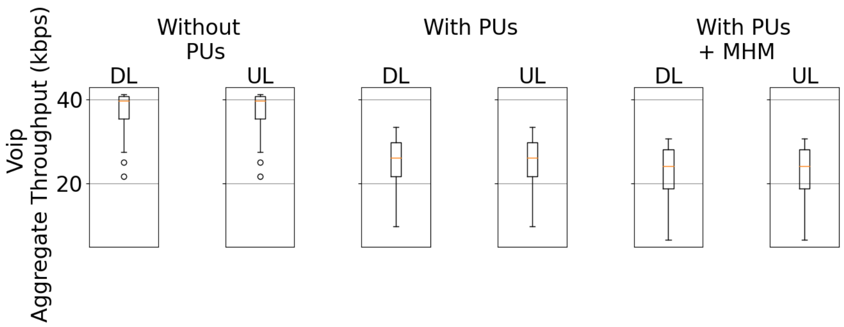

Figure 56. Simulation results for throughput, scenario with two UEs establishing a VoIP.

Figure 57 shows the simulation results in a scenario with three UEs. In this case the UEs send web traffic to connect with a remote server outside the cell. The traffic pattern used in this simulation is the one described in Figure 53. Without PU interference, the aggregate throughput is above 60 kbps which shows consistency with the generated traffic at each UE. The simulation shows the asynchronous nature of HTTP communication and its different impact on DL and UL channels. The aggregate throughput on UL is near 25 kbps. Also, for this case, the simple OR and MHM fusions are not effective in this scenario.

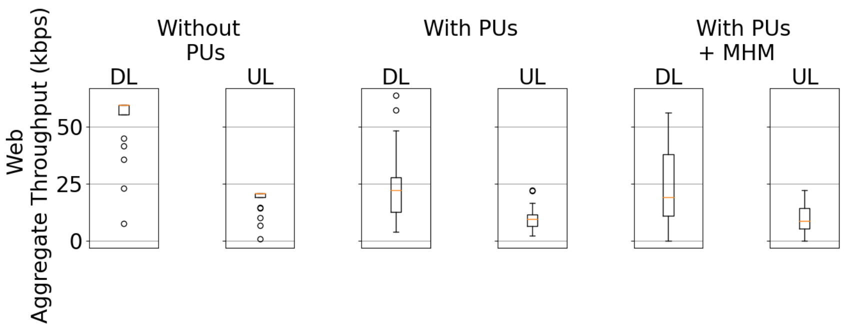

Figure 57. Simulation Results for throughput, 3 UEs using HTTP to connect with a remote server

Figure 58 shows a simulation scenario with 20 UEs, as the one illustrated in Figure 55. In this scenario, 30% of UEs establish VoIP calls with each other, and 70% are sending web traffic to a remote server outside the cell. For the VoIP application, the aggregate throughput is near 120 kbps, without PU interference. It's near 20 kbps for each one of the 6 UEs, which remains befitting with the previous result. The fourteen UEs are able to achieve a Web aggregate throughput near 1100 kbps, which is slightly better than the last presented result, reaching almost 78 kbps per UE. This number drops to near 60 kbps per UE with PU presence.

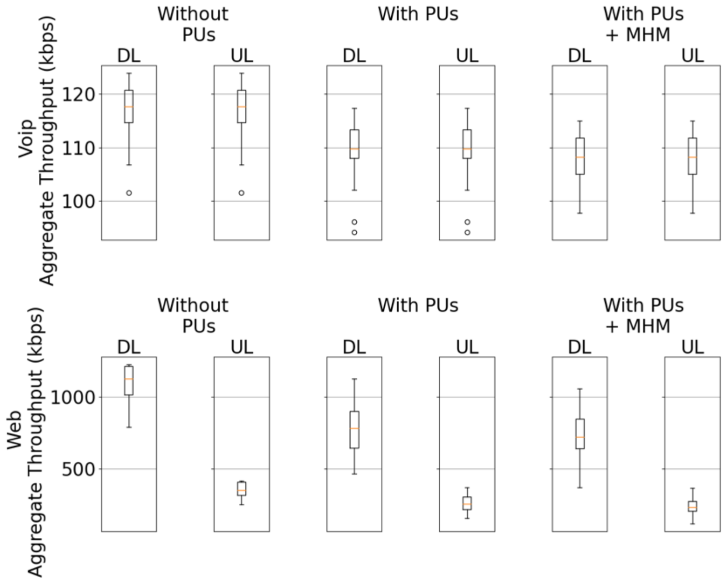

Figure 58 Simulation Results for throughput, 20 UEs, 30% VoIP calls with each other, 70% using HTTP to connect with a remote server

Figure 59 shows the simulation results for a scenario with fifty UEs. In this scenario, 30% of UEs establish VoIP calls between each other and 70% use HTTP to connect with a remote server outside the cell. The aggregate throughput for the VoIP application increases to near 245 kbps and the Web application throughput is 4 Mbps.

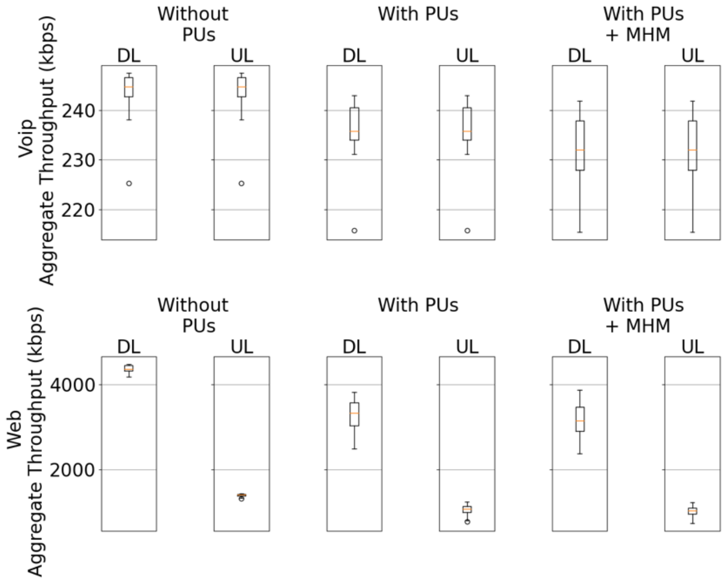

Figure 59. Simulation results for throughput, 50 UEs, 30% VoIP calls with each other, 70% using HTTP to connect with a remote server.

Figure 60 shows the result for a simulation scenario with 100 UEs. In this scenario, 30% of UEs make VoIP calls with each other, and 70% use HTTP to connect with a remote server outside the cell. The aggregate throughput for the VoIP application increases to near 560 kbps and the Web application reaches 10 Mbps kbps. With PU communication, the aggregate throughput decreases as expected.

However, it is near 540 kbps using the MHM mechanism as a fusion algorithm. That is, each UE reaches 18 kbps for the VoIP application and near 107 kbps for Web data traffic HTTP.

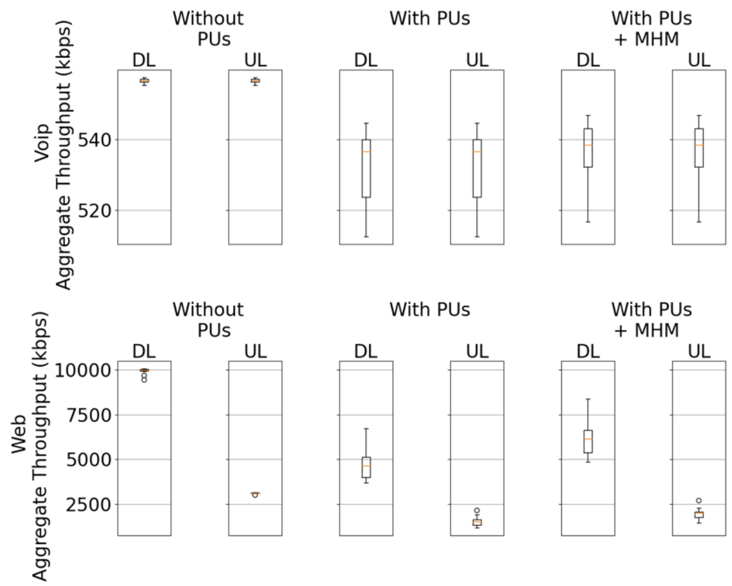

Figure 60. Simulation results for throughput, 100 UEs, 30% VoIP calls with each other, 70% using HTTP to connect with a remote server.

The results for all the VoIP and data connectivity scenarios in this section show that the 5G-Range solution is capable of achieving the throughput and reliability KPIs defined for VoIP and data connectivity as described in Table 12.

Figure 61, Figure 62 and Figure 63 show the results for delay/latency, jitter and packet loss, for the simulation scenario with two UEs. The values for delay are below 100 ms for the case of no PU interference and slightly above 100ms, while jitter is all cases is below 100ms and packet loss for all the cases is below 5%. The delay for the simulation scenario may be higher since the scheduling algorithm that is being using is round robin, which is not CQI aware. So, the traffic is being transmitted using a best effort model. The best effort effect can be better observed in a more complex scenario, as shown in Figure 64 and Figure 65, with 50 and 100 UEs respectively, where the delay for VoIP traffic and Web traffic remains very close, slightly lower for the Web traffic since it has a less constant behavior.

The results for jitter and packet loss for the 100 UEs scenarios, where 30% of UEs are using VoIP and 70% are transmitting Web traffic are shown in Figure 66 and Figure 67, respectively. As can be seen, in this more complex scenario, mean packet loss and jitter are below the defined KPI. Then, to evaluate the CCS and MHM implementation, Figure 68 shows the results for sensing efficiency. The results show that for the case of no PU interference, false positives and false negatives are zero, which is the expected result. Then, when there is PU interference, the MHM implementation shows much better values for false positives and false negatives, all of them around 10%.

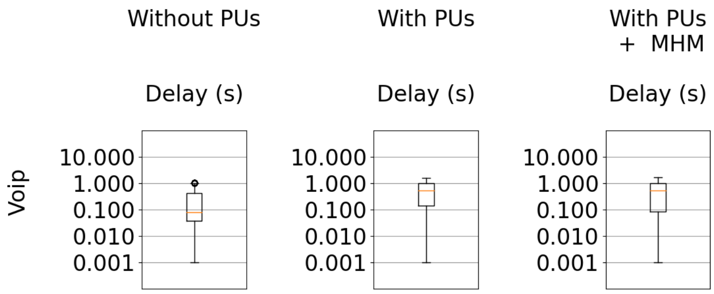

Figure 61. Simulation results for delay, scenario with two UEs establishing a VoIP.

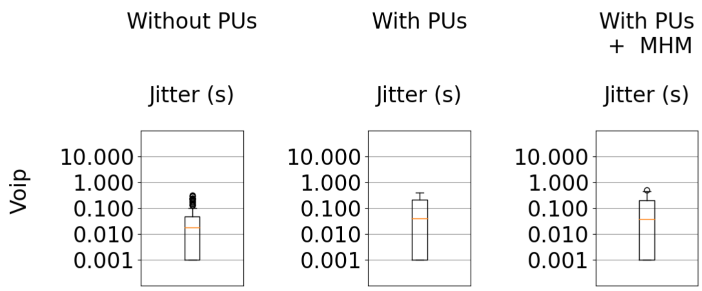

Figure 62. Simulation results for jitter, scenario with two UEs establishing a VoIP.

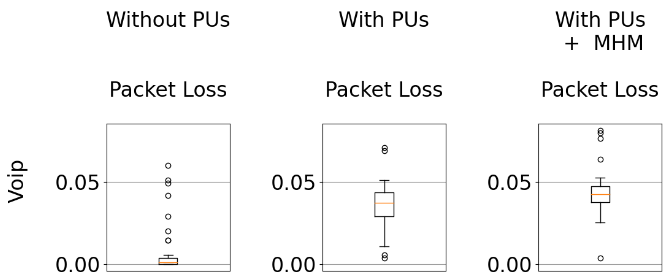

Figure 63. Simulation results for packet loss, scenario with two UEs establishing a VoIP.

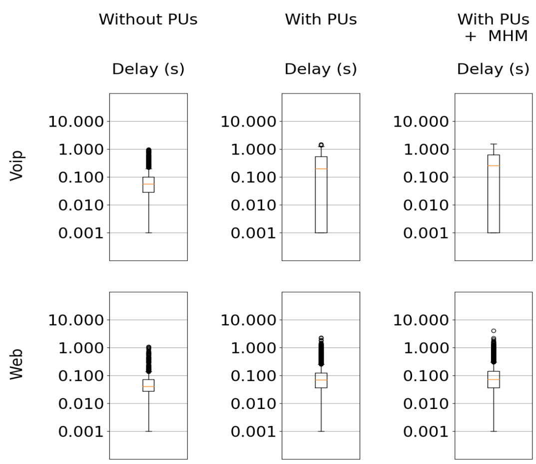

Figure 64. Simulation results for delay, 50 UEs, 30% VoIP calls with each other, 70% using HTTP to connect with a remote server.

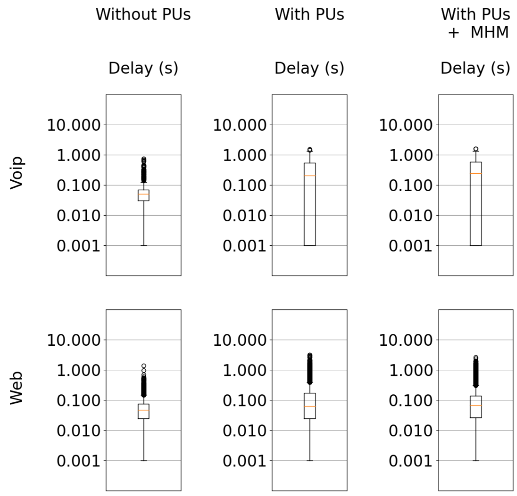

Figure 65. Simulation results for delay, 100 UEs, 30% VoIP calls with each other, 70% using HTTP to connect with a remote server.

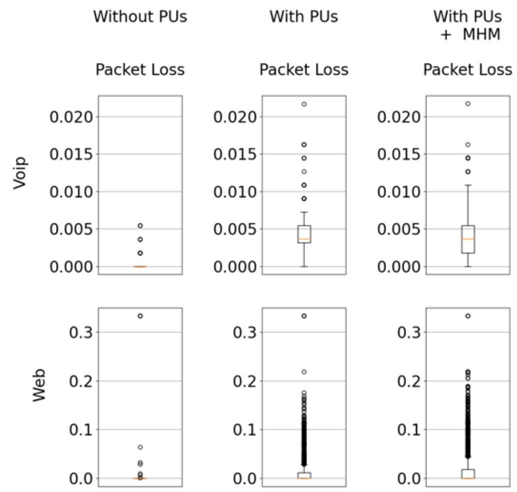

Figure 66. Simulation results for packet loss, 100 UEs, 30% VoIP calls with each other, 70% using HTTP to connect with a remote server.

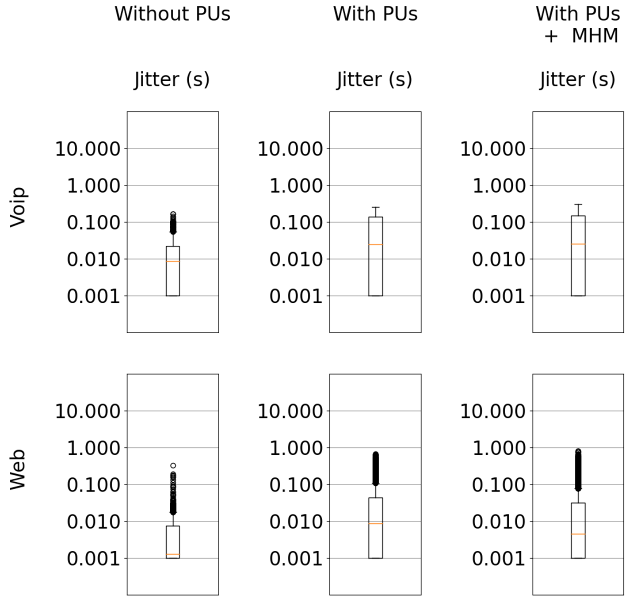

Figure 67. Simulation results for jitter, 100 UEs, 30% VoIP calls with each other, 70% using HTTP to connect with a remote server.

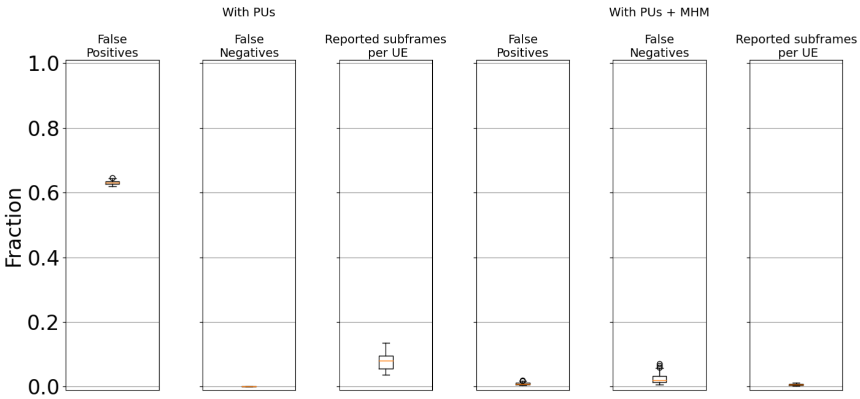

Figure 68. Simulation results for sensing efficiency, 100 UEs, 30% VoIP calls with each other, 70% using HTTP to connect with a remote server.

The simulation results in this section show that the 5G-Range network achieves the defined KPIs for the use case for VoIP and data connectivity.

4.2 Core Use Case 2: Wireless Backhaul

This use case focuses on the usage of TV broadcast network infrastructure (towers and frequency channels) for wireless backhaul implementation for rural area network. Figure 69 illustrates this use case scenario. Regions that currently have a relatively good TV-coverage, the use of that infrastructure for backhaul implementation could be a cost-effective solution. By utilizing low frequencies (VHF and UHF), large multi-antenna systems, beamforming and high TV-towers, enough long wireless backhaul link distances and required capacity may be achieved. The assumption is that a 5G-RANGE base station that is installed to TV tower, can provide line-of-sight (LOS) for a 50 km link using VHF or UHF band (unoccupied channels based on spectrum sensing reports) to the local small cell BS which is located at the rural location. This link works in a transparent way to connect the small cells with the network core. Mobile users are connected to small cell BS in this local rural area. A further assumption is that the population density is low in this area, but the user at small cell BS coverage (< 500 m) must be supported by a high throughput (100 Mbps) connection.

4.2.1 Description

In the Wireless Backhaul scenario, the 5G-RANGE BS (Figure 69) has in most of the cases a directly line-of-sight communication link with 5G-RANGE radio on the TV Tower infrastructure. Behaving like a 5G-RANGE UE for direct communication with the TV tower, the 5G-RANGE BS is also able to create a WiFi local infrastructure to route and distribute the Internet access link locally among several devices. This infrastructure is able to provide a **data transport service**. Due to the nature of the use case, the service that is intended to be covered by the backhaul link is the indiscriminate transport of data among subcells and the core network.

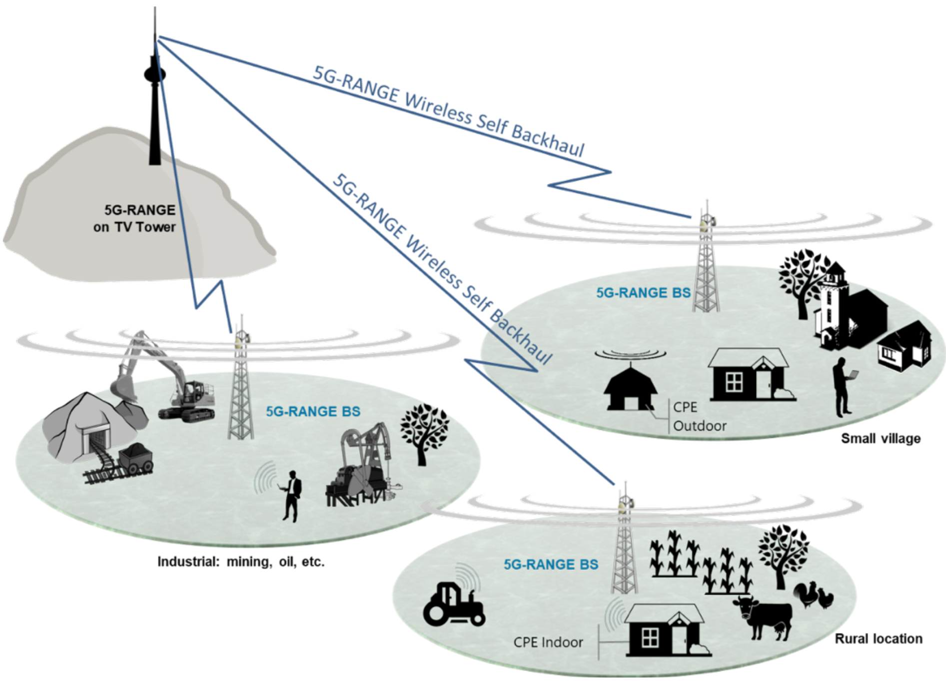

Figure 69. Illustration of the wireless backhaul scenario.

Table 13 presents the quantitative requirements for wireless backhaul use case, originally presented and explained in the deliverable D2.1 [6]. For the backhaul data throughput, 100 Mbps is the Peak of the DL data rate at cell edge (50 Km, one link), in static position.

Table 13. Specific requirements (Wireless Backhaul) [6].

Attribute	Description	KPI
Spectrum	Carrier Frequency	< 3.5 GHz Priority on 700 MHz band
Traffic model	Low-density areas	≤ 0.1 users/km^2
	Backhaul data throughput	100 Mbps (DL)
	Reliability	99.5%
UE	Mobility	Static

For the backhaul downlink and uplink traffic, since it represents the aggregation of multiple applications, the most suitable traffic type to use in this use case is the fractal model, using an *H* parameter above 0.5, which represents bursty traffic and long dependance correlation, which is typically observed in network backbones. Figure 70 and Figure 71 show the parameters of the traffic series used the represent the backhaul traffic for downlink and uplink respectively, both achieving above 100 Mbps.

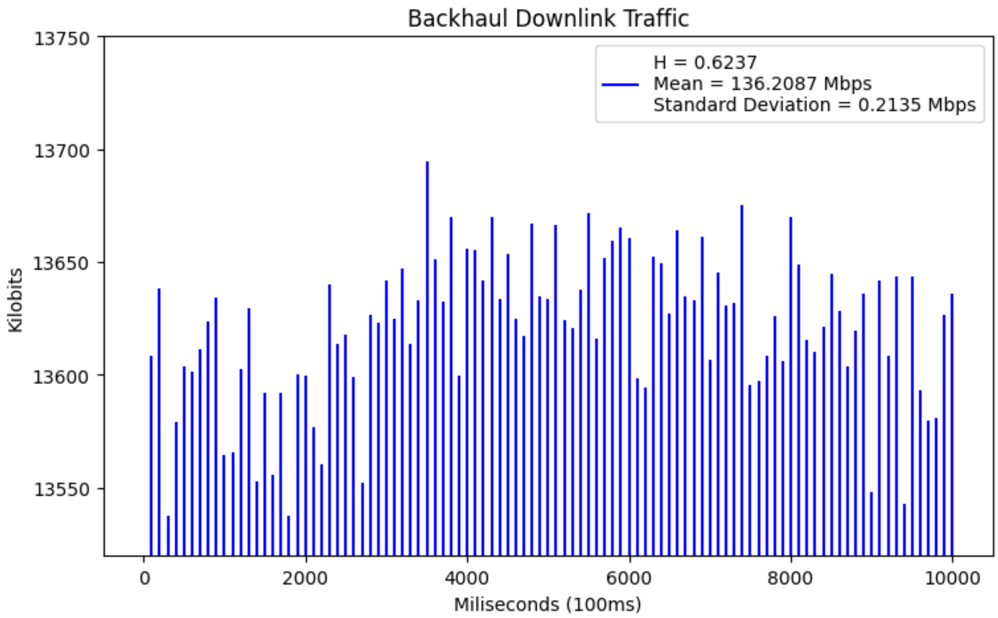

Figure 70. Traffic Series for Downlink Backhaul Traffic.

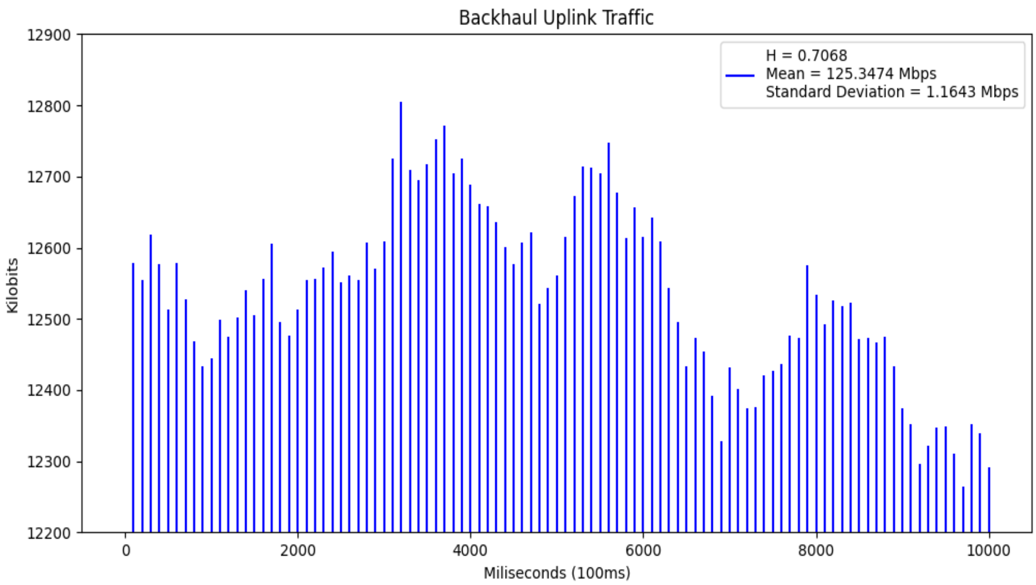

Figure 71. Traffic Series for Uplink Backhaul Traffic.

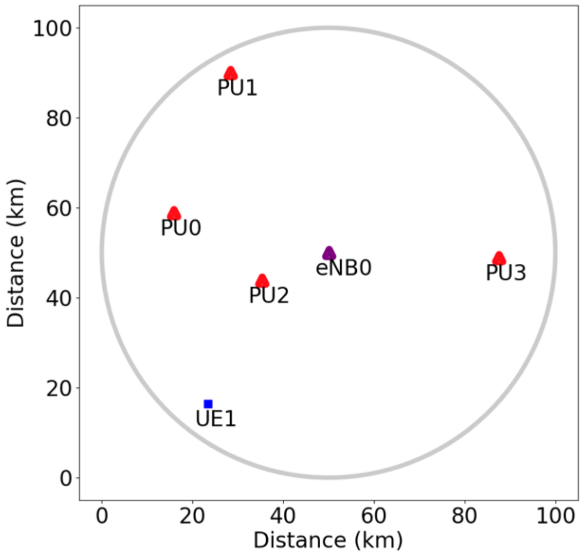

Figure 72. Example of one of the simulated topologies for the backhaul scenario: 1 UE acting as backhaul at the border cell and 4 PUs

4.2.2 Simulation Results

For the simulation backhaul scenario, the distance from the 5G-RANGE on TV-Tower and the 5G-RANGE BS were randomly chosen, varying from 2 km until 50 km distance from each other. As presented in Figure 70 and Figure 71, the traffic has an average throughput of 136 Mbps and 125 Mbps in the downlink and uplink channel, respectively.

Figure 73 shows the simulation results for the backhaul scenario, achieving an aggregate throughput of 75 Mbps on the downlink and 12.5 Mbps on the uplink channel, without PU communication. For the case of PU interference, the throughput is around 25 Mbps. It is important to note that in this scenario, there is the consideration that the backhaul does not have a direct line of sight, so its affected by shadowing effects. Then, the simulation was executed considering the CDL-A (NLOS) channel model. However, the results show an interval of 75Mbps and 25Mbps for the downlink channel, which is acceptable for many applications in the rural area.

Figure 74 and Figure 75 show the results for delay and packet loss. The results show that the delay in for all the cases remains below 1s and packet loss has a mean value around 8%. For this scenario, the defined KPIs for the downlink channel were a peak rate of 100Mbps and packet loss of 0,5%. The KPIs were not fully achieved, but some factors may have influenced the simulation: (a) the type of traffic, transmitted without any traffic shaping, which is highly burst and may produce higher packet loss; b) the simulation considered a NLOS communication between the BS and the backhaul device, to consider shadowing effects and the possibility of not a totally static device; c) buffers configuration in the BS and backhaul point may improve the packet loss metrics in the real world. These four items may have influenced the metrics, however, the simulation results show a good potential of using the 5G-Range in the backhaul scenario.

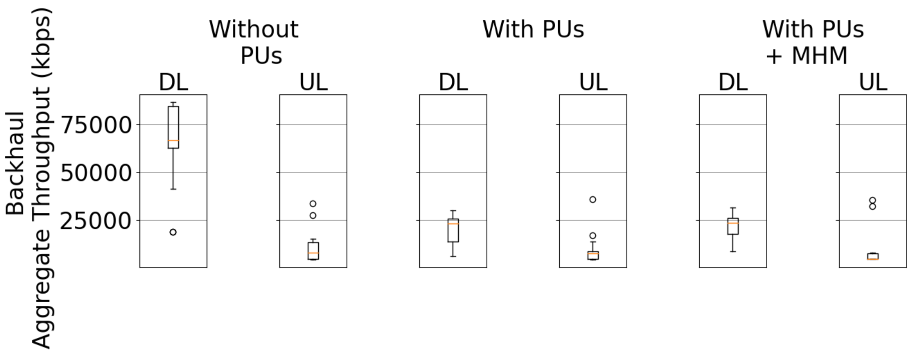

Figure 73. Aggregate throughput for the Wireless Backhaul scenario (CDL-A).

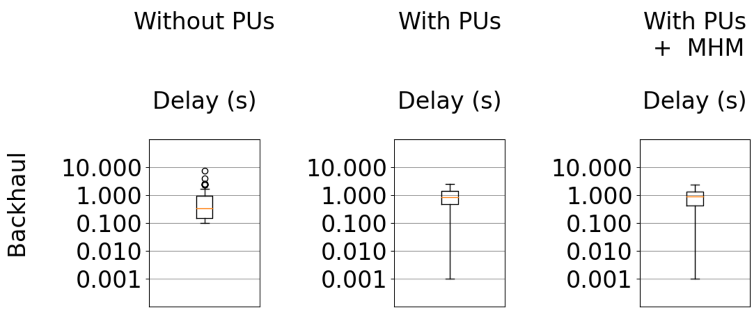

Figure 74. Delay for Wireless Backhaul scenario (CDL-A).

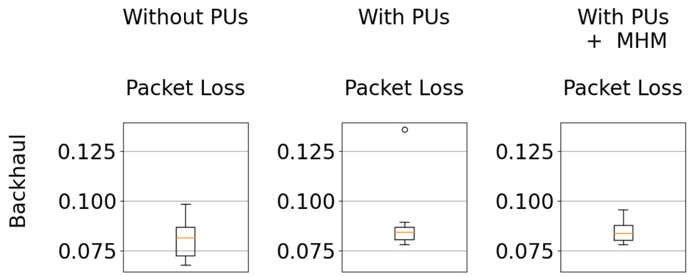

Figure 75. Packet loss for Wireless Backhaul scenario (CDL-A).

4.3 Core Use Case 3: Smart Farm

This use case scenario addresses the agribusiness vertical market with the goal to provide reliable connectivity and networking for underserved and remote rural areas. It intends to enable smart farming and broadband Internet access in a sustainable and cost-effective way. Moreover, it deals with real-time services (not necessarily low latency) such as data collection and analysis, crop monitoring, production traceability, remote maintenance and diagnosis, cattle counting, etc.

4.3.1 Description

Figure 76 shows the conceptual architecture for the Smart Farm scenario, with UEs acting as sink points and several IoT devices connected to them. Each UE will receive the IoT data traffic generated from a different number of IoT devices. Each one of these devices generates IoT traffic that follows the traffic distribution defined in Table 11.

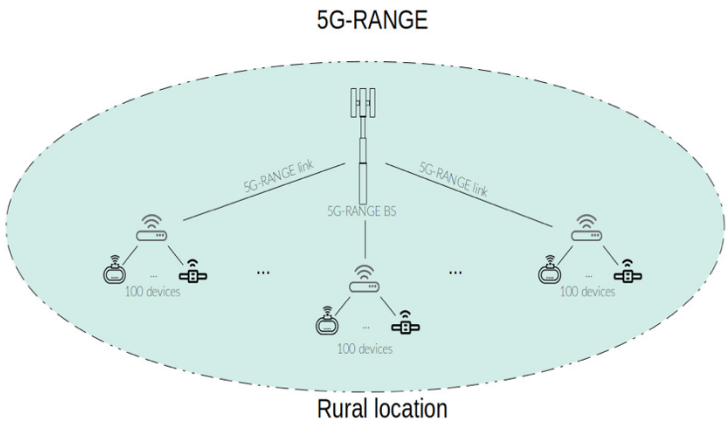

Figure 76. Example of the Smart Farm communication scenario.

Table 14 presents the quantitative requirements for the smart farming use case, originally presented and explained in the deliverable D2.1 [6]. According to D2.1, it is important to highlight the end-to-end latency KPI is defined between the IoT device to the interface to the remote host. Also, the survival time is defined as the time that an application consuming a communication service may continue without an anticipated message.

Table 14. Specific requirements (Smart Farming) [6].

Attribute	Description	KPI
Spectrum	Carrier Frequency	< 3.5 GHz Priority on 700 MHz band
Traffic model	Low-density areas	≤ 2 gateway/km^2
	User Experience data throughput (per IoT device)	1 Mbps
	Payload size	Small: payload typically ≤ 256 bytes
UE	Medium mobility	Speed up to 60 km/h
System	Reliability	> 99.9%
	End-to-end latency	50 ms
	Survival time	100 ms
	Cell range	Up to 100 km range

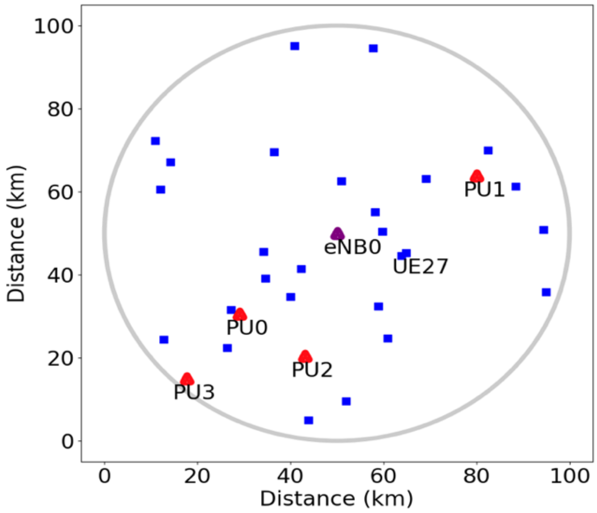

Figure 77. Example of the simulated topology for Smart Farm: 1 UE (IoT Server), 26 UEs (sinks) each one with 100 IoT devices and 4 PUs.

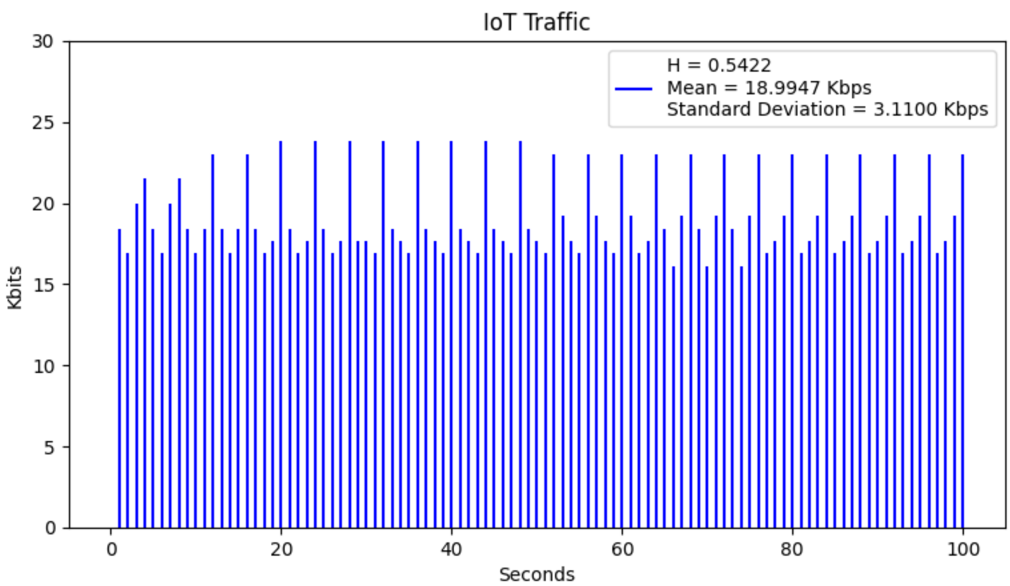

Figure 78. IoT Traffic Series (per IoT device).

4.3.2 Simulation Results

Figure 77 illustrates the simulation topology for the IoT scenario. For each simulation round, of a total of 20, the sinks and IoT devices were set in random positions. In this scenario, 26 5G-RANGE UEs behave as IoT sink nodes. Each sink has 100 IoT nodes, for a total of 2600 IoT devices in the cell that will collect and transmit data to an IoT server inside of the 5G-RANGE infrastructure. Figure 78 shows the IoT traffic series used to simulate the IoT device traffic. The traffic series achieves an average of 19 kbps throughput for each IoT device in the application layer.

Figure 79 shows the results for the Smart Farm simulation scenario. The aggregate throughput, without PU interference is 55 Mbps. Thus, the average throughput is 20 kbps per IoT device, which is enough to provide IoT communication for all 2600 nodes. In this topology is important to highlight that only the 26 UEs (sinks and IoT server) are running the channel sensing mechanism.

Figure 80 and Figure 81 show the results for packet loss and delay in the smart farm scenario, respectively. The results show that for all the cases, the packet loss is below 5%, when a mean value

around 2%. The delay is below 1 second for all the cases and below 100ms for the case of no PU interference.
Regarding sensing efficiency, for all the results it is clear that the PU presence has a direct impact on system performance. Figure 82 shows the results for sensing efficiency. Figure 79 shows that the aggregate throughput drops to near 20 Mbps. The sensing shows a false-positive rate near 20% for the OR algorithm and a false-negative rate around 10% for the MHM algorithm. As mentioned before, in this topology only the sinks are running the sensing algorithm.
The simulations in the smart farming scenario show the achievement of the KPIs for throughput and packet loss. The KPI end-to-end latency is achieved for the case of no PU interference but it is important to highlight that the simulation considered the delay between the sink and the remote host since the complexity of simulating a cell with 2.600 devices was not feasible to be performed in the simulation tool.

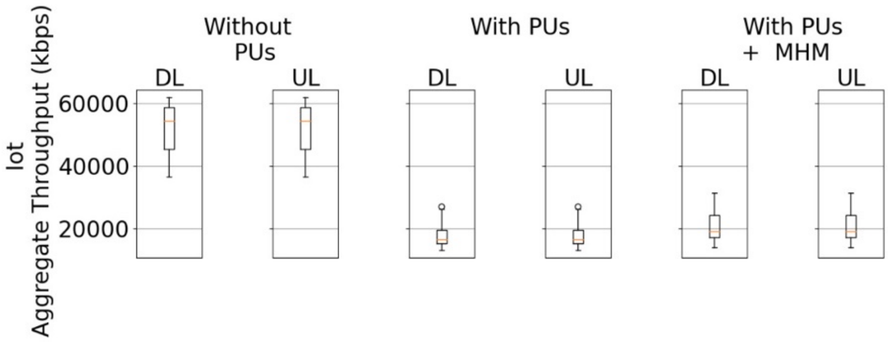

Figure 79. Simulation results for throughput, Smart Farm scenario: 26 UEs (sinks) each one with 100 IoT.

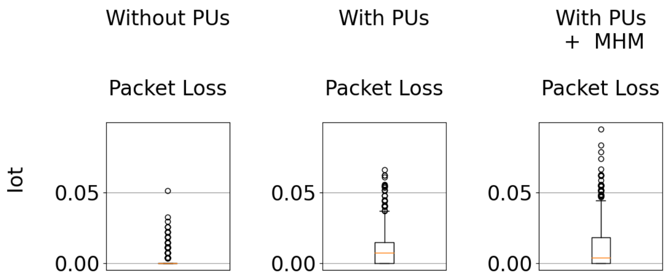

Figure 80. Simulation results for packet loss, Smart Farm scenario: 26 UEs (sinks) each one with 100 IoT.

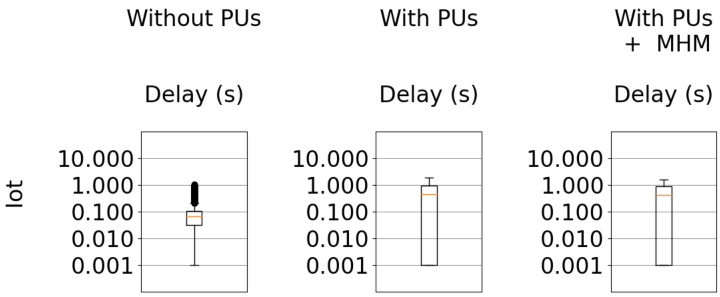

Figure 81. Simulation results for delay, Smart Farm scenario: 26 UEs (sinks) each one with 100 IoT.

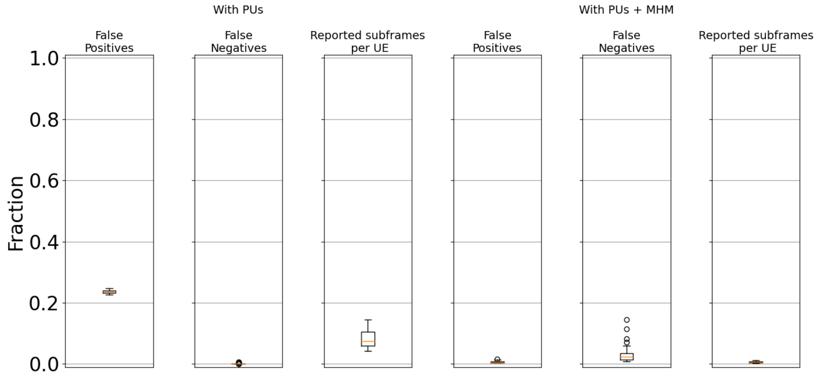

Figure 82. Simulation results for sensing efficiency: Smart Farm scenario

4.4 Core Use Case 4: e-Health

The Remote Health Care (e-Health) use case is focused on providing health/medical assistance to Underserved Rural and Remote Areas. It assumes broadband communication with acceptable latency, so the e-Health Ecosystem can provide real-time assistance. Thus, one facet of this scenario deals with high-speed ambulance traveling through the super cell coverage area without losing connection to video and voice services, and with high data rate and low latency capable of handling full definition video conference.

4.4.1 Description

This section shows the scenario used to simulate the Remote Health Care (e-Health) in regions where health infrastructure is still precarious or even absent. The goal is to demonstrate the viability of 5G-RANGE in providing broadband communication with acceptable latency so that the e-Health Ecosystem can provide real-time assistance, as presented in Figure 83 and Figure 84.
In this scenario, the UEs will use 5G-RANGE connectivity to make VoIP calls inside of the infrastructure, that simulates the online monitoring, even with higher requirement that IoT devices, video conferencing that simulates e-health multimedia services at home and web traffic, that simulates background traffic that will compete with the other ones. To simulate this scenario, the number of UEs was varied between 20, 50 and 100. For the traffic model, in concurrent time, 30% of the UEs will make VoIP calls, 70% will use HTTP for browsing on the Internet, and 5% will make videoconference calls. This simulates an rural area in which, 30% of the users are using online monitoring, 70% of the users generate background traffic as web traffic and 5% generate video-streaming. The traffic model parameters used in this scenario by the different types of UEs are defined in Table 11.
The following services, as described in deliverable D2.1 [6], are implemented in this scenario, as follows:

- **High mobility ambulance sceneries monitoring (Figure 83):** In an emergency situation, such as ambulance transportation, it is necessary to have real-time monitoring of vital functions of the patient for good planning in the hospital. Due to the emergency situation and the critical time that takes to arrive to the hospital, it is important to have the hospital team updated, providing real-time information to get ready for the patient's arrival. Thus, one facet of this scenario deals with high-speed ambulance traveling through the supercell coverage area without losing connection, and consequently, the doctor will have direct access to the patient's information.

- **E-Health Multimedia services at home (Figure 84):** Multimedia services, like videoconference, will be possible in remote areas scenarios. It is necessary to keep a high data rate to provide this service. In this use case, people can have professional medical assistance at their own homes. This service enables rural patients to reach urban doctors through a telemedicine solution. In this case, the doctor remotely manages a remote device to obtain medical parameters and provide a prescription to the patient.

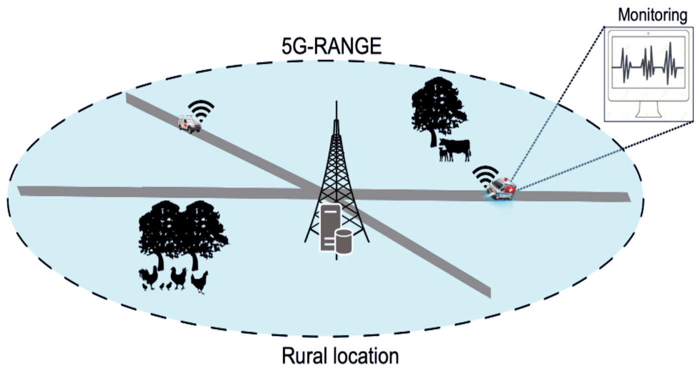

Figure 83 Illustration of the remote health care and high mobility ambulance scenarios.

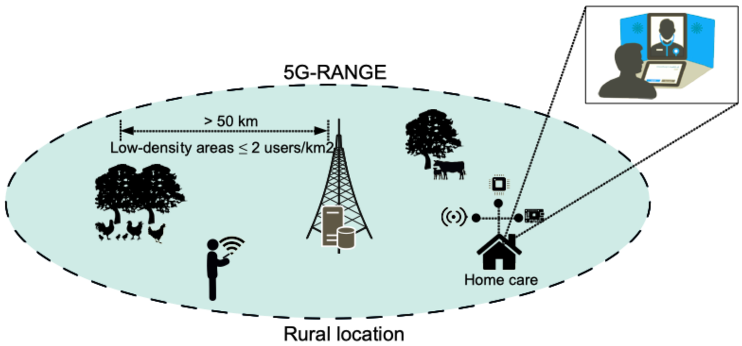

Figure 84. Example of remote health care and the e-health multimedia services.

Table 15. Specific requirements (Remote Health Care) [6].

Attribute	Description	KPI	
		Monitoring	Multimedia
Spectrum	Carrier Frequency	< 3.5 GHz Priority on 700 MHz band	
Traffic model	Low-density areas	≤ 2 users/km^2	
	Uplink /Downlink ratio	Mostly UL	25%/75%
	User experience data rate	1 Mbps (per IoT device)	100 Mbps
UE	Mobility	Speed up to 120 km/h	Static
System	Reliability	> 99.9%	>99%
	End-to-end latency	50 ms	100 ms
	Range	Up to 100 km	

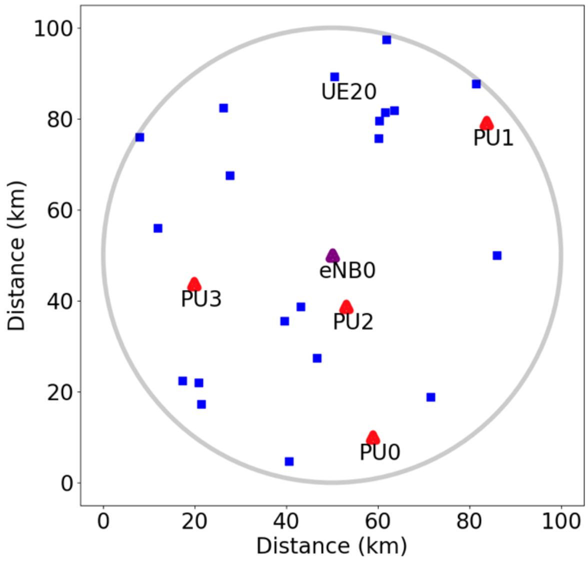

Figure 85. Example of the simulated topology with 20 UEs and 4 PUs within the 50km radius cell.

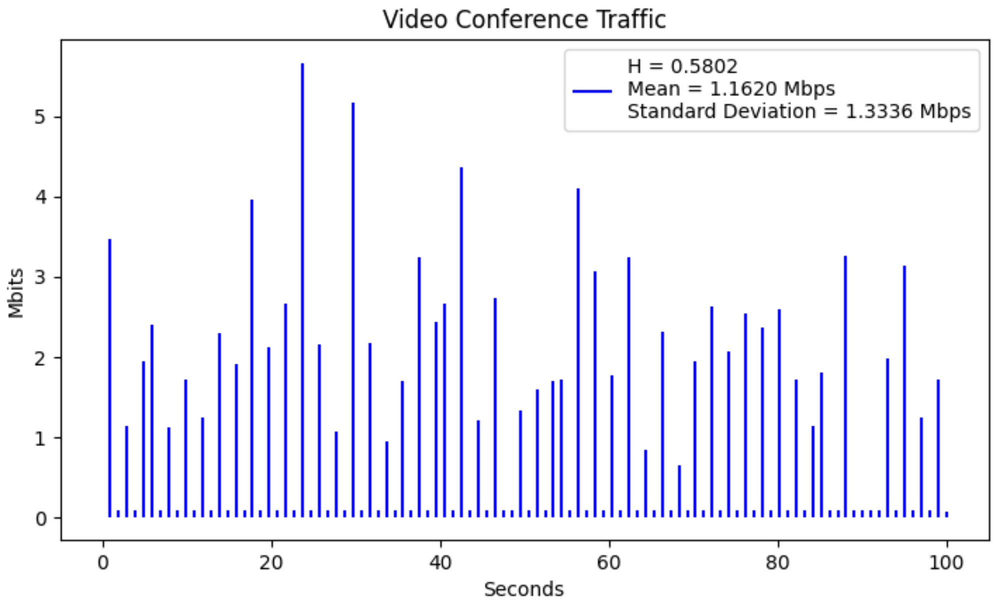

Figure 86. Video Conference Traffic Series (per UE).

4.4.2 Simulation Results

The first evaluation result for the e-Health scenario has 20 UEs with the following division of applications: 30% of UEs with VoIP calls, 5% with videoconference calls (VoIP + 2 Mbps stream interleaved) with each other inside of 5G-RANGE cell and 70% of the total UEs use HTTP to connect with a remote server. There is overlap of traffic generated by UEs which are randomly selected to generate the defined traffic in each simulation round. As defined in Table 11, the G.711 is one of the used codecs for VoIP calls simulation, with a packet size of 214 bytes. Then, considering 8 and 20 bytes for UDP and IP headers, respectively, the achieved rate is 1936 bits at every 0.02 seconds (as defined in Table 11). That is, a VoIP call using G.711 codec generates 96.8 kbps, for each UE communication direction. G.711 codec is also used in the video conference application. Figure 86 shows the traffic series used to generate video conference data traffic, with a mean data rate of 1.16Mbps.

Figure 87 shows the results for the aggregate throughput for each type of application. VoIP is near 605 kbps, showing that 6 UEs generate each near 100 kbps average throughput. Without PU interference, the UEs are able to achieve 1,200 kbps and 1,300 kbps for video conference and web applications, respectively. As mentioned above, in this scenario, 5% of the UEs execute video conference calls (VoIP + 2 Mbps stream interleaved) inside of 5G-RANGE infrastructure. The achieved throughput of 1,200 kbps matches the video conference traffic series used in this simulation.

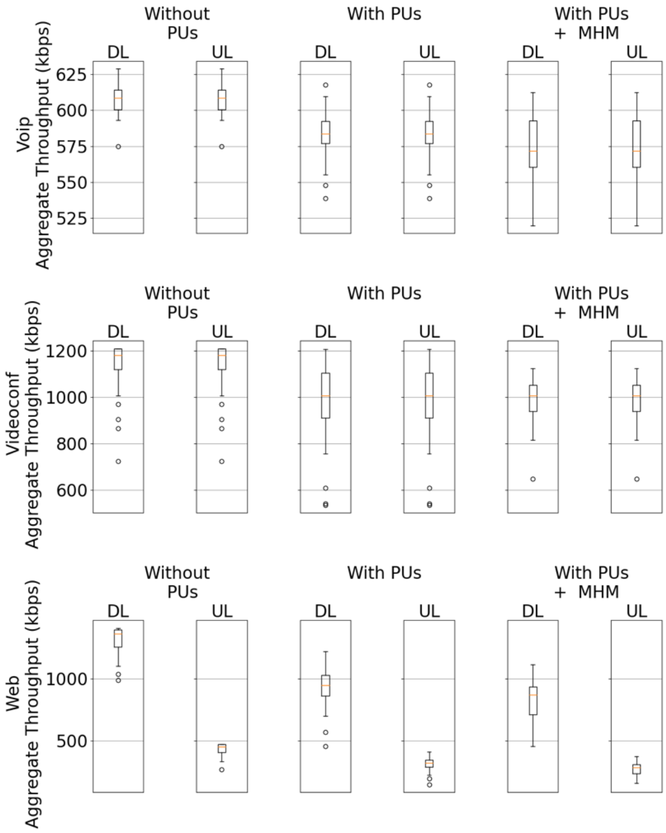

Figure 87. Simulation Results for throughput in the e-health scenario: 20 UEs

The second scenario increases the number of UEs to 50, using the same division for applications: 30% of UEs with VoIP calls, 5% with videoconference calls (VoIP + 2 Mbps stream interleaved) with each other inside of 5G-RANGE cell and 70% of the total UEs use HTTP to connect with a remote server. Figure 88 shows the results of the aggregated throughput for this scenario. All the values proportionally increased following the number of UEs. Using video conference application, 5% of UEs, achieved 2375 kbps, with VoIP reached almost 1250 kbps, and using HTTP, 70% of UEs, achieves almost 4700 kbps.

In the third scenario the number of UEs increases to 100, following the same application division than the previous scenarios. The results are shown in Figure 89. The results show that the VoIP application achieves 2900 kbps, without PU interference and confirms the system capability to offer 96.6 kbps throughput for each one of the 30 UEs participating in this simulation. With the PU interference and using MHM fusing algorithm, it is possible to provide VoIP communication for 28 UEs using G.711 codec. The aggregate HTTP throughput is 10.3 Mbps for seventy UEs, which provides almost 150 kbps throughput for each one. It is important to highlight that 5% of UE's will also run a video conference application in parallel. Those were able to achieve 4.9 Mbps of aggregate throughput.

Figure 90and Figure 91 show the results for delay with 20 UEs and 100 UEs. For the VoIP application, in all the cases the mean delay remains below 100s and below 100ms where there is no PU interference. The web application has a mean delay for all the cases below 100ms and the video streaming application has for all the cases a delay below 100ms.

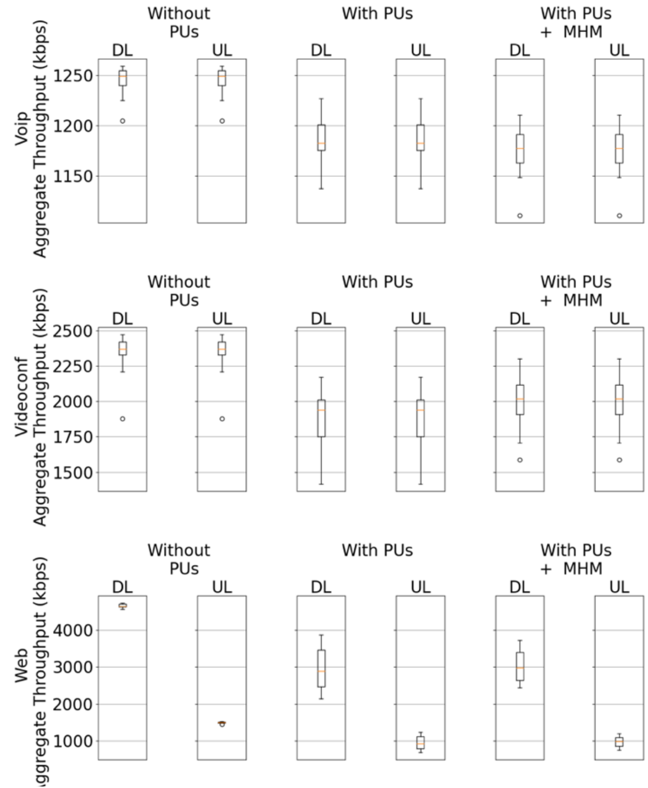

Figure 88. Simulation Results for throughput in the e-health scenario: 50 UEs.

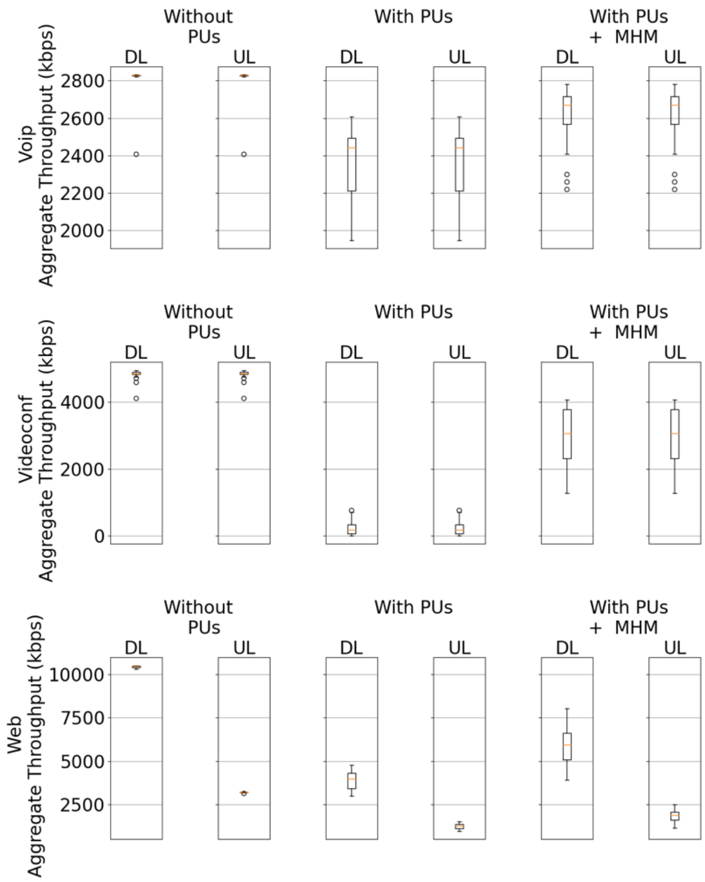

Figure 89. Simulation Results for throughput in the e-health scenario: 100 UEs

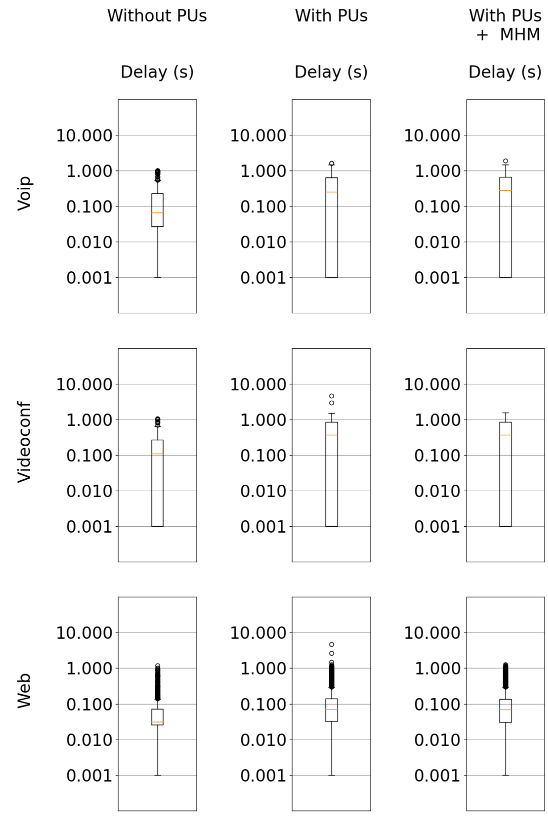

Figure 90. Simulation Results for delay in the e-health scenario: 20 UEs

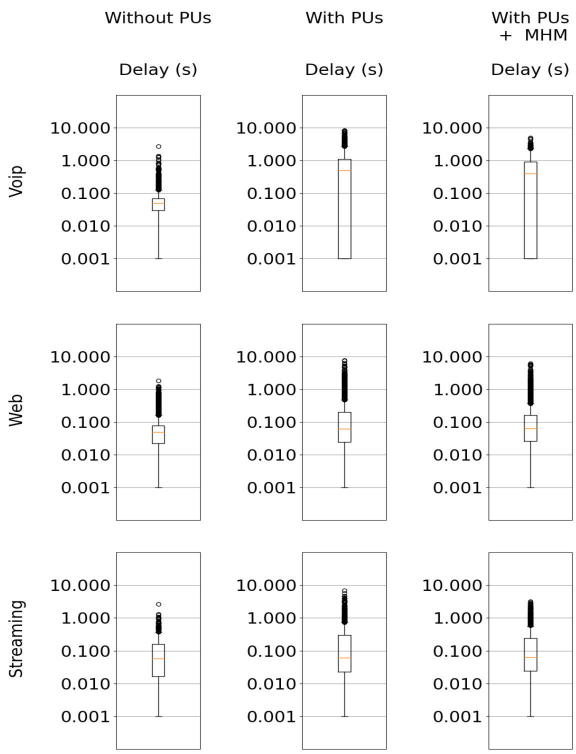

Figure 91. Simulation Results for delay in the e-health scenario: 100 UEs

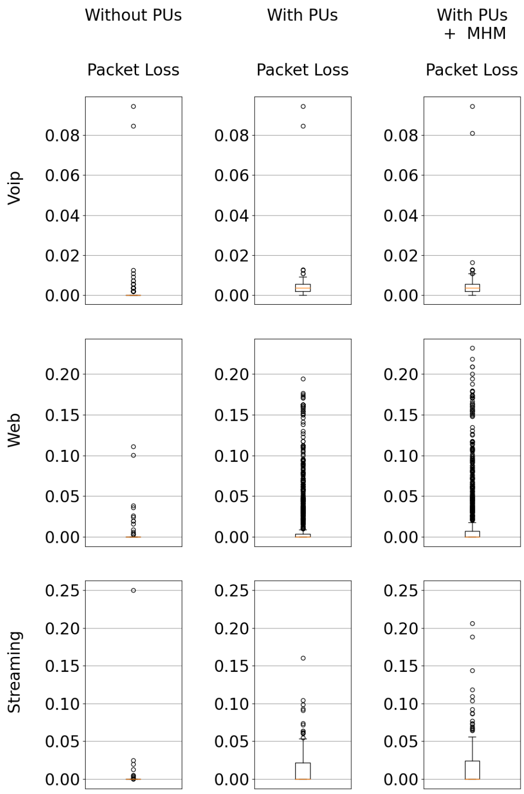

Figure 92. Simulation Results for packet loss in the e-health scenario: 100 UEs

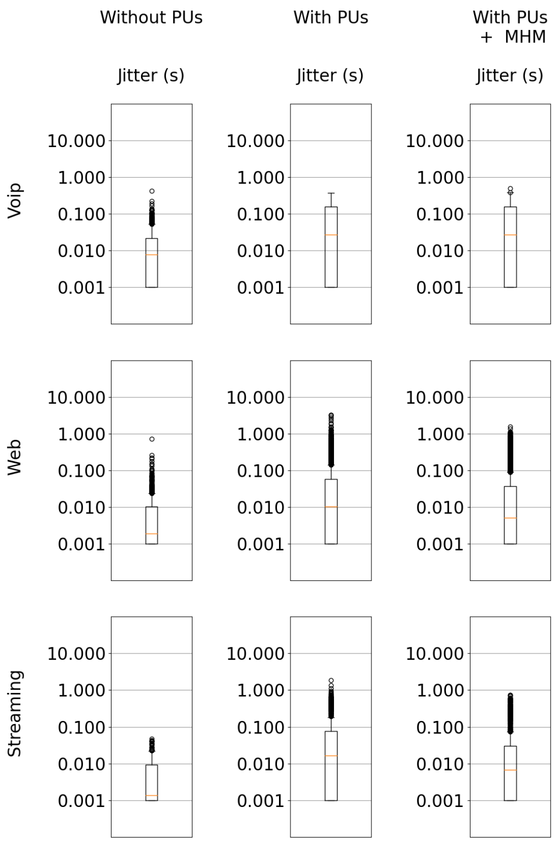

Figure 93. Simulation Results for jitter in the e-health scenario: 100 UEs

Figure 92 and Figure 93 show the results for packet loss for and jitter for the scenario with 100 UEs, respectively. Packet loss for the VoIP application is under 2% for all the cases, while for web applications it remains under 5% for the case without PU interference and around 12% for the other cases. Jitter, which is only meaningful for the VoIP and video streaming is under 100ms for both applications in all the cases, with or without PU interference.

Figure 94 and Figure 95 show the sensing simulation results for scenarios with 20 and 100 UEs, respectively. The results show that increasing the number of UEs in the cell also increases the false-positive fraction for the OR fusion algorithm. The false-positive reports increase from 20% to 62%. A false-positive detection impacts the system throughput. With PU interference, 14 UEs were able to achieve near 1 Mbps of aggregated throughput using web traffic (Figure 87), which is almost 71 kbps per UE. The average throughput per UE drops almost 13% to 62 kbps, when the number of UEs increases to 70 (Figure 89). On the other hand, the MHM fusion algorithm was able to increase almost 29%, from 62.5 kbps to 80.35 kbps the average throughput per UE (Figure 89). This is related to the performance improvement of MHM algorithm when increasing the UEs quantity in the cell. As shown in Figure 95 , the UE frame sensing reports increases near to 15% for 100 UEs using the OR fusion algorithm approach. The MHM approach it is near to zero even keeping lower results for false-positive and false-negatives values.

The simulation of the e-health scenario considered a mix of different applications and background traffic. For the VoIP and video-streaming applications, codecs with higher data rates were considered, which requires more available bandwidth in the network. The results in this section show that for these applications, the throughput per application was maintained, which is vital for monitoring. Then, for throughput, considering the complex scenario, the KPI was achieved. Delay shows values around 100ms for all the applications but is important to highlight that the scheduling algorithm used in the simulation is round robin, not being aware of implementing CQI requirements. Finally, packet loss show values below 2% for all the simulations, with a reliability around 98%. The delay and packet loss metrics may be improved when introducing a scheduling algorithm CQI-aware.

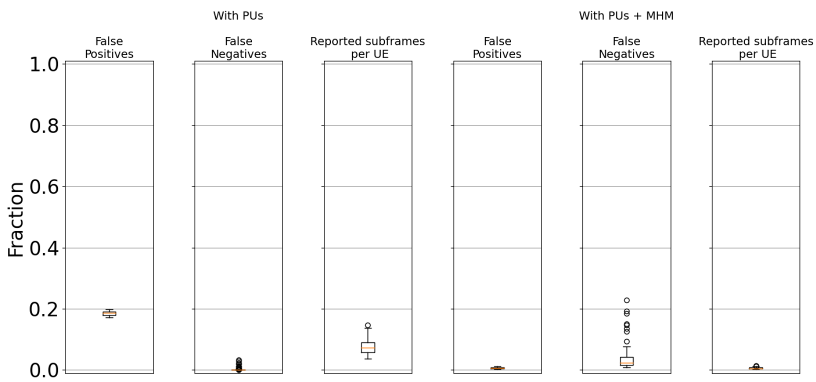

Figure 94 Simulation Results for sensing efficiency in the e-health scenario: 20 UEs

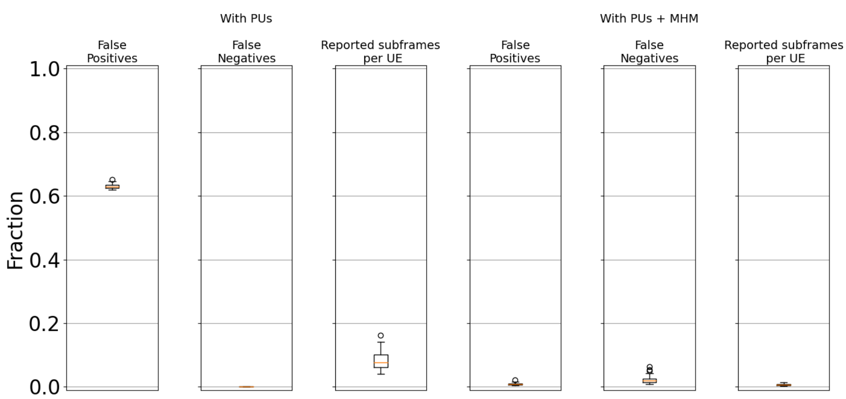

Figure 95 Simulation Results for sensing efficiency in the e-health scenario: 100 UEs

5 Conclusions

This deliverable presented the performance evaluation and simulation of the 5G-Range network. Since the project had budget and time restrictions to demonstrate in real world scenarios (with tens of users and different applications in rural areas) the capabilities of the 5G-Range network, the adopted approach was to integrate the main features developed during the project in a real-time PoC, intended to cover smaller versions of the most important uses cases which are voice and data connectivity, smart farm and wireless backhaul. Then, the software simulator, that integrates the PHY and MAC functionalities of the 5G-Range Network with a customized IP layer, integrated the models developed in WP3, WP4 and WP5 and after a proper validation when comparing field trial measures with simulation results, was used to simulate the four core use cases defined in D2.1.

As explained in deliverable, D6.1, the software simulator is composed by a link-level simulator and a system level simulator, which provided a mean to abstract the PHY layer in a set of set of tables and models that were integrated into the software simulator. A similar procedure was adopted with the spectrum sensing and CSS procedures. Therefore, the features regarding 5G-COSORA and 5G-DARA modules were fully implemented in the software simulator, also including some extensions for security and CSS optimization.

Section 2 shows the development and verification of the PHY and MAC Layer in the simulation tool. Then, in Section 3, the software simulator presented satisfactory results when comparing with field trial results obtained with the PoC results. The validate software simulation tool then was named and COLAB-5 and is available at [22].

Section 5 shows the simulation of the four core use cases defined in D2.1. Also, to improve the proximity with real world applications, was developed a traffic generation tool, the EROS-5, which is capable of generating VoIP, traffic, Web traffic, video streaming and fractal traffic, available at [17][18]. The simulation results in this section show a very acceptable picture and were able to show the potentiality of the 5G-Range Network to comply with most of the KPIs defined for each use case. Due to the computational complexity needed to simulate some scenarios with higher complexity (hundreds of UEs for example), the results in this section are restricted to scenarios with 100 UEs, which in many cases may represent the reality of rural scenarios.

Finally, we expect that the software tool can be considered as a customized experimental testbed, that may allow to evaluate the performance and metrics of miscellaneous configurations of the 5G-Range use cases and aid in future developments and research activities for 5G.

References

[1] 5G-RANGE, “Deliverable 3.1 Physical layer of the 5G-RANGE – Part I,” December 2018.

[2] J. C. Ikuno, M. Wrulich, M. Rupp, “System level simulation of LTE networks,” in Proc. IEEE Vehicular Technology Conference, pp. 1-5, May 2010.

[3] E. M. G. Stancanelli, C. H. M. Lima, and D. C. Moreira, “Strategies for Link-Level Performance Assessment in the Simulation of Wireless Systems,” in Optimizing Wireless Communication Systems, F. R. P. Cavalcanti, S. Andersson, Ed. Springer, 2009, pp. 269-309.

[4] M. of WINNER, “Assessment of advanced beamforming and MIMO technologies”, WINNER, Tech. Rep. IST-2003-507581, 2005.

[5] 5G-RANGE, “Deliverable 3.2 Physical layer of the 5G-RANGE – Part II,” February 2019.

[6] 5G-RANGE, “Deliverable 2.1 Application and requirements report,” April 2018.

[7] A. Faustine, M. Gabriel, and B. Shao. "Open source cellular technologies for cost effective cellular connectivity in rural areas." International Journal of Computer Applications 146.15 (2016).

[8] E. Bratu, B. Harper. "Open Source Mobile Network Using OpenBTS and USRP 9." The University of Mississippi Undergraduate Research Journal 2.1 (2017): 12.

[9] Ericsson & Telstra - A, R1 - 166599, Measurements for extreme rural scenario, Göterberg, 2017.

[10] Ericsson & Telstra - B, R1-167451 Channel model for extreme rural scenario, Göteberg, 2016.

[11] Ericsson & Telstra - C, R1-167452 Path loss model for extreme rural scenario, Göteborg, 2016.

[12] J. Olmos, S. Ruiz, M. García-Lozano, D. Martín-Sacristán, “Link abstraction models based on mutual information for LTE downlink,” COST 2100 TD. 10, pp. 1-18, Jun. 2010.

[13] 5G-RANGE, “Deliverable 6.1 Software-based system integration”, June 2019.

[14] M. Miozzo et al., "SDR and NFV extensions in the ns-3 LTE module for 5G rapid prototyping," 2018 IEEE Wireless Communications and Networking Conference (WCNC), Barcelona, 2018, pp. 1-6, doi: 10.1109/WCNC.2018.8377237.

[15] 5G-Wise, ‘5G K-Simulator’, Available at : [http://5gopenplatform.org], last access: November 2020.

[16] A. A. Barakabitze, A. Ahmad, R. Mijumbi, A. Hines, “5G network slicing using SDN and NFV: A survey of taxonomy, architectures and future challenges”, Computer Networks,Volume 167, 2020, 106984, ISSN 1389-1286, doi: 10.1016/j.comnet.2019.106984.

[17] R. Amaral, ‘‘EROS-5: Gerador Sintético de carga de tarbalho para ambientes 5G’’, Available at: [https://notopoloko.github.io/Eros/], last access: November 2020.

[18] R. Amaral, ‘‘EROS-5 Git Source Code Repository’’, Available at: [https://github.com/notopoloko/Eros], last access: November 2020.

[19] A. Ferreira *et al.*, "5G-RANGE Project Field Trial,"2019 European Conference on Networks and Communications (EuCNC), Valencia, Spain, 2019, pp. 490-494, doi: 10.1109/EuCNC.2019.8802021.

[20] Z. Li *et al.*, "Probe and Adapt: Rate Adaptation for HTTP Video Streaming At Scale," in IEEE Journal on Selected Areas in Communications, vol. 32, no. 4, pp. 719-733, April 2014, doi: 10.1109/JSAC.2014.140405.

[21] J. Vartiainen, M. Matinmikko-Blue, H. Karvonen, L. Mendes, A. Matos, and C. Silva (2019). Performance of WIBA energy detector in rural and remote area channel. In *2019 16th International Symposium on Wireless Communication Systems (ISWCS)*. IEEE.

[22] G. Ferreira, ‘‘COLAB-5G Tool’’, Available at: [https://gabrielcarvfer.github.io/NS3/COLAB_5G], last access: November 2020.

[23] C. Tarver, A. B. Stimming and J. R. Cavallaro, “Design and Implementation of a Neural Network Based Predistorter for Enhanced Mobile Broadband,” IEEE International Workshop on Signal Processing Systems (SiPS), Oct. 2019

[24] G. J. M. Llames and A. S. Banacia, “Spectrum sensing system in software-defined radio for determining spectrum availability,” International Conference on Electronics, Information, and Communications (ICEIC), 2016.

[25] M. Vaezi, Z. Ding, and H. V. Poor, Multiple Access Techniques for 5G Wireless Networks and Beyond, 08 2018.

[26] 3GPP TR 136.141 version 15.4.0, "Evolved Universal Terrestrial Radio Access (E-UTRA)".

[27] S. Shellhammer, 'Spectrum sensing in IEEE 802.11', 06 2010.

[28] 3GPP, "Procedures for the 5G System; Stage 2," 3rd Generation Partnership Project; Technical Specification Group Services and System Aspects, 3GPP Technical Specification 23.502, version 16.2.0., September 2019.

[29] C.I. Mattos, E.P. Ribeiro, E.M.G. Fernandez, C.M. Pedroso, 'An Unified VoIP model for workload generation'. Multimedia Tools and Application, 70 (3): 2309—2329.